



Contents lists available at ScienceDirect

## Marine Micropaleontology

journal homepage: [www.elsevier.com/locate/marmicro](http://www.elsevier.com/locate/marmicro)

# The Miocene Climatic Optimum at the interface of epicontinental sea and large continent: A case study from the Middle Miocene of the Eastern Paratethys

Yuliia V. Vernyhorova<sup>a,\*</sup>, Katarína Holcová<sup>b</sup>, Nela Doláková<sup>c</sup>, Bettina Reichenbacher<sup>d</sup>, Filip Scheiner<sup>b,e</sup>, Lukáš Ackerman<sup>e</sup>, Jan Rejšek<sup>e</sup>, Lorenzo De Bortoli<sup>b</sup>, Jakub Trubač<sup>f</sup>, Torsten Utescher<sup>g,h</sup>

<sup>a</sup> Department of Stratigraphy and Paleontology of Cenozoic Deposits, Institute of Geological Sciences of National Academy of Sciences of Ukraine, O. Honchr str. 55-b, 01601 Kyiv, Ukraine

<sup>b</sup> Charles University, Institute of Geology and Palaeontology, Faculty of Sciences, Albertov 6, 128 43 Praha 2, Czech Republic

<sup>c</sup> Masaryk University, Institute of Geological Sciences, Faculty of Science, Kotlářská 2, 611 37 Brno, Czech Republic

<sup>d</sup> Department for Earth and Environmental Sciences, Palaeontology and Geobiology, Ludwig-Maximilians-Universität München, Richard-Wagner-Str. 10, 80333 Munich, Germany

<sup>e</sup> Institute of Geology of the Czech Academy of Sciences, Rozvojová 269, 165 00, Prague 6, Czech Republic

<sup>f</sup> Charles University, Institute of Geochemistry, Mineralogy and Mineral Resources, Faculty of Sciences, Albertov 6, 128 43 Praha 2, Czech Republic

<sup>g</sup> Senckenberg Research Institute and Natural History Museum / Biodiversity and Climate Research Centre, Frankfurt, Germany

<sup>h</sup> Institute for Geosciences, Bonn University, Bonn, Germany

## ARTICLE INFO

## Keywords:

Paleoclimate  
Paleoenvironments  
Miocene Climatic Optimum  
Age-model  
Langhian  
Tarkhanian-early Chokrakian  
Eastern Paratethys

## ABSTRACT

The Miocene Climate Optimum (MCO) and the subsequent Miocene Climate Transition (MCT) are important biotic, environmental and geologic events. Here we address whether this holds true for the epicontinental Eastern Paratethys Sea (today's Black – Caspian Sea region). Two Tarkhanian – lower Chokrakian sequences of Middle Miocene age in the Kerch Peninsula were investigated using foraminifera, calcareous nannofossils, molluscs, fish otoliths, spores and pollen, oxygen and carbon stable isotopes and strontium isotope stratigraphy (SIS). Our results show that the marine environment during the Tarkhanian to early Chokrakian in the study area was characterized by open shelf conditions (near upper part of lower sublittoral zone), variable water column stratification and bottom water oxygen levels. Biostratigraphy and new SIS data suggest an age of >15.5 (~16.0?) – 14.75 Ma for the Tarkhanian, which implies a considerably longer duration (> 0.75 Ma vs. 0.1 Ma) than was previously suggested. The maximum transgression seen in the middle Tarkhanian could be dated to ~15.5–15.1 Ma and correlates with the highstand of sequence Bur 5/Lan 1 (15.2 Ma) and terminal phase of the MCO. The vegetation indicates a gradual change from subtropical humid (early Tarkhanian) to arid (early Chokrakian) conditions, which reflect the MCT. The climate change in the Eastern Paratethys occurred slightly earlier than in the Central Paratethys, possibly related to the existence of the large flat Eurasian continent.

## 1. Introduction

The late Burdigalian, Langhian and Serravallian time span (17.3–11.6 Ma) represents a very significant Neogene period from the view of climatic evolution and palaeogeographic reorganisation. It started with the last warm interval of the Neogene – the Miocene

Climatic Optimum (MCO; ~17.0–15.0 Ma, Zachos et al., 2001). It was followed by an important climatic change associated with the Antarctic ice sheet expansion, which is known as Miocene Climate Transition (MCT; ~15.0–13.0 Ma, Holbourn et al., 2005; Shevenell et al., 2006). These global climatic events were described from the oceanic realm, but their manifestation in the epicontinental seas and on land is not well

\* Corresponding author.

E-mail addresses: [july.vern@gmail.com](mailto:july.vern@gmail.com) (Y.V. Vernyhorova), [holcova@natur.cuni.cz](mailto:holcova@natur.cuni.cz) (K. Holcová), [nela@sci.muni.cz](mailto:nela@sci.muni.cz) (N. Doláková), [b.reichenbacher@lrz.uni-muenchen.de](mailto:b.reichenbacher@lrz.uni-muenchen.de) (B. Reichenbacher), [scheinerfilip@gmail.com](mailto:scheinerfilip@gmail.com) (F. Scheiner), [ackerman@gli.cas.cz](mailto:ackerman@gli.cas.cz) (L. Ackerman), [rejsek@gli.cas.cz](mailto:rejsek@gli.cas.cz) (J. Rejšek), [lurensdebortoli@gmail.com](mailto:lurensdebortoli@gmail.com) (L. De Bortoli), [jakub.trubac@gmail.com](mailto:jakub.trubac@gmail.com) (J. Trubač), [torsten.utescher@senckenberg.de](mailto:torsten.utescher@senckenberg.de) (T. Utescher).

<https://doi.org/10.1016/j.marmicro.2023.102231>

Received 26 September 2022; Received in revised form 7 March 2023; Accepted 8 March 2023

Available online 15 March 2023

0377-8398/© 2023 The Authors. Published by Elsevier B.V. This is an open access article under the CC BY-NC-ND license (<http://creativecommons.org/licenses/by-nc-nd/4.0/>).

known. From this viewpoint, the system of the Paratethys Sea, a large, semi-closed epicontinental sea, represents a unique archive (Piller et al., 2007). Several works interpreted the climatic and paleoceanographic evolution during the MCO and MCT in the area of the Central Paratethys in Central Europe (Hohenegger et al., 2009; Böhme et al., 2011; Kováč et al., 2017, 2018; Sant et al., 2017; Holcová et al., 2019; Doláková et al., 2021; Scheiner et al., 2019). According to these studies, global climate, as recorded from the oceanic archives, probably had a clear impact on the Central Paratethys environments. However, a different paleoclimatic evolution due to strong influence of continental climate can be supposed for the Eastern Paratethys (today's Black Sea – Caspian Sea region) as the Middle Miocene sea interfaced here with the large continent of Eurasia (Rögl, 1998). Although a complex circulation model has recently been created for the Middle Miocene Eastern Paratethys sea (Palcu et al., 2017, 2019), the interaction between marine palaeoenvironments and adjacent continental settings has not yet been studied considering the perspective of regional versus global climate evolution. The present study aims to fill this gap and to test the hypothesis that both the MCO and MCT can be detected in the area of the Eastern Paratethys. The specific objectives were (1) to refine the age model of the Tarkhanian and early Chokrakian, (2) to carry out paleoenvironmental reconstructions of the Tarkhanian to early Chokrakian marine habitats (bathymetry, trophic conditions, bottom water oxygenation, water column stratification), and (3) to reconstruct the continental vegetation as a proxy for the palaeoclimate during the MCO and MCT. To achieve this, we conducted a multiproxy approach using marine microfossils, pollen and spores, stable isotope analyses (oxygen, carbon, strontium) from two large outcrops on the Kerch Peninsula (Eastern Paratethys) that expose the Tarkhanian and Chokrakian of the regional Eastern Paratethys chronostratigraphy (Langhian of the Global Time Scale).

## 2. Geological setting

### 2.1. Tarkhanian – Chokrakian stratigraphy

The Tarkhanian and Chokrakian deposits were first discovered on the Azov Sea shore near the Tarkhan Cape and the Chokrak Lake (Fig. 1) by Andrusov (1889, 1893, 1961a, 1961b). The Tarkhanian and Chokrakian regional Eastern Paratethys stages were formally defined in 1975 (Nevekkaya et al., 1975; Nevekkaya et al., 1984). The Tarkhanian can be further subdivided into three regional substages in some areas of the Eastern Paratethys, whereas the Chokrakian is not (Nevekkaya et al., 1975; Nevekkaya et al., 1984; Nevekkaya et al., 2003).

The Chokrakian corresponds to the Langhian based on the recognition of the nannofossil zone NN5 (*Sphenolithus heteromorphus* Zone) (Kononkova and Bogdanovich, 1994) (Fig. 2). However, the correlation of the Tarkhanian with the standard chronostratigraphy (Raffi et al., 2020) is still under discussion (see Fig. 2). It was correlated with the late Early Miocene (e.g. Kononkova and Bogdanovich, 1994; Barg and Ivanova, 2001), the early Middle Miocene (e.g. Andreyeva-Grigorovich and Savitskaya, 2000; Krashennikov et al., 2003; Golovina, 2012), or with the transition between the Early and Middle Miocene (e.g. Nosovsky et al., 1976; Nevekkaya et al., 2003). These discrepancies are mainly based on the presence, respectively absence, of the calcareous nannofossil index species *Helicosphaera ampliaperata*, which is characteristic for the nannofossil zone NN4 and has its last appearance datum at 14.8 Ma (Raffi et al., 2020). Tarkhanian deposits containing this index species are correlated with the upper Burdigalian to lower Langhian (e.g. Studencka et al., 1998; Barg and Ivanova, 2000), whereas deposits which do not contain this species are correlated to the middle to upper Langhian (e.g. Rögl, 1998; Andreyeva-Grigorovich and Savitskaya, 2000; Golovina, 2012). Based on magnetostratigraphic data (Ciscaucasian sections), the base of the Tarkhanian has been dated at ~14.85 Ma, while the base of the Chokrakian has been dated at 14.75 Ma (Palcu et al., 2019). Accordingly, the Tarkhanian would represent a very short interval of 100 ka.

### 2.2. Regional geology

The study area is located in the northern-eastern part of the Kerch Peninsula. This region is part of the Kerch-Taman folded zone between the mountain structures of the Crimea and the Caucasus; it is characterized by tectonic and mud-volcanic activity and formation of anticlines and synclines in the Neogene (e.g. Andrusov, 1893; Shnyukov et al., 2006). Generally, Tarkhanian and Chokrakian deposits are widespread on the Kerch Peninsula (e.g. Andrusov, 1889, 1893; Arkhanguelsky et al., 1930; Archangelsky, 1940; Nosovsky et al., 1976; Barg and Stepaniak, 2003; Rostovtseva, 2012; Vernigorova et al., 2012; Vernyhorova, 2014). In this region, the Tarkhanian deposits follow above the Maikop deposits without visible hiatuses and are overlain, also without visible hiatuses, by sediments of the Chokrakian, or, after an erosion gap, by younger sediments (Andrusov, 1889, 1893; Arkhanguelsky et al., 1930; Nosovsky et al., 1976; Barg and Stepaniak, 2003; Vernigorova et al., 2012; Vernyhorova, 2014). The Tarkhanian sediments were considered by Andrusov (1961b) as upper (final) part of the Maikop strata as both deposits have a similar lithofacies. Following this interpretation, the Tarkhanian deposits of the Kerch Peninsula are considered as the upper part of the Arabatska and Alahol Formations (Fig. 3).

The Tarkhanian deposits of the eastern and north-eastern parts of the Kerch Peninsula (Alahol Formation) are represented by Maikop-like clays. Only in the middle part of the sections a marl layer (near 0,2 m), oyster banks and characteristic molluscs (e.g. *Lentipecten corneus denudatus*) occur (e.g. Nosovsky et al., 1976; Vernyhorova, 2014). These fossiliferous beds are indicative of the middle Tarkhanian (Terskie Beds or Beds with *Lentipecten corneus denudatus*, see Muratov and Nevekkaya, 1986). In the remaining region of the Kerch Peninsula, the Tarkhanian deposits are represented by Maikop-like clays (Arabatska Formation) and fossils only rarely occur (e.g. Nosovsky et al., 1976; Vernyhorova, 2014).

The lower part of the Chokrakian deposits on the Kerch Peninsula comprises dark-gray to gray clays, thin-, thick and not laminated with fine-grained sands and small amounts of molluscs on the bedding planes; common thickness is near 90 m (see “spirialis clays” in Nosovsky et al., 1976; Goncharova, 1989; Barg and Stepaniak, 2003; Rostovtseva, 2012; Vernigorova et al., 2012; Vernyhorova, 2014). These deposits are termed Bulhanak Beds (Vernigorova et al., 2012; Vernyhorova, 2014) (Fig. 3).

### 2.3. Study sites

The Malyi Kamyshlak section (45°26'04.2"N 36°30'53.8"E) and the Skelia section (45°25'34.0"N 36°31'52.9"E) are located on the north-eastern part of the Kerch Peninsula on the Azov Sea shore with a distance of 1.8 km from each other (Fig. 1). They form the western and eastern wings of the Bulhanak anticline (Table 1 in Arkhanguelsky et al., 1930) or northern part of the Bulhanak mud volcanic center (e.g. Shnyukov et al., 2006) (Fig. 1). The Malyi Kamyshlak section is the neostatotype of the Tarkhanian and Chokrakian of the Eastern Paratethys. At the Malyi Kamyshlak section, a 43 m thick sedimentary sequence was studied (Fig. 4), while at the Skelia section only about 0,5 m of deposits were accessible for our work (Fig. 5). A detailed lithological description of both sections is given in Figs. 4 and 5 and Supplementary Fig. S1.

The litho- and biostratigraphic subdivisions of the Maly Kamyshlak and Skelia sections have already been established in previous works (Vernigorova et al., 2012; Vernyhorova, 2014). The corresponding stratigraphic scheme (Fig. 3) is used in this work.

## 3. Methods

We used (micro) palaeontology, palynology, biostratigraphy, palaeoecology and Strontium Isotope Stratigraphy (SIS) dating to obtain new

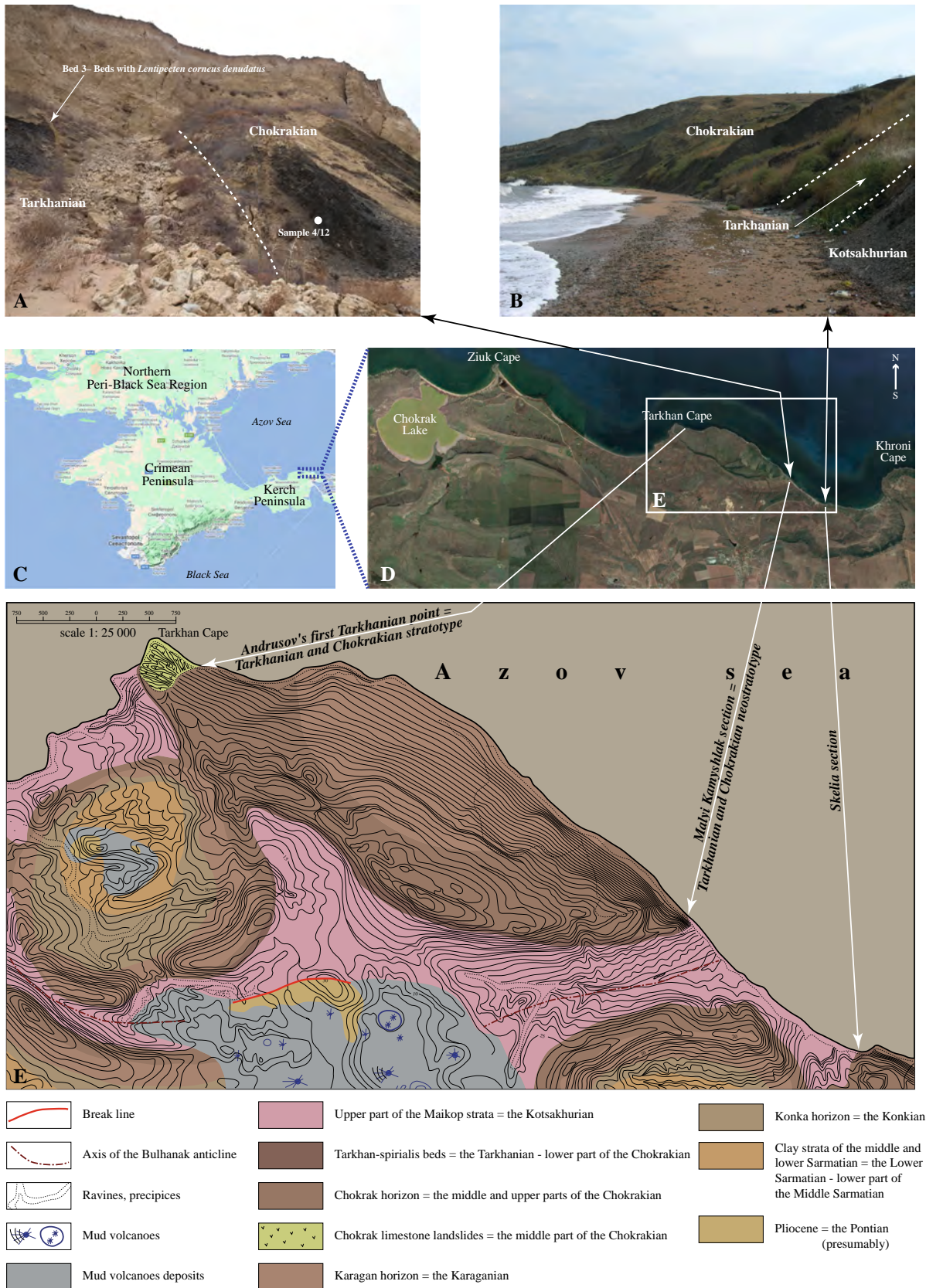


Fig. 1. The location of the Malyi Kamyshlak and Skelia sections in the northern part of the Kerch Peninsula: A – Malyi Kamyshlak section; B – Skelia section; C, D – Google maps with study area; E – restored part of the Geological map of the Bulhanak area (– its northern part) [scale 1: 25000] by (Aleksandrova, 1952).



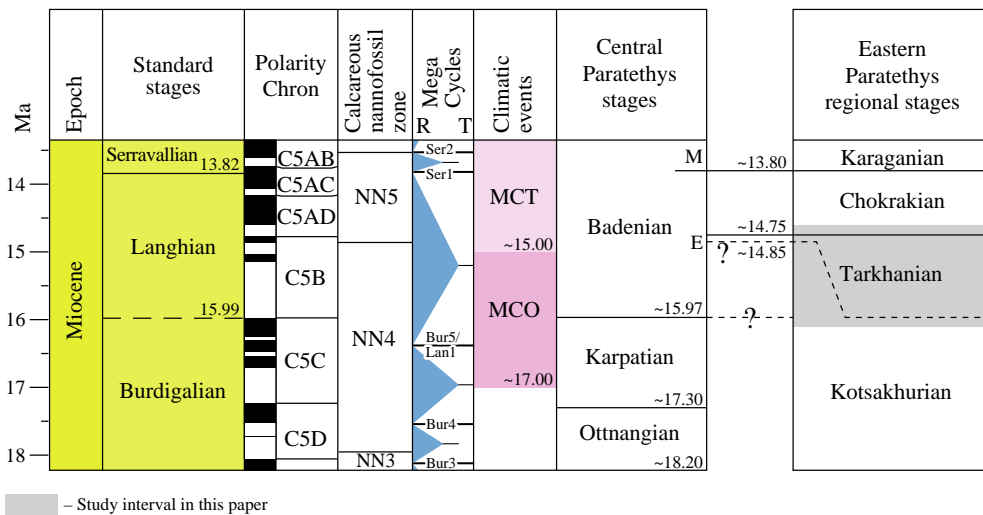


Fig. 2. Stratigraphic framework and correlation of the Lower-Middle Miocene of the Central and Eastern Paratethys.

Legend: Stratigraphic framework – after Palcu et al., 2017, 2019; Raffi et al., 2020. Mega Cycles – after Hilgen et al., 2012. Climatic events – after Zachos et al., 2001; Holbourn et al., 2005; Shevenell et al., 2006.

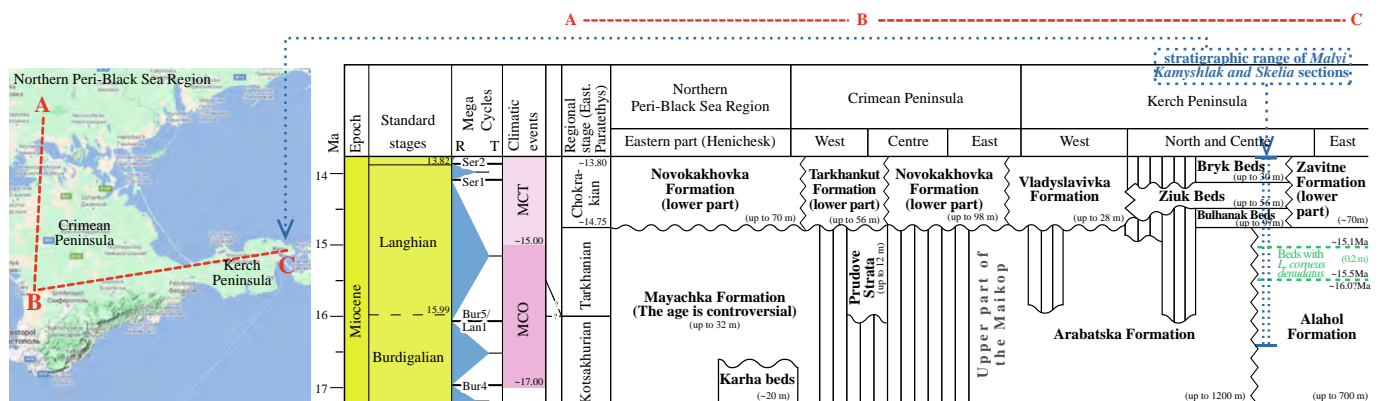


Fig. 3. The stratigraphic scheme of the Lower-Middle Miocene deposits of the Southern Ukraine (after Vernyhorova, 2014–2016 with changes).

Legend: Stratigraphic framework – after Palcu et al., 2017, 2019; Raffi et al., 2020. Mega Cycles – after Hilgen et al., 2012. Climatic events – after Zachos et al., 2001; Holbourn et al., 2005; Shevenell et al., 2006.

stratigraphical and paleoenvironmental data for the Malvi Kamyshlak and the Skelia sections and also compare with previous works. A total of 55 rock samples were selected for these analyses (43 from Malvi Kamyshlak, 12 from Skelia; each sample contained 400 g sediments).

### 3.1. Foraminifera

Foraminifera were present in 40 samples from the Malvi Kamyshlak section (Fig. 4) and nine samples from the Skelia section (Fig. 5). They were picked after washing and sieving the rock sample through a 63  $\mu$ m sieve and were identified under a stereomicroscope. Representative specimens were examined in detail using scanning electron microscope (SEM) (see Plates 1–4). Species determination of benthic foraminifera was based on Bogdanovich (1952), Dzhanelidze (1963, 1970), Krashennnikov (1959), Krashennnikov et al. (2003), and Bugrova et al. (2005). Revision of genera was based on Bogdanovich (1971) and Loeblich Jr. and Tappan (1988). Unfortunately, tests of planktic foraminifera from both sections are very small (up to ~100–150  $\mu$ m) and only three species could be identified: *Globigerina tarchanensis* Subbotina et Chutzieva, *Globigerinella obesa* (Bolli) (= *G. praebulloides* Blow) and *Globigerinita* cf. *uvula* (Ehrenberg) (with specific surface structure of tests – see Plate 4). Benthic foraminifera species diversity (after Boltovskoy and Totah, 1985) was the number of

species per sample (based on 400 g sample). Dominant (>20% of tests in the sample) and accompanying (between 10 and 20% of shells in the sample) species were identified (after Boltovskoy and Totah, 1985) in each sample. Dominant species formed the name for each foraminifera association. All benthic foraminiferal associations were statistically analysed using a Principal Component Analysis (PCA) and a Cluster Analysis (Bray-Curtis Similarity Index, Paired group), as implemented in the PAST software (Hammer et al., 2001). Epifaunal and infaunal species of benthic foraminifera were classified according to Rosoff and Corliss (1992), Báldi (2006) and Murray (2006). The ratio of these groups of benthic foraminifera (after the TROX-model by Jorissen et al., 1995) was used to estimate changes in trophic conditions and bottom water oxygen levels. The ratio of oxic-suboxic-dysoxic benthic foraminiferal indicators was used to monitor changes in bottom water oxygenation according to Kaiho (1994, 1999) and Murray (2006).

### 3.2. Calcareous nannofossils

Calcareous nannofossils were studied from the Malvi Kamyshlak section. Totally, 27 samples were analysed from the uppermost Kotsakhurian to the lower part of the Chokrakian (see Supplementary Fig. S2 for sample numbers and position). Smear slides were prepared using the method described in Zágorský et al. (2007). The slides were examined

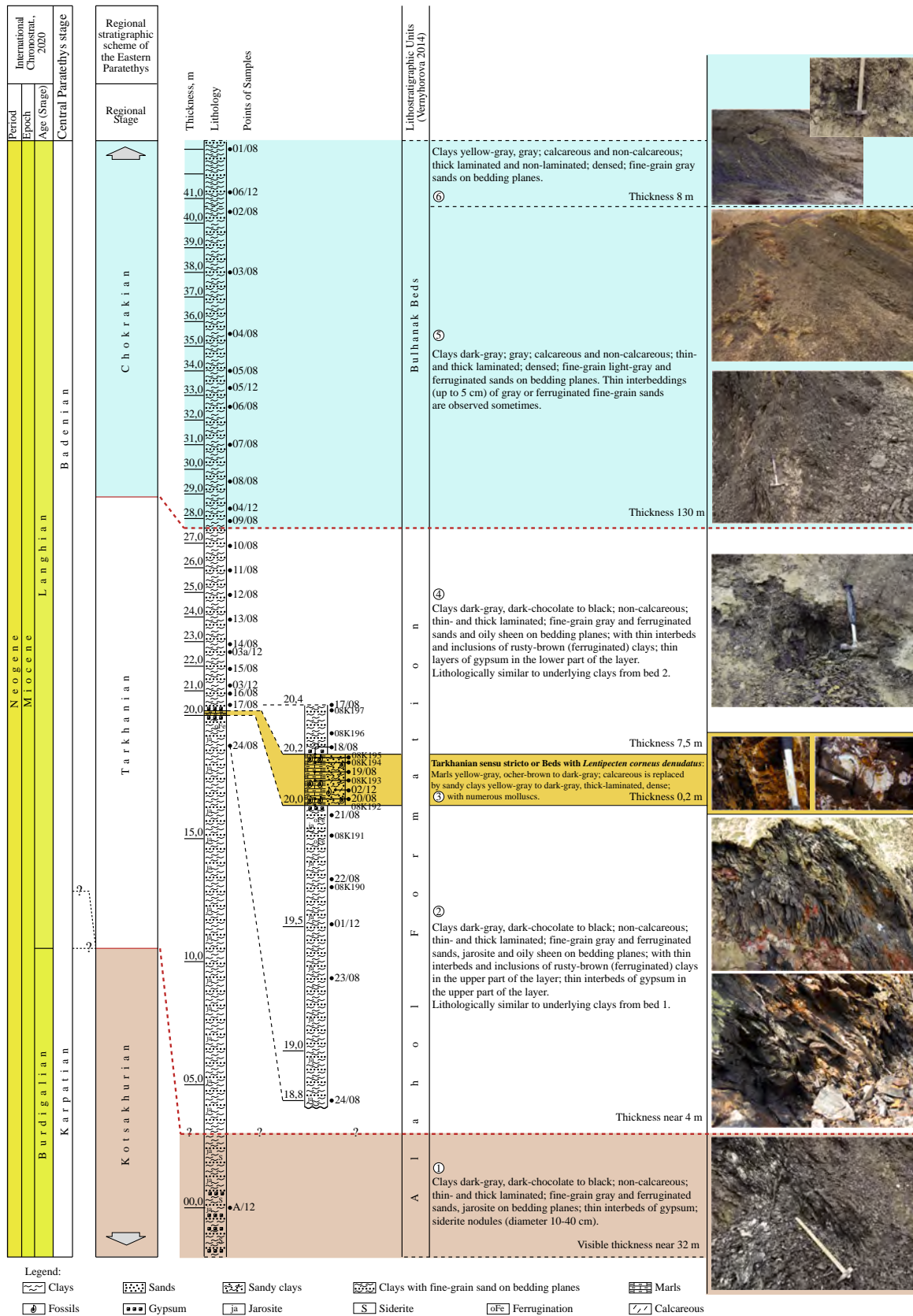


Fig. 4. Lithological log of Malyi Kamyshlak section with sampling points for micropaleontological analysis.



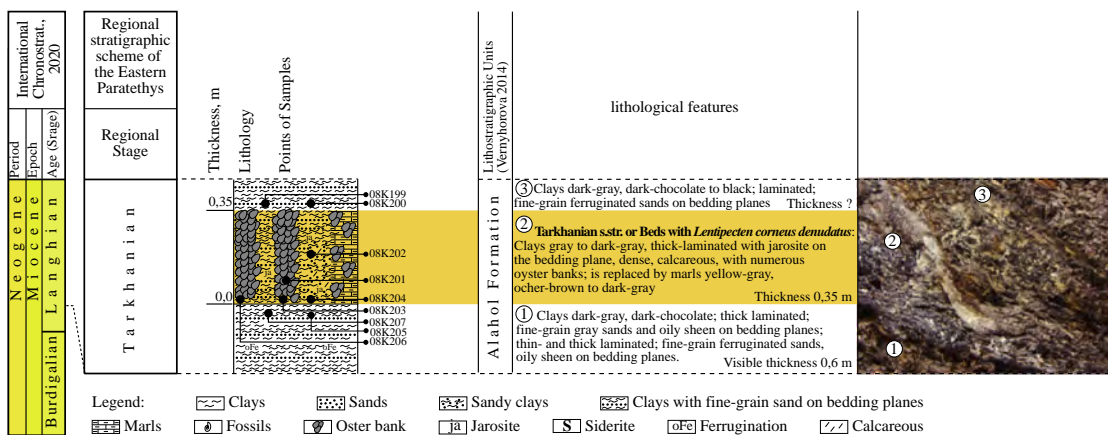


Fig. 5. Lithological log of Skelia section with sampling points for micropaleontological analysis.

using polarizing microscope at 1000× magnification in cross polarized and plane light. Abundances of calcareous nannofossils in individual samples were estimated semi-quantitatively based on the scheme of Rio et al. (1990) and Fornaciari et al. (1996) as follows: 1) = very abundant ( $\geq 50$  specimens/field of view), 2) = abundant (20–49 specimens/field of view), 3) = common (1–19 specimens/field of view) and 4) = rare (1 specimen/field of view). If the number of individuals was not sufficient only binary data is presented. Species determination of calcareous nannofossils was based on the Nannotax3 database (Young et al., 2021) and the calcareous dinoflagellate genus *Thoracosphaera* was included. Presence of diatoms in nannofossil slides was also recorded. Due to scarcity of calcareous nannofossils, statistical analysis using quantitative data was possible only for 14 samples. The Principal Component Analysis (PCA) of the PAST software was used (Hammer et al., 2001).

### 3.3. Molluscs

Molluscs were found in 16 samples from the Malyi Kamyshlak section and 3 samples from the Skelia section (Figs. 4 and 5) and were studied as a complementary group for a better understanding of the Tarkhanian-Chokrakian regional stratigraphy. The identification of molluscs was carried out directly during sampling of the sections, as well as under a stereomicroscope. Traditional conchological methods were used for species identification (Ilyina, 1993; Nevesskaya et al., 1993). Previous data on mollusc ecology were used for additional environmental interpretation.

### 3.4. Fish otoliths

Seven of the samples that have been used for the foraminiferal analyses yielded also fish otoliths: 4 samples from the middle Tarkhanian (Bed 3, Malyi Kamyshlak section, samples 19/08, 08 K194, 08 K195, Bed 2, Skelia section, sample 08 K202), 1 sample from the upper Tarkhanian (Bed 4, Malyi Kamyshlak section, 08 K196), and 2 samples from the lower Chokrakian (Bed 5, Malyi Kamyshlak section, 04/12, 05/12). Species determination and paleoecological interpretation followed previous works on the otoliths from the Tarkhanian and Middle Miocene of the Central and Eastern Paratethys (Weiler, 1950; Pobedina et al., 1956; Strashimirov, 1972; Brzobohatý and Nolf, 2002; Nolf, 2013; Bratishko et al., 2015; Schwarzahns, 2017). Information on otoliths preserved in situ in skeletons of *Vinciguerria merklini* Daniltschenko, 1946 from a historical collection at the Malyi Kamyshlak section was available by courtesy of Alexander Bannikov (Moscow).

### 3.5. Spores, pollen and terrestrial palaeoclimate interpretation

Palynomorphs were studied from 12 samples from the Malyi Kamyshlak section (see Supplementary Fig. S2 for sample numbers and position, C). The sediments of the middle Tarkhanian were not suitable for the preservation of palynomorph due to the coarse grain size. Samples were processed using standard maceration with HCl and HF acids and heavy liquid  $ZnCl_2$  (2 g/cm<sup>3</sup>). Determination of the palynomorphs was conducted with optical microscope and a SEM (JEOL JSM – 649 OLV).

Standard pollen diagrams were simultaneously analysed using the Palaeotropical/Arctotertiary concept (P/A), synthesized diagrams, the Coexistence Approach (CA) and Plant Functional Types (PFT) (see below for details). A standard pollen diagram was calculated (min. 150 determined grains) using the POLPAL programme (Walanus and Nalepka, 1999). The pollen diagram was divided into two parts to eliminate the possibility of oversizing the content of conifers in the marine realm and enabling comparison with the Central Paratethys (left part – 100% of all taxa excluding *Pinus* and *Cathaya*, right part – proportion of *Pinus* and *Cathaya* to all determined grains) (see Doláková et al., 2014; Doláková et al., 2021 and below).

The P/A concept was applied according to Mai (1981, 1991),

Planderová (1990) and Stuchlik (1994). The terminology of vegetation type was used according to Kvaček et al. (2006), Kovar-Eder et al. (2008a, 2008b), Teodoridis et al. (2011a, 2011b), and Kovar-Eder and Teodoridis (2018). The Coexistence approach (CA) was used for quantitative palaeoclimate reconstruction (Mosbrugger and Utescher, 1997; Utescher et al., 2014). The reconstructed climatic parameters are: mean annual temperature (MAT), mean temperature of the warmest month (WMT), mean temperature of the coldest month (CMT), mean annual precipitation (MAP), mean precipitation of the wettest month (MPwet), mean precipitation of the warmest month (MPwarm), and mean precipitation of the driest month (MPdry). Moreover, the mean annual range of temperature (MART) can be determined as the difference between summer and winter temperatures (MART = WMTmean – CMTmean) by using means of coexistence intervals (CIs) resulting for each microflora. Accordingly, the mean annual range of precipitation (MARP) is calculated as the difference between wettest and driest month precipitation (MARP = MPwetmean – MPdrymean). The climatic tolerances of all NLRs known for the fossil floras are taken from the PALAEOFLORA database (Utescher and Mosbrugger, 2015).

The plant functional type (PFT) approach was developed in relation to the CARAIB model (Carbon Assimilation in the Biosphere), a global dynamic vegetation model (Warnant et al., 1994; Otto et al., 2002; Laurent et al., 2008; Dury et al., 2011). According to Popova et al. (2013), the 26-PFT classification including 15 arboreal, 3 herbaceous, 8 shrub PFTs, and 1 additional aquatic PFT (PFT 27) (Supplementary Fig. S4) was applied. In the CA and PFT analyses, all taxa were recorded without their abundances to minimize taphonomic effects (Popova et al., 2013; Utescher and Mosbrugger, 2015).

### 3.6. Carbon and oxygen stable isotope data

For carbon and oxygen stable isotope analyses, 13 samples from the Malyi Kamyshlak section containing well-preserved foraminiferal tests were used (see Supplementary Fig. S2 for sample numbers and positions). The foraminiferal preservation was evaluated based on the inner-wall structure check (overgrowths, crystal alignment) under SEM. Various crushed individuals from each sample were examined to evaluate possible diagenetic alteration and only those with no or minor signs of recrystallization were selected for the isotopic analysis.

Foraminiferal species were selected with respect to their ecological positions within the water column. Planktic foraminifera of the *Globigerina bulloides/praebulloides* group were analysed as representatives of surface waters, whereas the benthic foraminifera *Nonion commune* were used as a marker of bottom waters. Other taxa were extremely scarce in the studied materials and therefore were not selected for isotopic analysis.

The conventional C, O isotope analysis was performed by employing GasBench II (ThermoFisher Scientific) equipped with a CTC Combi-Pal (PALSYSTEM) linked to a MAT253 isotope ratio mass spectrometer (ThermoFisher Scientific) in a Continuous Flow IV (ThermoFisher Scientific) system housed at the Faculty of Sciences, Charles University, Prague. The procedure comprised of weighing of foraminiferal samples for the subsequent linearity corrections (routinely about 150–450 µg). The internal precision (SD) is typically 0.02 and 0.09 for raw  $\delta^{13}C$  and  $\delta^{18}O$  values, respectively, given a sample size above 50 mg. Calibration of the raw results versus the VPDB scale is achieved using the in-house calcite standards that have been calibrated against NBS-18, L-SVEC, and IAEA-603 international reference materials (IAEA, Vienna, Austria).

### 3.7. Strontium isotope data

Several foraminiferal tests, fish otoliths and parts of molluscs shells (*Ostrea*) (samples 08 K195 from the Malyi Kamyshlak section, samples 08 K201, 08 K202 from the Skelia section, see Supplementary Fig. S2) were processed at the clean lab of the Institute of Geology of the Czech Academy of Sciences (IG CAS). Planktic organisms were removed from

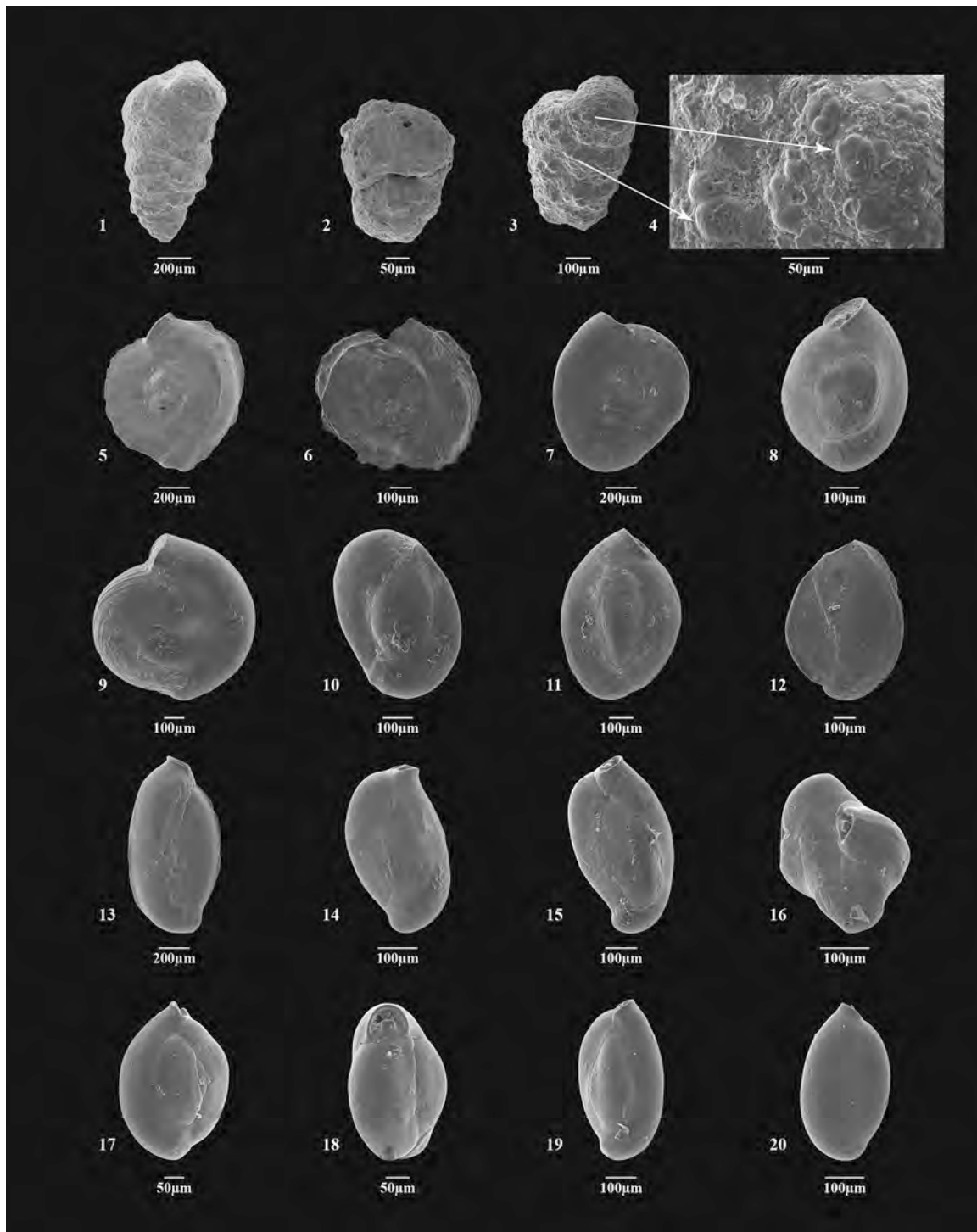


**Plate 1.** Benthic foraminifera from the Tarkhanian – early Chokrakian of the Kerch Peninsula:

1–4 *Textularia tarchanensis* Bogdanowicz: 1 – sample 08 K201; Skelia section; 2 – sample 19/08; Malyi Kamyshlak section; 3 – test with broken umbilical chambers; sample 08 K201; Skelia section); 4 – shell's surface of the test number 3.

5; 6 *Spiroloculina bicarinata* O. Djanelidze: 5 – sample 08 K202; Skelia section; 6 – sample 08 K202; Skelia section.

7 *Spiroloculina tarchanensis* O. Djanelidze: 7 – sample 08 K201; Skelia section.

8 *Quinqueloculina boueana* d'Orbigny: 8 – sample 08 K202; Skelia section.

9 *Quinqueloculina boueana* var. *plana* O. Djanelidze: 9 – sample 08 K201; Skelia section.

10 *Quinqueloculina* cf. *obliqua* Reuss: 10 – sample 08 K201; Skelia section.

11; 12 *Quinqueloculina ungeriana* d'Orbigny: 11 – sample 08 K202; Skelia section; 12 – sample 08 K204; Skelia section.

13 *Quinqueloculina elongato-carinata* (Bogdanowicz): 13 – sample 06/08; Malyi Kamyshlak section.

14; 15 *Quinqueloculina* aff. *Laevigata* d'Orbigny 14 – sample 07/08; Malyi Kamyshlak section; 15 – sample 08/08; Malyi Kamyshlak section.

16 *Quinqueloculina akneriana* d'Orbigny (abnormal forms): 16 – sample 03/12; Malyi Kamyshlak section.

17; 18 *Quinqueloculina akneriana* d'Orbigny: 17 – sample 05/12; Malyi Kamyshlak section; 18 – the same test.

19; 20 *Quinqueloculina akneriana* subsp. *longa* (Gerke): 19 – sample 05/12; Malyi Kamyshlak section; 20 – sample 05/12; Malyi Kamyshlak section.



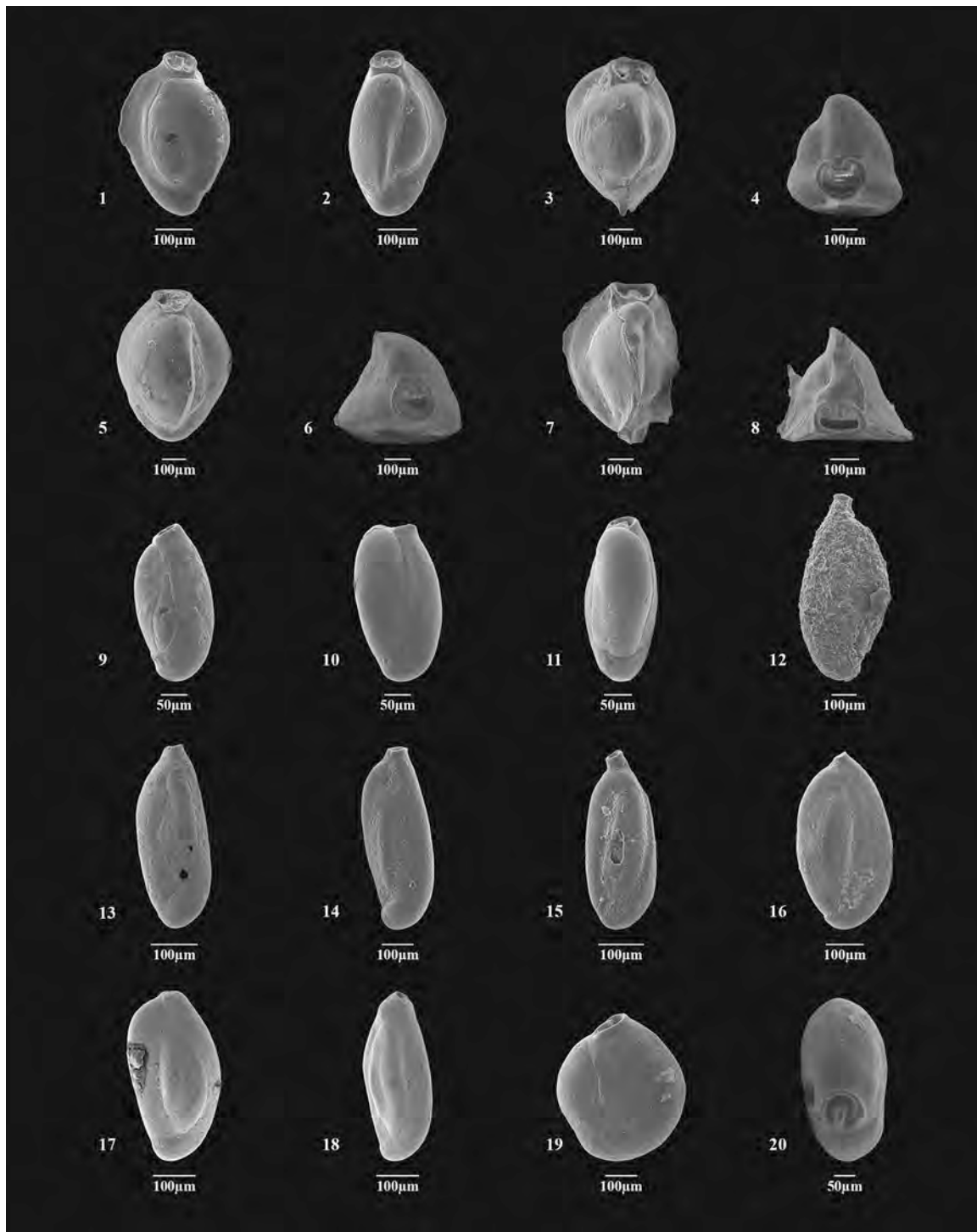
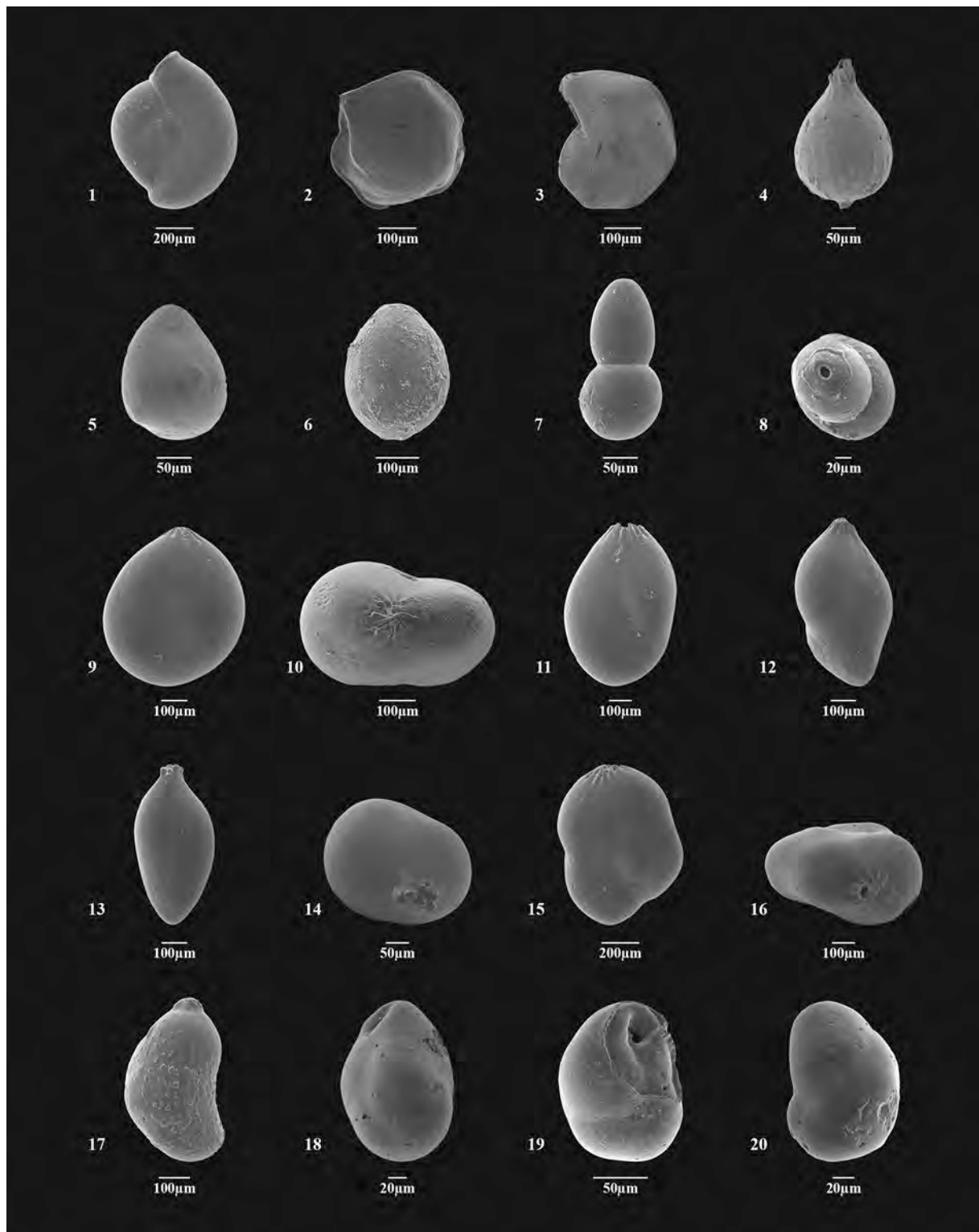


**Plate 2.** Benthic foraminifera from the Tarkhanian – early Chokrakian of the Kerch Peninsula:

- 1; 2 *Triloculina subfoliacea* (Bogdanowicz): 1 – sample 05/12; Malyi Kamyshlak section; 2 – sample 05/12; Malyi Kamyshlak section.  
 3; 4 *Triloculina austriaca* d'Orbigny: 3 – sample 08 K201; Skelia section; 4 – the same test.  
 5; 6 *Triloculina gibba* d'Orbigny: 5 – sample 08 K202; Skelia section; 6 – the same test.  
 7; 8 *Triloculina trigonula* (Lamarck): 7 – sample 08 K201; Skelia section; 8 – the same test.  
 9–11 *Triloculina gubkini* (Bogdanowicz): 9 – sample 13/08; Malyi Kamyshlak section; 10 – sample 05/12; Malyi Kamyshlak section; 11 – sample 05/12; Malyi Kamyshlak section.  
 12 *Sigmoinilina mediterraneensis* Bogdanowicz: 12 – sample 05/12; Malyi Kamyshlak section;  
 13; 14 *Sigmoinilina tschokrakensis* Gerke: 13 – sample 09/08; Malyi Kamyshlak section; 14 – sample 05/12; Malyi Kamyshlak section.  
 15 *Sigmoinilina* sp.1: 15 – sample 13/08; Malyi Kamyshlak section.  
 16 *Sigmoinilinita tenuis* (Czjzek): 16 – sample 02/12; Skelia section.  
 17; 18 *Sigmoinilinita tenuis* (Czjzek) var. *tarchanensis* (O. Dzanelidze): 17 – sample 20/08; Malyi Kamyshlak section; 18 – sample 20/08; Malyi Kamyshlak section.  
 19; 20 *Sigmoinilina haidingerii* var. *haidingeriia* (D'Orbigny): 19 – sample 05/12; Malyi Kamyshlak section; 20 – sample 05/12; Malyi Kamyshlak section.



(caption on next page)

**Plate 3.** Benthic foraminifera from the Tarkhanian – early Chokrakian of the Kerch Peninsula:

- 1 *Sigmoilina haidingerii* (D'Orbigny) var. *tschokrakensis* Bogdanowicz: 1 – sample 05/12; Malyi Kamyshlak section.
- 2 *Lenticulina* cf. *californiensis* Trujillo: 2 – sample 20/08; Malyi Kamyshlak section.
- 3 *Lenticulina* sp.1: 3 – sample 19/08; Malyi Kamyshlak section.
- 4 *Lagena* cf. *striata* (d'Orbigny): 4 – sample 16/08; Malyi Kamyshlak section.
- 5 *Fissurina laevigata* Reuss: 5 – sample 20/08; Malyi Kamyshlak section.
- 6 *Entosolenia mironovi* Bogdanowicz: 6 – sample 05/12; Skelia section.
- 7; 8 *Nodosaria* sp.: 7 – sample 04/12; Malyi Kamyshlak section; 8 – the same test.
- 9; 10 *Globulina gibba* d'Orbigny var. *globosa* (Von Munster): 9 – sample 19/08; Malyi Kamyshlak section; 10 – sample 19/08; Malyi Kamyshlak section.
- 11 *Globulina inaequalis* Reuss: 11 – sample 08 k193; Malyi Kamyshlak section.
- 12 *Guttulina austriaca* d'Orbigny: 12 – sample 08 k195; Malyi Kamyshlak section.
- 13; 14 *Pseudopolymorphina tschokrakensis* O.Djanelidze: 13 – sample 08/08; Malyi Kamyshlak section; 14 – the same test.
- 15; 16 *Pseudopolymorphina variata* (Jones, Parker and Brady) var. *fischeri* (Terquem): 15 – sample 19/08; Malyi Kamyshlak section; 16 – the same test.
- 17 *Pyrrulina fusiformis* (Roemer): 17 – sample 08 K195; Malyi Kamyshlak section.
- 18 *Cassidulina* aff. *Tarchanensis* Khutzieva: 18 – sample 20/08; Malyi Kamyshlak section.
- 19; 20 *Cassidulinoides tarchanensis* Khutzieva: 19 – sample 14/08; Malyi Kamyshlak section; 20 – sample 08 K196; Malyi Kamyshlak section.

Sr isotope analysis due to their low oxygen isotope values which might indicate influence of fresh waters; this could shift the strontium values (El Meknassi et al., 2018; McArthur et al., 2020 and references therein).

The samples were crushed and then treated using an ultrapure water (Millipore Element), alkali-buffered 1% H<sub>2</sub>O<sub>2</sub> solution and weak HNO<sub>3</sub> to remove possible clay particles, organic matter, coarse-grained silicate and other contaminations (Barker et al., 2003). Afterwards, the samples were quickly (30 s) leached using 0.001 M HNO<sub>3</sub> and finally dissolved in 1 M HNO<sub>3</sub> and processed for Sr separation. Strontium was isolated from the matrix by ion exchange chromatography using a Sr resin (Triskem, France) with 2 ml of 0.05 M HNO<sub>3</sub> used for Sr collection (Pin et al., 2014). The solution was dried and loaded in a 6 M HCl onto degassed Re filaments in the presence of Ta activator and <sup>87</sup>Sr/<sup>86</sup>Sr determination was performed on a Thermo Triton Plus thermal ionization mass spectrometer (TIMS) housed at the IG CAS using Faraday cups employed in a static mode and <sup>88</sup>Sr/<sup>86</sup>Sr of 8.3752 for mass fractionation correction.

External reproducibility of the measurements was accessed through the periodical analyses of the NIST SRM 987 solution that yielded <sup>87</sup>Sr/<sup>86</sup>Sr of 0.710239 ± 0.000008 (2σ, n = 20). <sup>87</sup>Sr/<sup>86</sup>Sr values were converted into numerical ages using the regression curve LOWESS look-up Table version 6 (McArthur et al., 2020). Minimum and maximum ages were obtained by combining the statistical uncertainty (2σ) of the mean values of the Sr-isotope ratios of the samples with the uncertainty of the seawater curve.

### 3.8. Palaeoenvironmental analyses

The paleoenvironmental features of the sea floor and the characteristics of the surface water were interpreted from data synthesis of the marine biota (foraminifera, calcareous nanoplankton, fish, molluscs) and geochemical parameters (stable carbon and oxygen isotopes). The vertical zoning of the benthic zone (e.g. upper and lower sublittoral zones) in combination with other characteristics (e.g. water column stratification, photic zone) was also used for the palaeoenvironmental reconstructions (e.g. Derjugin, 1915, 1928; Hedgpeth, 1957; Andriyashchev, 1979; Longhurst, 2007). Moreover, to trace the degree of isolation of the Eastern Paratethys during the Tarkhanian – early Chokrakian (the first half of the Langhian), the ratio of endemic and non-endemic benthic foraminifera species was calculated.

## 4. Results

### 4.1. Foraminifera

#### 4.1.1. Statistical analysis of foraminiferal assemblages

PCA was conducted to assess the general similarity in the benthic foraminifera species composition from the Tarkhanian and lower Chokrakian deposits of the Malyi Kamyshlak section. Three assemblages were classified: (1) The *Nonion commune*-*Globulina*-*Guttulina* assemblage

occurs in all samples of the middle Tarkhanian and in some samples of the upper Tarkhanian; (2) the *Bolivina tarchanensis* assemblage was distinguished in samples from the upper Tarkhanian and in some samples from the lower Chokrakian and (3) the *Quinqueloculina* assemblage was recorded in some of the lower and upper Tarkhanian samples and also in some of the lower Chokrakian samples (Fig. 6).

Cluster Analysis using the Bray-Curtis similarity index (Paired group) was used to determine the stratigraphic sequence of benthic foraminifera species composition through the studied Tarkhanian – lower Chokrakian interval of the Malyi Kamyshlak and Skelia sections. Six clusters are recognizable (I, II, IV, V, VI in Malyi Kamyshlak section and III in Skelia section) (Fig. 7). For each cluster the dominating and accompanying species were determined (see Appendix Figs. A1 and A2; Supplementary Figs. S5 and S6), which resulted in 6 different associations of benthic foraminifera: (I) *Quinqueloculina* association (lower Tarkhanian; Malyi Kamyshlak and Skelia sections); (II) *Nonion-Globulina-Guttulina* association (middle Tarkhanian; Malyi Kamyshlak section); (III) *Triloculina-Textularia-Guttulina-Nonion* association (middle Tarkhanian; Skelia section); (IV) *Nonion* association (upper Tarkhanian; Malyi Kamyshlak section); (V) *Nonion-Quinqueloculina* association (upper Tarkhanian; Malyi Kamyshlak section); (VI) *Bolivina-Nonion-Quinqueloculina* association (lower Chokrakian; Malyi Kamyshlak section).

#### 4.1.2. Characteristic of foraminiferal associations

**4.1.2.1. Upper Kotsakhurian.** The single sample from the Malyi Kamyshlak section (Bed 1, sample A/12, see Fig. 4) yielded only 3 planktic foraminifera tests (small 4-chambers *Globigerina*) (Appendix Fig. A1).

**4.1.2.2. Lower Tarkhanian.** Several samples from Bed 2 of the Malyi Kamyshlak section (Fig. 4) comprised a small number of two groups of planktic foraminifera: small 4-chambers *Globigerina* and small 5-chambers *Globigerina* (Appendix Fig. A1). The coeval deposits of the Skelia section (Bed 1, Fig. 5) did not yield planktic foraminifera (Appendix Fig. A2). Benthic foraminifera are represented in Bed 2 of the Malyi Kamyshlak section and Bed 1 of the Skelia section by the *Quinqueloculina* association (I, see above) which consists of 10 species from 7 genera (a detailed species list is provided in Appendix Figs. A1 and A2 and Supplementary Figs. S5 and S6). Species diversity ranges from 0 to 5 taxa per sample, numbers of tests are 0–8 per sample. In addition to representatives of *Quinqueloculina*, single tests of *Textularia tarchanensis*, *Sigmoilinita tenuis*, *S. mediterraneensis*, *Globulina gibba*, *Nonion commune*, *Ammonia beccarii*, and *A. tepida* were found. All tests have small sizes, thin walls and are often broken.

**4.1.2.3. Middle Tarkhanian.** Almost all samples of Bed 3 of the Malyi Kamyshlak section (Fig. 4) and Bed 2 of the Skelia section (Fig. 5)



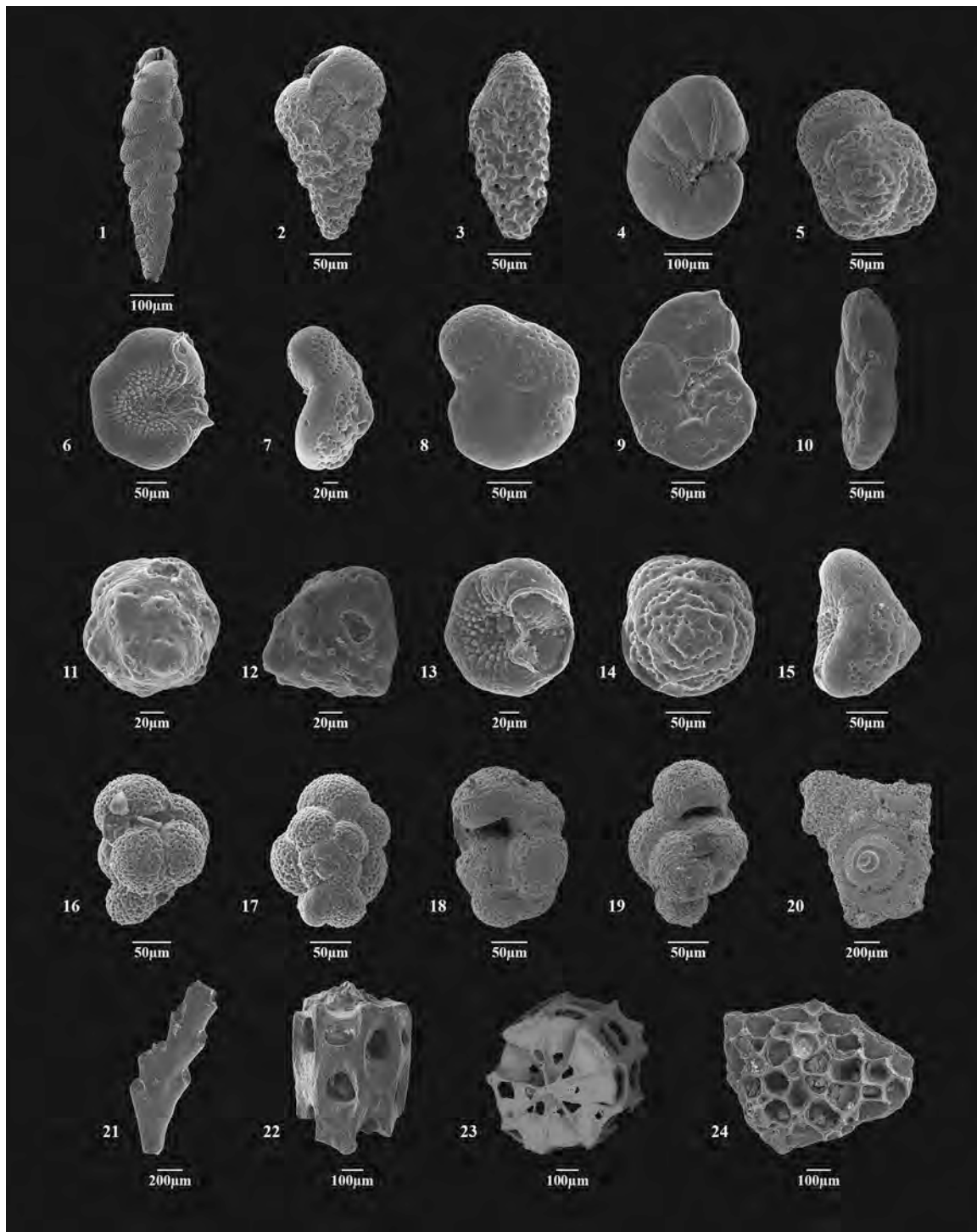


**Plate 4.** Benthic foraminifera from the Tarkhanian – early Chokrakian of the Kerch Peninsula:

1 *Bolivina tarchanensis* Subbotina and Khutsieva in Bogdanowicz: 1 – sample 09/08; Malyi Kamyshlak section.

2 *Bolivina crenulata* Cushman: 2 – sample 11/08; Malyi Kamyshlak section.

3 *Bolivina albatrossi* Cushman: 3 – sample 16/08; Malyi Kamyshlak section.

4 *Nonion commune* (d'Orbigny): 1 – sample 20/08; Malyi Kamyshlak section.

5–7 *Discorbis tarchanensis* O.Djanelidze: 5–7 – sample 14/08; Malyi Kamyshlak section.

8–10 *Discorbis tschokrakensis* Bogdanowicz: 8 – sample 08/08; Malyi Kamyshlak section; 9 – sample 08/08; Malyi Kamyshlak section; 10 – the same test.

11–15 *Discorbis* sp.1: 11 – sample 05/12; Malyi Kamyshlak section; 12 – the same test; 13–15 – sample 05/12; Malyi Kamyshlak section.

16–19 *Globigeriinita* cf. *uvula* Ehrenberg: 16; 17; 19 – sample 19/08; Malyi Kamyshlak section; 18 – sample 16/08; Malyi Kamyshlak section.

20 Echinoid remains: 20 – sample 19/08; Malyi Kamyshlak section.

21–24 Briozoans: 21 – sample 05/12; Malyi Kamyshlak section; 22 – sample 08 K195; Malyi Kamyshlak section; 23 – the same test; 24 – sample 18/08; Malyi Kamyshlak section.

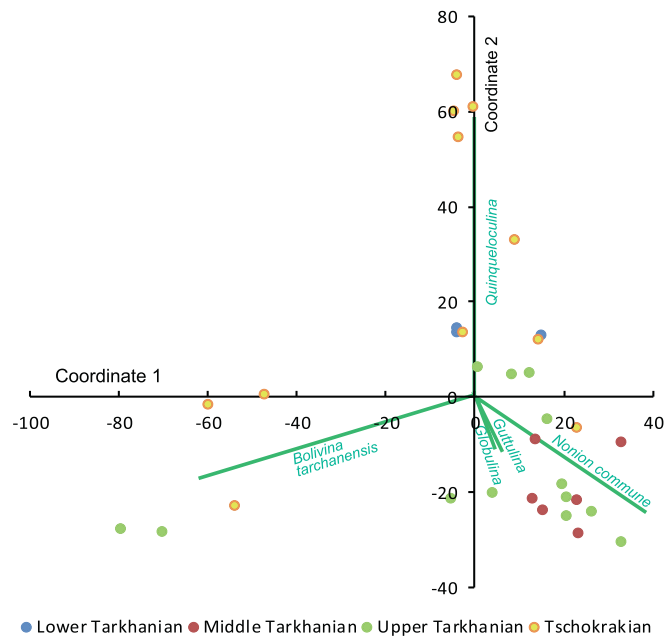


**Fig. 6.** Classification of foraminiferal assemblages using PCA. Coordinates 1 and 2 capture 91.2% of the variation.

comprised different amounts of planktic foraminifera: small 4-chambers *Globigerina* (5–173 tests per sample) and small 5-chambers *Globigerina* (3–68 tests per sample). Benthic foraminifera are represented in Bed 3 of the Malyy Kamyshlak section by the *Nonion-Globulina-Guttulina* association (II, see above) which consists of 39 species from 18 genera (Appendix Fig. A1 and Supplementary Fig. S5). Species diversity ranges from 11 to 23 taxa per sample, numbers of tests are 80–567 per sample. The tests are whole or broken, some of them are ferruginous. They have small and big sizes and different wall thicknesses. Dominant species are *Nonion commune*, *Globulina gibba*, *G. inaequalis*, *Guttulina austriaca*, *G. problema*, and *Guttulina* sp. 1. Also, *Sigmoilinita tenuis*, *Textularia tarchanensis* and *Cycloforina contorta* are accompanying in the lower part of Bed 3. In Bed 2 of the Skelia section, benthic foraminifera are represented by the *Triloculina-Textularia-Guttulina-Nonion* association (III, see above) which consists of 27 species of 15 genera (Appendix Fig. A2 and Supplementary Fig. S6). Species diversity ranges from 0 to 19 taxa per sample, numbers of tests change from 0 to 230 per sample. All tests are thick-walled and have a big size, which is in contrast to the coeval deposits of the Mali Kamyshlak section (Bed 3). Most tests are complete, some are broken and/or ferruginous. The dominant species are *Triloculina gibba*, *Textularia tarchanensis*, *Guttulina austriaca*, and *Nonion commune*. Accompanying species are *Spiroloculina bicarinata*, *Sigmoilina mediterraneensis* and *Quinqueloculina boueana*.

**4.1.2.4. Upper Tarkhanian.** All samples of Bed 4 of the Malyy Kamyshlak section (Fig. 4) revealed different numbers of planktic foraminifera: small 4-chambers *Globigerina* (3–277 tests per sample) and small 5-chambers *Globigerina* (3–181 tests per sample) (Appendix Fig. A1). Furthermore, this bed is characterized by a heterogeneous benthic foraminifera species diversity. Its lower part (from sample 08 K196 to sample 03/12) is represented by the *Nonion* association (IV, see above) which consists of 28 species from 18 genera (Appendix Fig. A1 and Supplementary Fig. S5). It is characterized by low species diversity (1–13 per sample), the numbers of tests vary between 2 and 87 per sample. All tests have small sizes and are sometimes corroded and broken. *Nonion commune* (d’Orbigny) is the dominant species. Accompanying species are *Sigmoilinita tenuis*, *Bolivina* sp. 1, *Guttulina austriaca*, *Globulina* sp. 1 (in the lower part of the deposits with the *Nonion* association) and *Cassidulinoides tarchanensis* and *Ammonia tepida* (in the

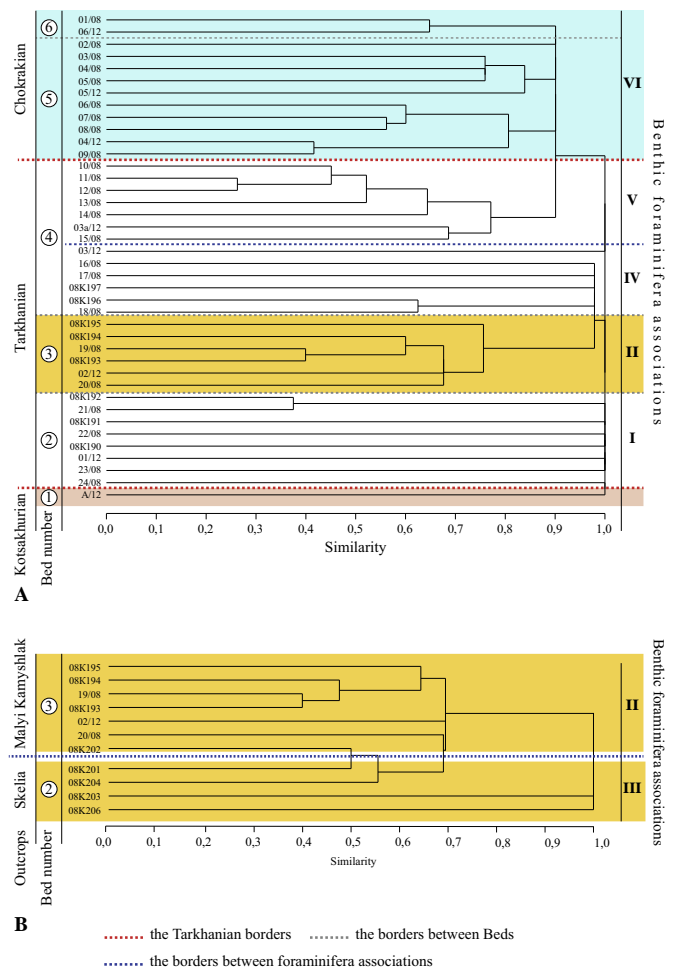


**Fig. 7.** Results of Cluster Analysis (Bray-Curtis Similarity Index, Paired group) benthic foraminiferal associations from the Tarkhanian – lower part of the Chokrakian of the Malyy Kamyshlak (A) and comparison of the middle part of the Tarkhanian deposits of Malyy Kamyshlak and Skelia sections (B) sections.

uppermost part of the deposits with this foraminifera association). The upper part of Bed 4 (from sample 15/08 to sample 10/08) is represented by the *Nonion-Quinqueloculina* association (V, see above) which consists of 25 species from 16 genera (Appendix Fig. A1 and Supplementary Fig. S5). It is characterized by higher species diversity compared with association IV (6–19 taxa per sample), the numbers of tests are 15–248 per sample. As before, all tests have small sizes and sometimes corroded and broken walls. The dominant species are *Nonion commune* and *Quinqueloculina akneriana*. Accompanying species are *Triloculina gubkini*, *Sigmoilina mediterraneensis*, *Bolivina crenulata* and *Ammonia tepida*.

**4.1.2.5. Lower Chokrakian.** All samples from Beds 5 and 6 of the Malyy Kamyshlak section (Fig. 4) comprised different numbers of planktic foraminifera: small 4-chambers *Globigerina* (3–457 tests per sample) and small 5-chambers *Globigerina* (1–403 tests per sample) (Appendix Fig. A1). In addition, Beds 5 and 6 yielded the *Bolivina-Nonion-Quinqueloculina* association (VI, see above), which is a relatively heterogeneous association consisting of 35 species from 16 genera (Appendix Fig. A1 and Supplementary Fig. S5). Species diversity ranges between 2 and 21 taxa per sample, numbers of tests are 11–1081 per sample. Big-sized, well preserved tests occur in the lower part of Bed 5, while well preserved tests of small size occur in the upper part of Bed 5 and in the lower part of Bed 6. There is a change of dominant and accompanying species (see Appendix Fig. A1): *Bolivina tarchanensis*, *Nonion commune*,

*Quinqueloculina akneriana* (normal and abnormal forms), *Q. akneriana* subsp. *longa* change from the dominant to accompanying levels several times upsection. *Sigmoilina haidingerii* var. *tschokrakensis* and *Ammonia tepida* occur as additional to accompanying species in the middle part of this interval.

#### 4.2. Calcareous nannofossil assemblages

From 27 analysed samples, 14 were analysed quantitatively, 4 did not contain calcareous nannofossils, while 9 samples could not be analysed quantitatively with only presence-absence data for the individual taxa (Appendix Fig. A3 and Supplementary Figs. S2, S7, and S8). Generally, the calcareous nannofossil assemblages are rare and contain high ratios of reworked specimens from the Oligocene, Eocene and Cretaceous. The abundance and diversity of autochthonous nannofossils varied; the highest diversity and abundance were recorded in the uppermost lower Tarkhanian (uppermost part of Bed 2), the middle and upper Tarkhanian (Beds 3, 4) and the lowermost Chokrakian (Bed 5) (Appendix Fig. A3A). *Coccolithus pelagicus*, *Sphenolithus* sp. and *Reticulofenestra* sp. dominate in the autochthonous assemblages. Other common taxa are *Helicosphaera* sp. and *Cyclicargolithus floridanus* (Appendix Fig. A3C). Relative abundances of redeposited Cretaceous nannofossils decrease upward the section, and are replaced by reworked Paleogene taxa (Appendix Fig. A3B).

Due to scarcity of calcareous nannofossils, statistical analysis using quantitative data was possible only for 14 quantitatively analysed samples. PCA enables to distinguish three type assemblages: (1) *Coccolithus pelagicus* assemblage prevailing in the middle Tarkhanian; (2) *Sphenolithus* spp. assemblage occurring mainly in the lower Tarkhanian and the lower Chokrakian; (3) an assemblage dominated by reworked taxa and *Reticulofenestra* in the upper Tarkhanian and the lower Chokrakian (Fig. 8).

#### 4.3. Molluscs

Molluscs were not found in Bed 1 (upper Kotsakhurian) of the Malyy Kamyslyak section. Bed 2, Malyy Kamyslyak section (lower Tarkhanian) comprised only several small, thin-walled shells of *Limacina tarchanensis* (Kittl). Bed 3 of the Malyy Kamyslyak section (middle Tarkhanian) contained both whole and broken shells of the following species: *Abra parabilis* (Zhizhchenko), *Nucula (Nucula) nucleus* (Linne), *Nuculana (Saccella) subfragilis* (Hoernes), *Lentipeecten corneus denudatus* (Reuss), *Modiolus* sp., *Limacina tarchanensis* (Kittl). Bed 2 of the Skelia section comprised whole and broken shells of *Abra parabilis* (Zhizhchenko), *Nuculana (Saccella) subfragilis* (Hoernes), and *Corbula (Varicorbula) gibba* (Oliv). In addition, shells congestion of *Neopycnodonte cochlear* (Poli) formed oyster banks (Fig. 5). Bed 4 of the Malyy Kamyslyak section (upper Tarkhanian) comprised a few small, thin-walled shells of *Limacina tarchanensis* (Kittl), and Beds 5 and 6 of the Malyy Kamyslyak section (lower Chokrakian) yielded different numbers of small, thin-walled shells of *Limacina tarchanensis* (Kittl).

#### 4.4. Fish otoliths

Almost all fish otoliths were very small in size, indicating the presence of juvenile or even larval specimens. Three fish species could be identified. Most abundant is *Vinciguerria merklini* Daniktschenko, 1946 (family Phosichthyidae Weitzman, 1974, order Stomiiformes), which is present in Beds 3 to 5 (middle Tarkhanian to lower Chokrakian) of the Malyy Kamyslyak section. The characteristics of the otoliths of *V. merklini* include a rounded to trapezoid shape, a short rostrum (mostly broken in our material), and a sulcus with a thin but clear collum between ostium and cauda. The cauda is slightly wider than the ostium and can be subdivided into a deepened anterior part and a shallow posterior portion; the curvature of the crista superior is slightly convex (Plate 5, d–f). All characteristics conform very well to those of the otoliths

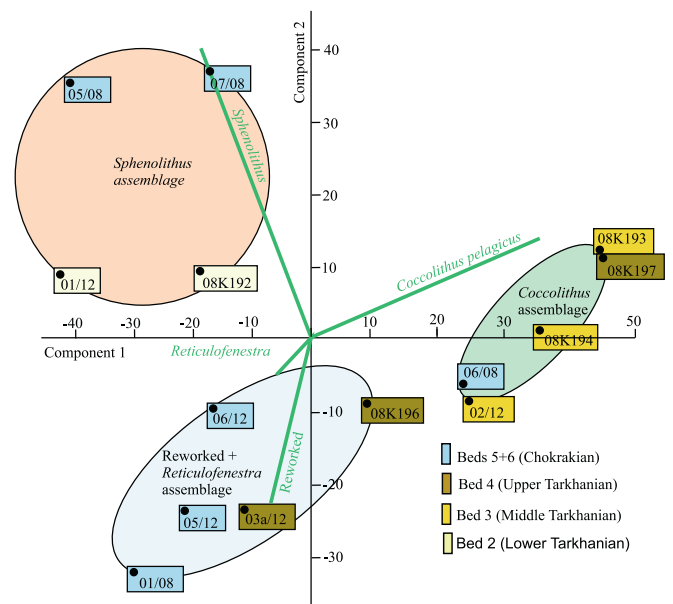


Fig. 8. Classification of nannofossil assemblages using the PCA. Coordinates 1 and 2 capture 94.5% of the variation.

preserved in situ in skeletal material of *V. merklini* of a previous collection at the Malyy Kamyslyak section from the same strata (Bannikov and Parin, 1997; Bannikov, 2010) (Plate 5, a–c). Furthermore, two small otoliths from the middle Tarkhanian (Bed 3) are tentatively identified as *Gonostoma? cyclomorphum* (Weiler, 1950) (family Gonostomatidae Cocco, 1838). Different taxonomic interpretations of this otolith-based species were proposed in previous works as *Argentina cyclomorpha* in Weiler (1950), ‘Gonostomatida’ *cyclomorpha* in Nolf (2013), or *Gonostoma? cyclomorphum* in Schwarzhans (2017). This species is known from the lower Badenian of Romania (Weiler, 1950) and the Tarkhanian of Bulgaria (Schwarzhans, 2017). A possible junior synonym of *G.? cyclomorphum* is “Otol. (inc. sed.) *rostratus* Pobedina, 1954” from the Tarkhanian (Strashimirov, 1972). The third species in our samples is tentatively referred to the genus *Aphia* Risso, 1827 (family Gobiidae Cuvier, 1816, order Gobiiformes) (Plate 5, g, h). It is represented with one specimen each in the middle and upper Tarkhanian (Beds 3 and 4). It can be recognized as a member of the Gobiidae based on the ‘shoe-sole-shaped’ sulcus that is typical for the family, and as a possible representative of *Aphia* based on its rounded shape, a slight shift of the sulcus towards the anterior margin, and a relatively long ostium, but short cauda (La Mesa, 1999). Otoliths of *Aphia* are relatively common in the Middle Miocene of the Central and Eastern Paratethys (e.g. Bratishko et al., 2015; Schwarzhans et al., 2020).

#### 4.5. Palynological data

##### 4.5.1. Vegetation types

A total of 108 taxa (Supplementary Fig. S3) were determined in the Malyy Kamyslyak section (28 herbs and dwarf shrubs, and 11 peritridophytes taxa). They belong to the lower and upper Tarkhanian and lower Chokrakian. Sediments from the middle Tarkhanian were not suitable for palynological studies. To interpret the vegetation composition, plant taxa were grouped according to their ecological and environmental requirements (Appendix Fig. A4a). Two principal vegetation types according to Kvaček et al. (2006), Kovar-Eder et al. (2008a, b 2018) and Teodoridis et al. (2011a, 2011b) could be recognized:

1. Ecotone Mixed-Mesophytic Forest/Broad – leaved evergreen forest.
2. Xeric grasslands or steppe.

In the lower Tarkhanian of the Malyy Kamyslyak section, the Mixed-



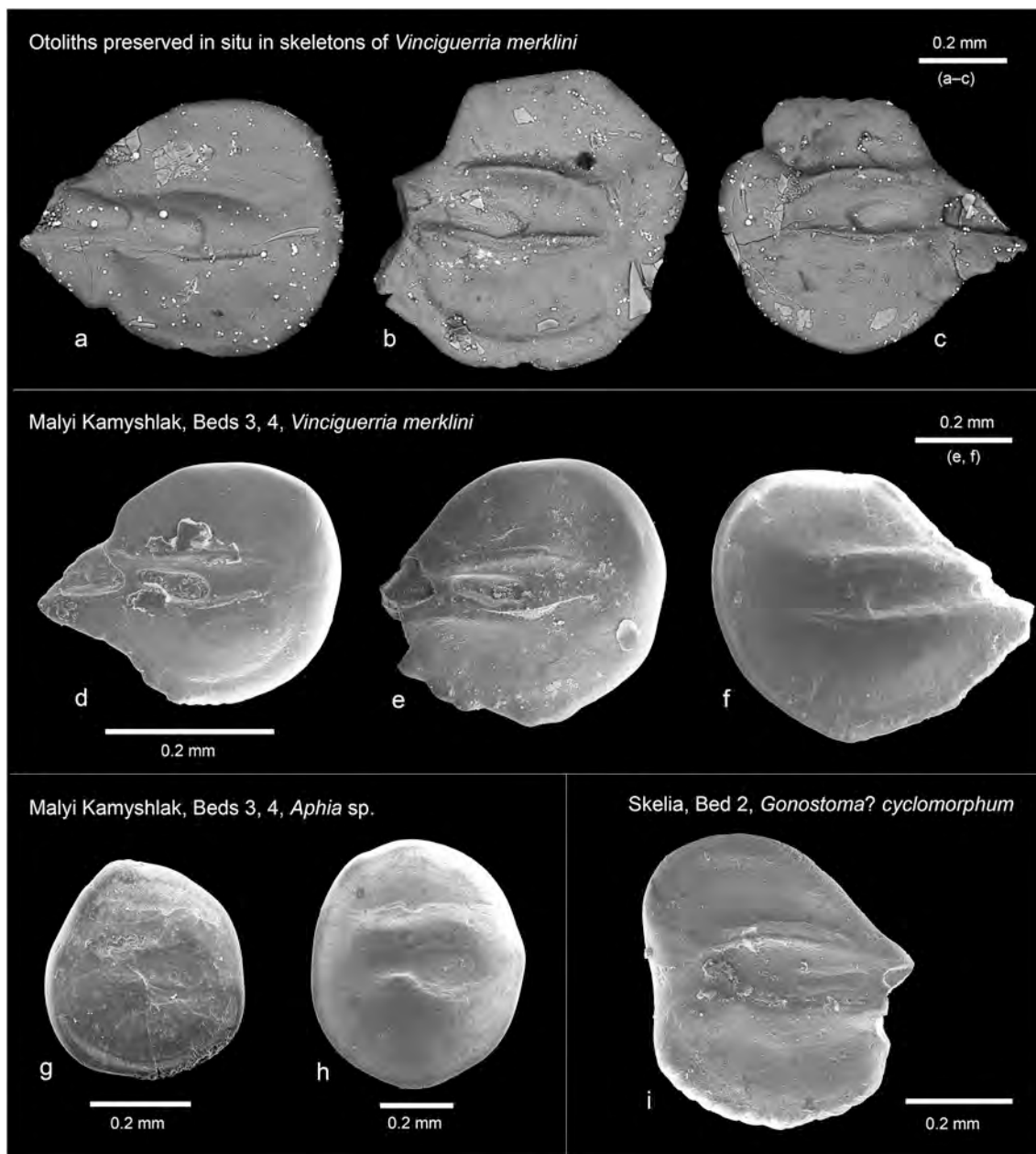


**Plate 5.** Explanation Otolith Figure:

A – c: Otoliths preserved in situ in three skeletons of *Vinciguerria merklini* from the Malyi Kamyshlak outcrop (collection in Moscow, photos by courtesy of A. Bannikov).

D – i: Isolated otoliths from Bed 3 (d, e, g) and Bed 4 (f, h) of the Malyi Kamyshlak outcrop and from Bed 2 (i) of the Skelia outcrop.

Mesophytic Forest/Broad – leaved evergreen forest with share of coastal swamp forest is dominant. In the upper Tarkhanian and lower Chokrakian of the Malyi Kamyshlak section its extent decreased and elements of xeric grasslands or steppe increased.

Zonal assemblages of Mixed-Mesophytic Forest/Broad – leaved evergreen forest are characterized by thermophylous/palaetropical elements (14–31%) such as Sapotaceae, Palmae, *Engelhardia*, *Platycarya*, evergreen Fagaceae (represented in pollen spectra by morpho-species *Quercoidites henrici*, *Quercoidites microhenrici*), *Trigonobalanopsis*, *Tricolpopollenites liblarensis*, Araliaceae, *Symplocos*, *Reevesia*, *Cornus-Mastixia*, Rutaceae, Styracaceae, *Parthenocissus*, Verbenaceae, and ferns *Lygodium*, Gleicheniaceae, Pteridaceae. The highest proportion of thermophylous elements was recorded in the lower Tarkhanian interval (Fig. 9; Plate 6; Appendix Fig. A4a).

Deciduous woody elements/arctotertiary (5–11%) comprise: *Quercus*, *Carpinus*, *Carya*, *Juglans*, *Tilia*, *Betula*, *Zelkova* and *Eucommia*.

The proportions of azonal communities such as coastal swamp (Taxodiaceae, Cyrillaceae, Myricaceae, *Decodon*) and deciduous riparian forest (*Alnus*, *Salix*, *Ulmus*, *Fraxinus*, *Liquidambar*, *Pterocarya*) were highest in the lower Tarkhanian. Their share decreases towards the younger parts of the profile (upper Tarkhanian and Chokrakian) steadily, with slight cyclical fluctuations.

Vegetation of open areas and insolated places (*Olea*, *Celtis*, *Buxus*, Rosaceae, *Ephedra*, Poaceae, Caryophyllaceae, Asteraceae, *Artemisia*, *Salvia*), including coastal salt marshes (Chenopodiaceae/*Salicornia* with Caryophyllaceae, *Armeria*, Daucaceae) (< 5% in the lower Tarkhanian, > 30% in the uppermost three samples of the Chokrakian) formed a significant component of vegetation (Fig. 9; Plate 6; Appendix Fig. A4a).

On the other hand, heliophilic shrubs, dwarf shrubs and herbs in wetland to aquatic habitats (*Ericaceae*, *Ilex*, *Ranunculaceae*, *Cyperaceae*, *Potamogeton*, *Sparganium* and unique *Pediastrum*) were more abundant in lower Tarkhanian sediments.

Extrazonal mountain elements such as *Cedrus* and *Picea* were very rare (negligible percentage). Conifer components (*Pinaceae* including *Cathaya*) complements the vegetation, being mostly at 10–15% and > 20% only in two samples (Fig. 9; Appendix Fig. A4a). The abundance of pollen found in clumps (*Chenopodiaceae*, *Caryophyllaceae*, *Poaceae*, *Decodon*) supports the assumption of low water dynamics and points to a short transport to the sedimentation area. Marine dinoflagellates (all samples), green algae such as *Prasinophyceae* and *Botryococcus* (MK 11, 23, 24), unique *Pediastrum* (MK 24), plant tissues, fungi (MK 1), amount of small medium to dark brown phytoclasts, are also present. Alterations in palynomorphs in forms of cubic caves caused by the crystallization of pyrite under anoxic or dysoxic conditions were observed in two samples (MK17, MK 9).

4.5.2. Coexistence approach, plant functional types (PFTs)

The reconstructed PFT diversity data show some variability that may also reflect sedimentary facies changes. Herbaceous diversity (PFTs 1–3) accounts for ca. 15–35% of total diversity and displays short-term variability. Highest diversities are recorded in the uppermost Tarkhanian (depth level 25.8 m) and at depth levels 31 m and 43 m of the Chokrakian. Aquatics are mainly present in the Tarkhanian where they may account for ca. 10% of total diversity. Arboreal diversity (Fig. 9; Appendix Fig. A4b; Supplementary Fig. S3) displays less variability among the samples, with conifer PFTs ranging from ca.15–30% of the total diversity, broadleaved evergreen components ca. 20–30%, broadleaved deciduous components at 30–45%, and tropical evergreen and rainingreen PFTs attaining ca. 8–15%. PFT 18 representing coastal swamp trees is present throughout the record.

Several indices are calculated to support the interpretation of the PFT spectra (Appendix Fig. A4b). The conifer/non-conifer ratio shows a relatively stable increasing upwards. The broadleaved evergreen/broadleaved deciduous ratio and the warm/cool woody PFTs indices, both potentially reflecting a climate signal, first show a steady decline up to 19.67 m and thereafter an increasing trend culminating at 34 m, followed by a poited decline towards the top. The dry/wet trees index has a considerable variability but may hide an overall increasing trend (Appendix Fig. A4b). The ratio of herbs and shrubs by trees is likewise highly variable, while the Chokrakian samples tend to have higher

values.

The reconstructed temperature records (Appendix Fig. A4a) show cyclical changes in the Tarkhanian, and a trend of moderate, gradual cooling in the Chokrakian. In the Tarkhanian CMTmin values mostly exceeded 10°C (means = 11°C), while in the Chokrakian CMTmin values dropped to 5°C (means <10°C). With MAT means mostly between 15 and 20°C, climate remained warm and temperate. With WMT means of ca. 24°C near the base to 27°C at the top of the section an increase in seasonality is evident, setting on in the latest Tarkhanian (Appendix Fig. A4a). The mean annual range of temperature (MART) is an important variable for estimating continentality of climate (MART = WMTmean – CMTmean). Range of MART lower than 15°C means more equable-temperature conditions throughout the year, while that of >15°C indicates higher climate continentality. In the Tarkhanian, some variability is visible (MART ~12–17°C), while in the Chokrakian a MART >15°C is pointing to higher continentality of climate.

Precipitation values also show higher variability in the Tarkhanian with drier intervals (MAP, MPwet) at 19.3–20.4 m and 25.8 m, respectively. Interval of mean annual precipitation (MAP) range from ~1000–1600 mm (with one exception), mean precipitation of the wettest month (MPwet) ~190–260 mm, mean precipitation of the driest month (MPdry) ~20–40 mm, mean precipitation of the warmest month (MPwarm) ~110–175 mm. These results point to a distinct seasonality in precipitation with the driest month not in the warmest season. The ratio of MPwarm on MAP is an important measure to estimate possible drought during summer. According to the results, summers were most humid at 19.67 m where MPwarm accounted for ca. 16% of annual rainfall. Thereafter, there was a step-wise decline to values around 9% as found in the Chokrakian samples (Appendix Fig. A4a).

4.6. Geochemistry

4.6.1. Stable oxygen and carbon isotopes

The foraminiferal oxygen isotope values vary from –0.78 to 0.90‰ for benthic specimens and from –7.98 to –3.90‰ for planktic taxa. δ<sup>18</sup>O values for the benthic foraminifera *Nonion commune* are comparable for the Chokrakian and Tarkhanian, whereas planktic δ<sup>18</sup>O values for the Chokrakian are higher than those of the Tarkhanian. Notably, δ<sup>18</sup>O values for benthic and planktic taxa are clearly different across the whole studied interval, although in the Chokrakian this difference slightly decreased (Fig. 10A). The very low values obtained from the planktic foraminifera raise concerns that these materials are

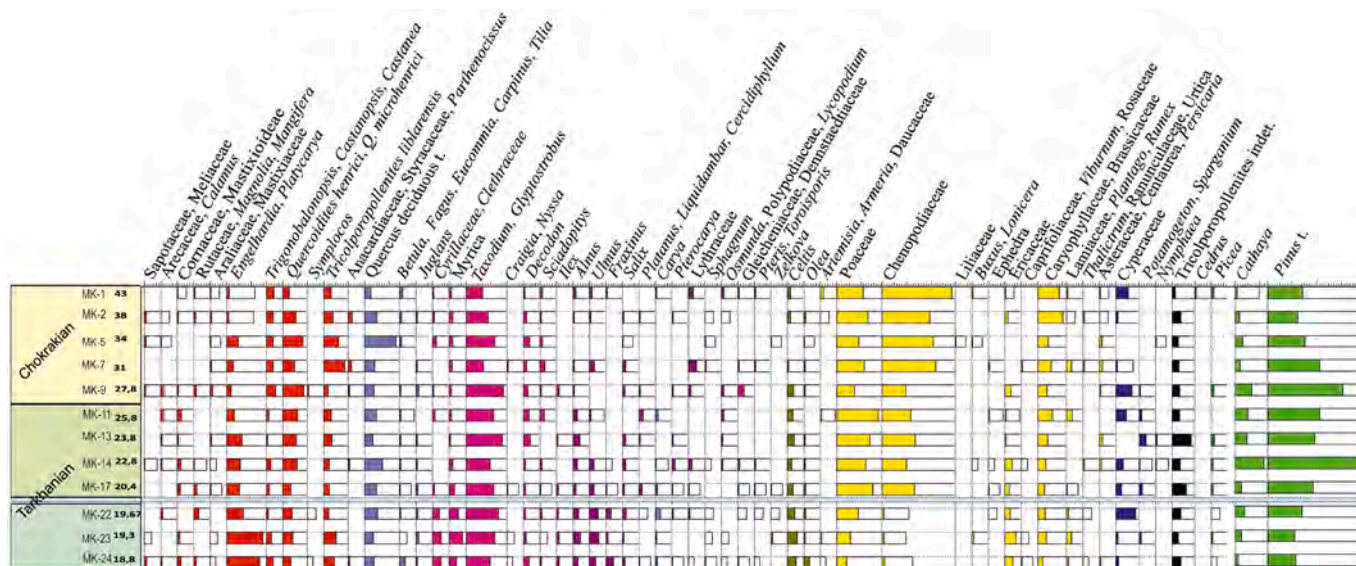
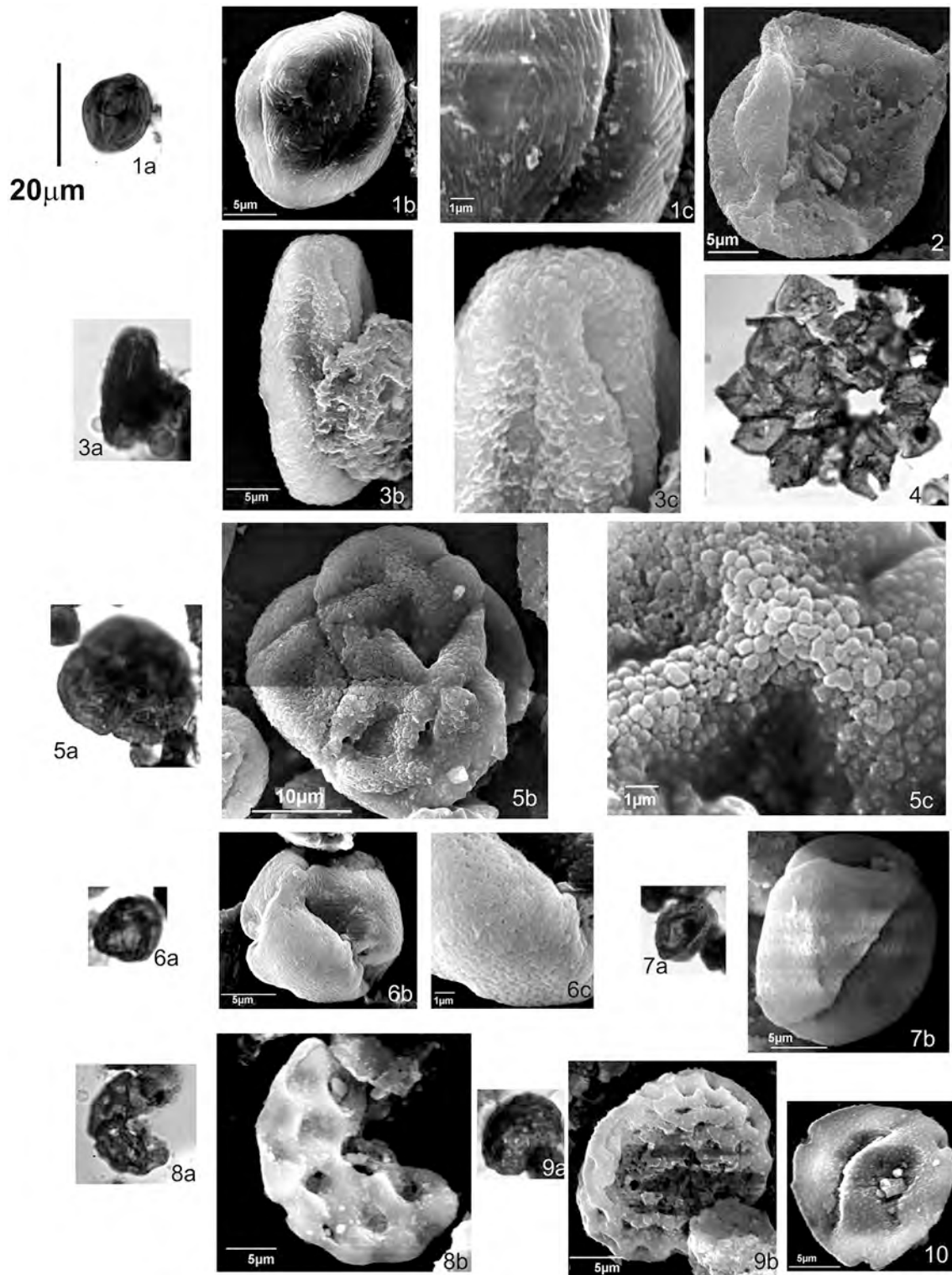


Fig. 9. Classic pollen diagram – percentage of determined taxa in Malyi Kamyshlak section.



**Plate 6.** Palynomorphs from Malyi Kamyshlak:

- 1 – Rosaceae, *Prunus* type; a – LM 1000×, b,c – SEM, MK-3.
- 2 – Cyperaceae ge.indet – SEM, MK-24.
- 3 – *Tricolpopollenites henrici* – *Quercus* sp. lobatae type; a – LM 1000×, b,c – SEM, MK-3.
- 4 – *Pedastrium* sp. – LM 1000×, MK-24.
- 5 – *Erica* sp. a – LM 1000×, b,c – SEM, MK-24.
- 6, 7 – Vitaceae gen indet; 6a,7a – LM 1000×, 6b,c, 7b – SEM, MK-24.
- 8 – Caryophyllaceae gen indet; a – LM 1000×, b – SEM, MK-3.
- 9a,b – Chenopodiaceae gen. Indet; a - LM 1000×, b – SEM, MK-3.
- 10 – *Platycarya* sp. – SEM, MK-24.



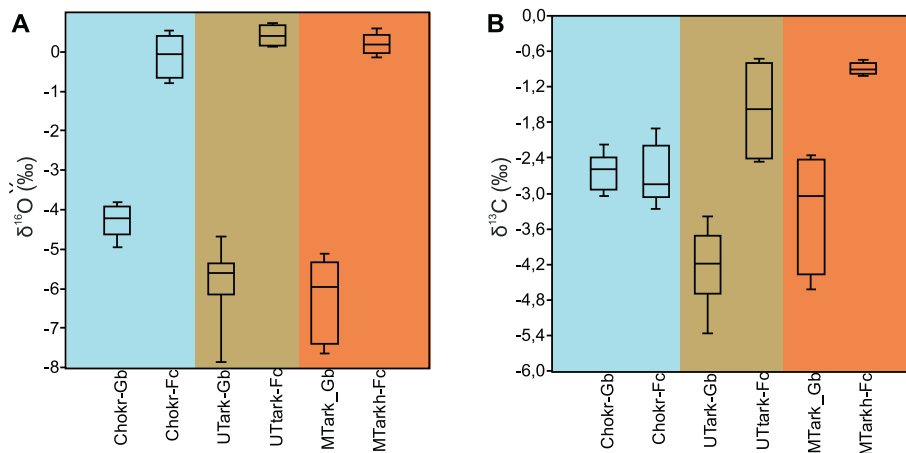


**Fig. 10.** Range of oxygen (A) and carbon (B) stable isotopic values obtained from tests of planktic *Globigerina bulloides* (Gb) and benthic *Nonion commune* (Fc) for Chokrakian (Chokr), upper Tarkhanian (UTark) and middle Tarkhanian (MTark).

**Table 1**

Strontium isotope values from the middle Tarkhanian (Bed 2, Skelia section – sample 08 K201, 08 K202, Bed 3, Maliy Kamyshlak section – sample 08 K195).  $^{87}\text{Sr}/^{86}\text{Sr}$  values were converted into numerical ages using the regression curve LOWESS look-up Table version 6 (McArthur et al., 2020).

Sample	Analysed material	$^{87}\text{Sr}/^{86}\text{Sr}$	2SE	Maximum age (Ma)	Mean age (Ma)	Minimum age (Ma)
MiKam 08 K195	Otolith	0.708751	0.000008	15.99	15.86	15.72
Skelia 08 K201	<i>Ostrea cochlea</i>	0.708759	0.000011	15.92	15.73	15.51
Skelia 08 K201	<i>Nonion commune</i>	0.708764	0.000010	15.82	15.63	15.42
Skelia 08 K202	<i>Ostrea cochlea</i>	0.708731	0.000009	16.32	16.18	16.04
Skelia 08 K202	<i>Nonion commune</i>	0.708766	0.000018	15.92	15.59	15.14

diagenetically affected. However, their internal test walls as well as dissections were carefully checked using SEM and revealed excellent preservation following Pearson and Burgess (2008) and Pearson (2012). For the analysis only empty tests were used. This, together with clearly different isotopic values for planktic and benthic foraminifera from the same sample, minimizes these doubts on diagenetic alteration.

The carbon isotope values for planktic foraminifera vary from  $-5.37$  to  $-2.18$ ‰, the values for the Chokrakian samples are higher than those from the Tarkhanian.  $\delta^{13}\text{C}$  values for benthic foraminifera vary from  $-3.26$  to  $-0.75$ ‰ and they decreased from the middle Tarkhanian to the Chokrakian. While the Tarkhanian  $\delta^{13}\text{C}$  values for benthos and plankton differ, the Chokrakian  $\delta^{13}\text{C}$  values are similar (Fig. 10B).

#### 4.6.2. Strontium isotope data

Five strontium isotope ( $^{87}\text{Sr}/^{86}\text{Sr}$ ) values were obtained based on fossils from the middle Tarkhanian of the Skelia (four values) and Mali Kamyshlak (1 value) sections. The sampled fossils were two shells of a benthic bivalve (*Ostrea cochlea* Poli), two tests of the infaunal foraminifera *Nonion commune*, and an otolith (1 value) (Table 1 and Fig. 11).

Including the statistical uncertainty ( $2\sigma$ ) of the strontium isotope results (Table 1), the chemostratigraphical data from the five studied samples provide an age range of 16.3–15.1 Ma (Fig. 11). Notably, the 16.3 Ma maximum age data point (sample 08 K202, *Ostrea cochlea*) is 0.3 Ma older than all other maximum ages obtained (Fig. 11; Table 1). As *Ostrea cochlea* is the index species of the middle Tarkhanian (it is not present in the lower Tarkhanian), its 16.3 Ma age could represent older middle Tarkhanian sediments from which it was reworked. Because it is a single value, we exclude it from our further discussion. Accordingly, SIS indicates an age range of 16.0–15.1 Ma for the middle Tarkhanian.

## 5. Interpretation and discussion

### 5.1. Age model

Here we use our new plankton data from the Mali Kamyshlak section, previously published nanofossil data from the same section, and the SIS results to propose a new age model for the Tarkhanian and lower Chokrakian. In the context of nanofossil biostratigraphy it must be noted that determination of First Occurrence (FOs) and Last Occurrence (LOs) may not always be precise because index species were rare.

No biostratigraphically informative nanofossil species were obtained from the lower Tarkhanian and the Chokrakian. In contrast, the middle and lowermost upper Tarkhanian yielded the index species *Helicosphaera waltrans* (FO 15.47 Ma, Iaccarino et al., 2011) (Supplementary Fig. S7). Also, the index species *Helicosphaera ampliiperta* (LO 14.8 Ma, Raffi et al., 2020) is present in these strata (see Studencka et al., 1998 and references cited therein). The lowermost upper Tarkhanian additionally contained the index species *Sphenolithus heteromorphus* (FO 18.0 Ma, LO 13.5 Ma; Young, 1994) (Supplementary Fig. S7). Furthermore, the absence of the planktic foraminifera *Praeorbulina* and *Orbulina* in the Chokrakian can be used as an additional age constraint because these taxa are common in Paratethys sediments younger than 14.6 Ma (Holcová et al., 2019). Taking the biostratigraphic evidence together, the middle and upper Tarkhanian and the lowermost Chokrakian range from 15.47 to 14.6 Ma.

Excluding the single 16.3 Ma maximum age value (see above), our SIS data indicate an age of 16.0–15.1 Ma for the middle Tarkhanian (Table 1), which is slightly older than that the biostratigraphic data suggest. A possible reason could be that riverine inflow has produced a local  $^{87}\text{Sr}/^{86}\text{Sr}$  signal in the middle Tarkhanian sea. This assumption is

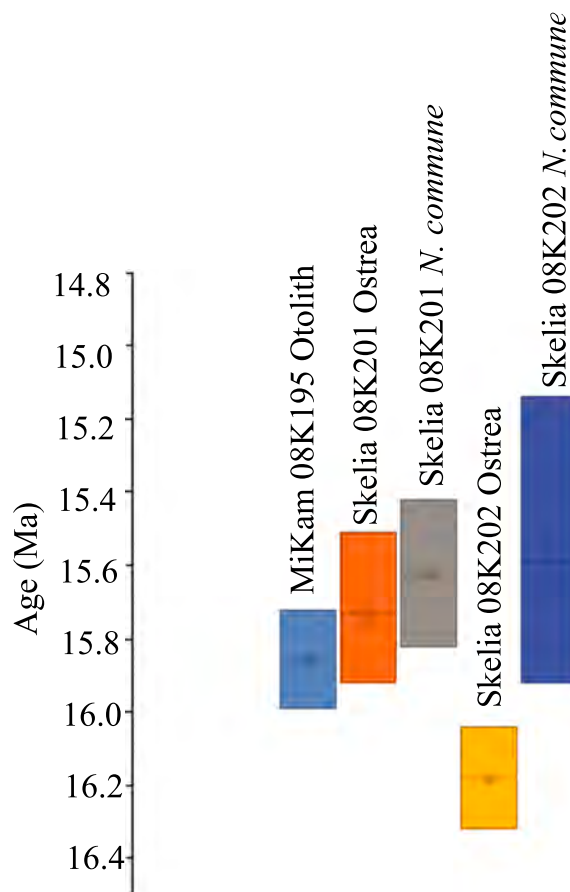


**Fig. 11.** Numerical ages of the middle Tarkhanian samples using SIS (Strontium Isotope Stratigraphy).  $^{87}\text{Sr}/^{86}\text{Sr}$  values were converted into numerical ages using the regression curve LOWESS look-up Table version 6 (McArthur et al., 2020). Crosses indicate mean ages; rectangles indicate the ranges of age including  $\pm 2\text{SE}$ .

supported by abundant presence of euryhaline bivalves (oysters) and by low oxygen values of planktic foraminifera (Fig. 10). That the riverine influx has led to 'too old' ages could be explained by a provenance area comprising pre-Middle Miocene carbonate rocks (Benito et al., 2020). An alternative explanation could be that the oyster banks of the middle Tarkhanian represent a slightly older time span than the oceanic water carrying nannofossils, and that slightly older oysters and benthic foraminifera co-occur with slightly younger nannofossil species due to low sedimentation rates and time averaging.

In conclusion, taking biostratigraphic and SIS data together, it can be assumed that the lower Tarkhanian is older than ~15.5 Ma (or even older than ~16.0 Ma), that the middle Tarkhanian ranges from ~15.5–15.1 Ma, and that the upper Tarkhanian and lowermost Chokrakian are 15.1–14.6 Ma old (Fig. 12). For the Tarkhanian-Chokrakian boundary, radiometric dating of ~14.75 Ma is available from the section Belaya (Palcu et al., 2019), and this age fits well with our model. For the entire Tarkhanian, however, Palcu et al. (2019) had proposed a very short duration (~14.85–14.75 Ma, magnetochron C5Bn.1n), but they also noted that a large part of the measured succession was disturbed by a massive olistostrome and slumps. In our model, both biostratigraphic and SIS data suggest a considerably longer duration of the Tarkhanian (>15.5 (16.0?)–14.75 Ma) (Fig. 12). Moreover, this new age model makes it plausible that the middle Tarkhanian flooding of the Eastern Paratethys can be correlated to the global sea level high-stand of sequence Bur 5/Lan 1 at ~15.2 Ma (Hilgen et al., 2012). Accordingly, the Middle Miocene flooding of the Eastern Paratethys occurred more or less simultaneously with the globally recognizable maximum

transgression of the Miocene (Haq and Schutter, 2008).

## 5.2. Reconstructions of the marine environments

### 5.2.1. Late Kotsakhurian (late Burdigalian – see Fig. 12) (Bed 1 at Malyi Kamyshtak)

In the Kotsakhurian, the Eastern Paratethys was isolated from the open ocean and presumably had only a limited connection to the Central Paratethys (Popov et al., 1993; Palcu et al., 2019). According to Merklin (1950), the study area was characterized by an open sea in the late Kotsakhurian, poor oxygenation of the bottom waters and short periods of hydrogen sulfide contamination. Harsh bottom water conditions for the biota are reflected by the presence of a monospecific assemblage of the agglutinating foraminifer *Saccamina zuramakensis* Bogdanowicz (e.g. Bogdanovich, 1965; Bogdanovich, 1971; Muratov and Nevevskaya, 1986). In our study, only three planktic foraminifera tests of *Globigerina* were found in the Kotsakhurian samples.

### 5.2.2. Early Tarkhanian (early Langhian) (Bed 2 at Malyi Kamyshtak, Bed 1 at Skelia)

In the early Tarkhanian (early Langhian), the Eastern Paratethys was characterized by a transgression and the occurrence of a new benthic biota (molluscs, foraminifera, ostracods) (e.g. Goncharova, 1989; Goncharova et al., 2001). The foraminifera species composition changed significantly and the monospecific assemblage of agglutinating *Saccamina zuramakensis* of the Kotsakhurian is replaced by a new, albeit still depleted assemblage of calcareous foraminifera (e.g. Archangelsky, 1940; Bogdanovich, 1965; Bogdanovich, 1971; Muratov and Nevevskaya, 1986; Vernyhorova and Ryabokon, 2020). It has been proposed that the new fauna had migrated through different straits from the Central Paratethys and the Indian Ocean to the Eastern Paratethys (Goncharova, 1989; Rögl, 1998, 1999, 2001; Goncharova et al., 2001; Popov et al., 2009, 2019; Palcu et al., 2019). Our data reveal the appearance of new benthic foraminifera (association I) and the prevalence of non-endemic species (Figs. 13 and 14), and thus confirm the open connection of the Eastern Paratethys with the surrounding marine basins.

According to previous works, deep-water environments of 200–400 m depth (pseudoabyssal zone, according to Derjugin, 1915; Derjugin, 1928; Andriyashvili, 1979) existed in the area of the Kerch and Taman Peninsulas at the beginning of the Tarkhanian (Goncharova, 1989; Goncharova et al., 2001; Palcu et al., 2019; Popov et al., 2019). The small numbers of molluscs and foraminifera have led to the assumption that oxygen exchange in the bottom water was still insufficient in the early Tarkhanian and caused a slow colonization of the sea floor (Goncharova, 1989; Goncharova et al., 2001).

Our new foraminifera data from Malyi Kamyshtak (Bed 2) and Skelia (Bed 1) clearly show that the early Tarkhanian Basin of the study area (Fig. 14) was part of the upper sublittoral zone (after Hedgpeth, 1957; Longhurst, 2007), rather than the pseudoabyssal zone (see below). The characteristic benthic foraminifera are represented by the *Quinqueloculina* association (I), which are shallow-water taxa (inner shelf; upper sublittoral zone) of the photic zone (predominance of herbivore species of *Quinqueloculina*, *Nonion*, *Ammonia* (?), see Murray, 2006), and possibly was resistant to some salinity fluctuations. A relatively shallow environment is additionally confirmed by the calcareous nannofossil species *Sphenolithus moriformis* (Perch-Nielsen, 1985; Andreyeva-Grigorovich, 2002; Ćorić and Hohenegger, 2008). Rare finds of shells of the pteropod *Limacina tarchanensis* (Kittl) do not contradict these assumptions (e.g. Davitashvili and Merklin, 1968).

As proposed earlier (Goncharova, 1989; Goncharova et al., 2001), deoxygenation in the bottom water is also seen in our data because epibenthic foraminifera, despite of their predominance in assemblage I, have small sizes and low abundance (suboxic A, after Kaiho, 1994) (Figs. 13 and 14; Appendix Fig. A1; Supplementary Fig. S5). Poor bottom water oxygenation might point to high nutrient availability and

enhanced bioproductivity in the surface water, but this cannot be unambiguously resolved with the data at hand. Dominance of sphenoliths in the early Tarkhanian calcareous nannofossil assemblages seems to indicate oligotrophic conditions (Young, 1994; Aubry, 1989; Bralower, 2002). However, *Sphenolithus moriformis*, which is dominant in the samples, is known as a specific representative of *Sphenolithus* which can survive also in eutrophic conditions (Wei and Wise, 1990; Agnini et al., 2007; Toffanin et al., 2011).

Our SIS age data indicate that the early Tarkhanian transgression can be related to the early Langhian sea level rise (megacycle Bur5/Lan1) and initial phase of the MCO (Figs. 12 and 14). Warm climate of mainly subtropical conditions, as can be assumed for the initial stage of the MCO, is supported by the dominance of sphenoliths (*Sphenolithus* spp.) in the calcareous nannofossil assemblage indicating warm-water conditions (Rio et al., 1990; Young, 1994; Aubry, 1989; Bralower, 2002).

5.2.3. Middle Tarkhanian (early Langhian – see Fig. 12) (Bed 3 at Malyi Kamyshlak, Bed 2 at Skelia)

In the middle Tarkhanian (early Langhian), the Eastern Paratethys retained its connections with the open ocean through the Central Paratethys and, possibly, the Indian Ocean (Goncharova, 1989; Goncharova et al., 2001) (Fig. 14). This is reinforced by our results based on the benthic foraminifera. The presence of a high percentage of cosmopolitan species, compared to the early Tarkhanian, and the predominance of non-endemic benthic foraminifera species (up to 80% in some samples of associations II, III – see Fig. 13A and B) clearly indicate open connections with the surrounding ocean basins.

The middle Tarkhanian is known to be characterized by a distinctive change in the benthic species composition (molluscs, foraminifera, ostracods) in many areas of the Eastern Paratethys (e.g. Archangelsky, 1940; Ananiashvili, 1985; Muratov and Nevesskaya, 1986; Nevesskaya et al., 1984, 2003). Likewise, our new data from Malyi Kamyshlak revealed a significant change in the genus and species composition of benthic foraminifera (Figs. 6, 7A, 13, and 14; Appendix Fig. A1; Supplementary Fig. S5). However, there is currently no agreement what has

caused the middle Tarkhanian biotic turnover. One possibility could be a change in water depth. Merklin (1950), who studied the mollusc assemblages, suggested that the middle Tarkhanian on the Kerch Peninsula represented the pseudoabyssal zone (after Derjugin, 1915, 1928; Andriyashev, 1979), whereas Goncharova (1989) and Goncharova et al. (2001), also based on molluscs, assumed that the area of the Kerch Peninsula was shoaling from the pseudoabyssal to the lower sublittoral.

The combination of our new foraminifera and fish data and previous mollusc data (Davitashvili and Merklin, 1966) supports the assumption that the middle Tarkhanian Basin of the Kerch Peninsula was part of the lower sublittoral, photic zone (after Hedgpeth, 1957; Longhurst, 2007) (see below). However, a shoaling during the middle Tarkhanian, as proposed by Goncharova (1989) and Goncharova et al. (2001), cannot be confirmed. Among the benthic foraminifera, species of *Globulina*, *Guttulina*, *Pseudopolymorphina*, *Fissurina*, and *Cassidulina* clearly indicate that the water depth in the study area had increased in comparison with the early Tarkhanian. A rather deep environment, most likely close to the outer shelf, is also supported by the occurrence of fish otoliths of the pelagic genera *Vinciguerria* (Phosichthyidae) and *Aphia* (Gobiidae) in the middle Tarkhanian samples. Today, *Vinciguerria* is abundantly present in all temperate, subtropical and tropical oceans (Nelson et al., 2016), where it undergoes daily migrations, with a usual 250–600 m depth range during daytime and a 50–500 m depth range during the night (Gradianu et al., 2020 and references cited therein). *Aphia* is a common element of the modern gobiid fauna of the Mediterranean Sea, Azov and Black Sea (La Mesa et al., 2005). The striking absence of otoliths of benthic gobiids, which mostly need water depth shallower than 80–100 m (Miller, 1986), reinforces the assumption of relatively deep water.

A further notable finding of our study is that strong local palaeoenvironmental differences existed in the middle Tarkhanian sea of the study area. At Malyi Kamyshlak, the *Nonion-Globulina-Guttulina* association (II) combines benthic foraminiferal species (Appendix Fig. A1; Supplementary Fig. S5), which predominantly inhabit the outer shelf (e.g. Ouda and Obaidalla, 1998; Rögl and Spezzaferri, 2003; Murray, 2006; Katz et al., 2013; Nurzalia et al., 2018). As during the early Tarkhanian,

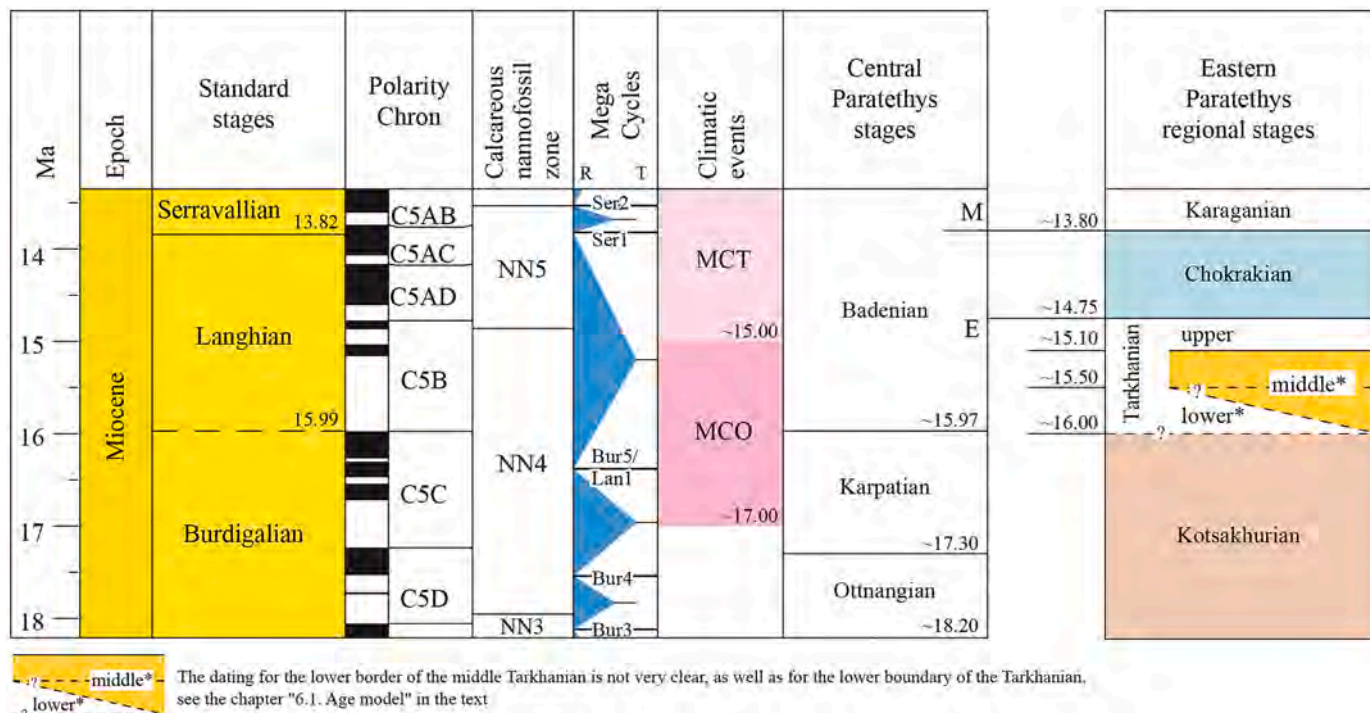


Fig. 12. The proposed age model of the Tarkhanian and its correlation with MCO and MCT.

Legend: Stratigraphic framework – Raffi et al., 2020. Lower borders of the Eastern Paratethys stages (Chokrakian and Karaganian) are used from Palcu et al., 2017, 2019. Mega Cycles – after Hilgen et al., 2012. Climatic events – after Zachos et al., 2001; Holbourn et al., 2005; Shevenell et al., 2006.



the presence of herbivore species of *Quinqueloculina*, *Spiroloculina*, *Triloculina*, *Ammonia* (?) and *Nonion* (after Murray, 2006) in this association indicates a photic zone of environment. The predominance of species belonging to suboxic B indicators (Fig. 13; Supplementary Fig. S5) (according to Kaiho, 1994, 1999; Murray, 2006) suggests low oxygen content in the bottom water. The significant dominance of infaunal over epifaunal species (from 70 to 90% in the sample) may indicate a low oxygen content (hypoxia) inside the sediments (after Rosoff and Corliss, 1992; Jorissen et al., 1995; Báldi, 2006; Murray, 2006; Drinia, 2009) (Fig. 13). The narrow range of the oxygen isotopic values of the benthic foraminifera suggests stable bottom water chemistry (Fig. 10). In comparison to Malyi Kamyshlak, the coeval deposits of the Skelia section revealed a very different association of benthic foraminifera, both in terms of species composition and qualitative characteristics (Figs. 7B and 13; Appendix Figs. A1 and A2; Supplementary Figs. S5 and S6). This is the *Triloculina-Textularia-Guttulina-Nonion* association (III)

(Appendix Fig. A2; Supplementary Fig. S6), which is inhabiting predominantly the inner-shelf, photic zone (Murray, 2006; Ouda and Obaidalla, 1998; Nurzalia et al., 2018; Trabelsi et al., 2017). Unlike association II (Fig. 13), oxic indicators (large-sized and thick-walled miliolids) prevail here indicating high oxygen content of the bottom water (according to Kaiho, 1994, 1999). Besides, the infauna / epifauna ratio changes significantly in this association compared to association II; their proportion is approximately 50 to 50% in all samples (Fig. 13) which may indicate a higher oxygen content inside the sediments of this sea zone. In addition, the presence of oyster banks at Skelia indicates hard substrate (stones, rocks or dense sandy silts) with high bottom waters dynamics, and relatively shallow water conditions.

Another feature of the middle Tarkhanian bottom environments (according to data from both sections) is persistence of low oxygen (up to hypoxia) in the sediment, but increased bottom water oxygenation compared to the early Tarkhanian (Fig. 14). This points to a distinctive

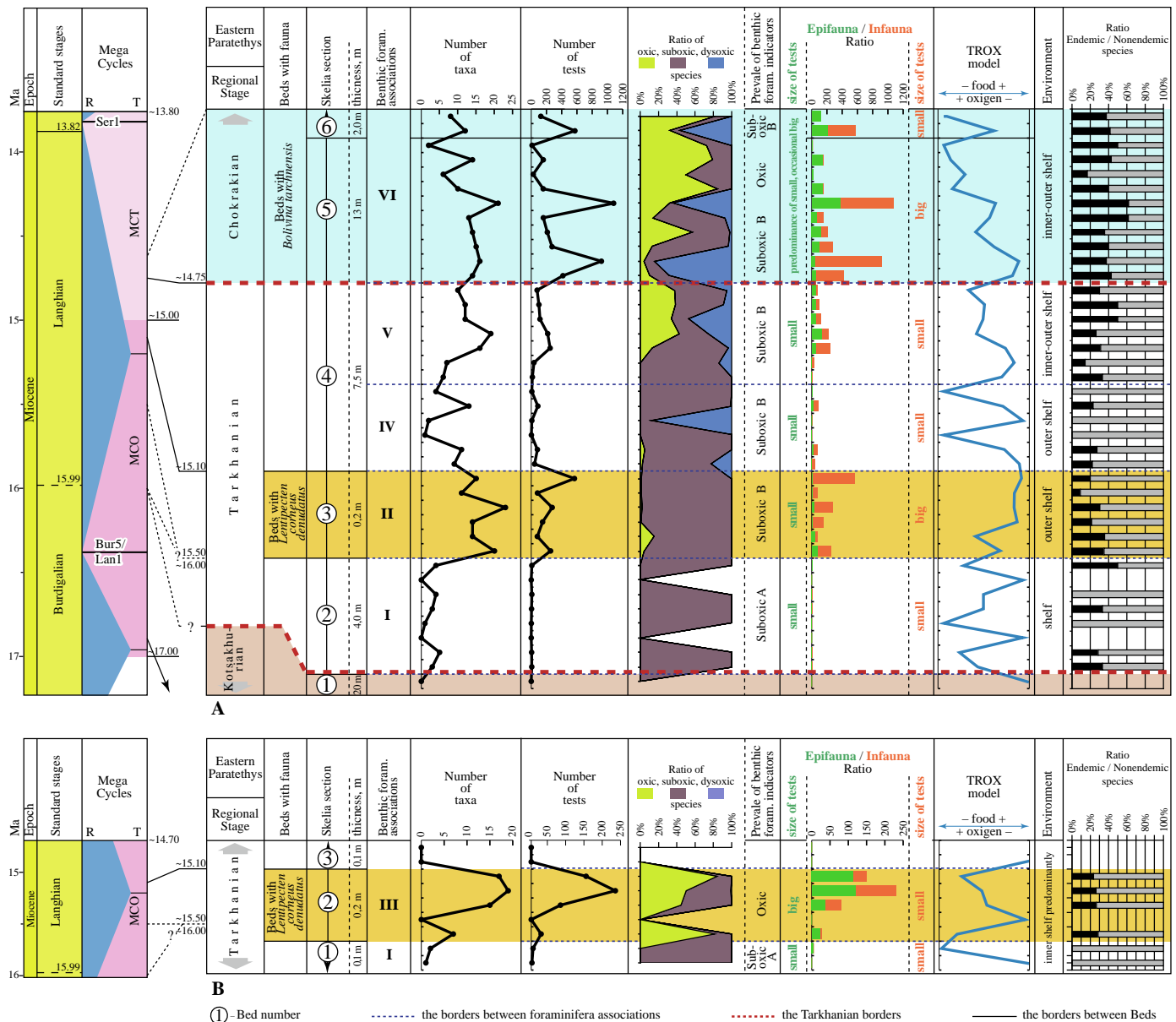


**Fig. 13.** Graphical representation of numerical data on benthic foraminifera associations and interpretation of some ecological conditions of bottom waters in the Tarkhan-Early Chorakian time in the areas of Malyi Kamyshlak (A) and Skelia (B). Legend: Stratigraphic framework – Raffi et al., 2020. Mega Cycles – after Hilgen et al., 2012. Climatic events – after Zachos et al., 2001; Holbourn et al., 2005; Shevenell et al., 2006.

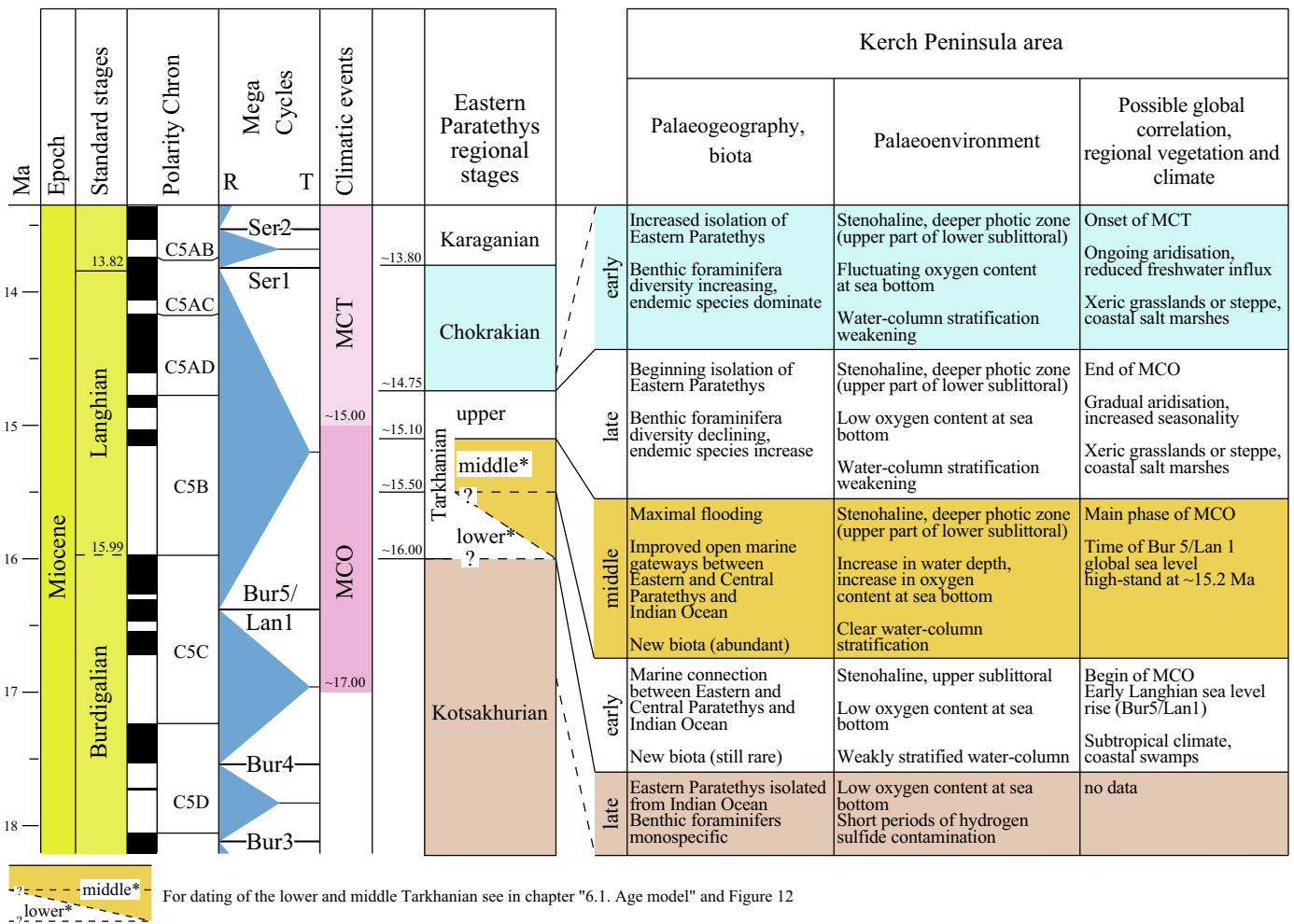


Fig. 14. Summary of changes in palaeogeography, marine environments, terrestrial vegetation and climate during the Tarkhanian – early Chokrakian based on this study and proposed correlation to global events (data for the Kotsakhurian according to Bogdanovich, 1965 Bogdanovich, 1971; Muratov and Nevesskaya, 1986; Popov et al., 1993; Palcu et al., 2019).

change in the quality of the surface water, as it is indicated by the nanofossil assemblages from the middle Tarkhanian samples, with the high-nutrient marker *Coccolithus pelagicus* as dominant species (see Okada and McIntyre, 1979; Winter et al., 1994; Cachão and Moita, 2000). Furthermore, clear differences of the isotopic values derived from benthic and planktic foraminifera, with unusually low oxygen isotopic values for the planktic species (Fig. 10), indicate that the water column was stratified (see also Palcu et al., 2019). Although the low oxygen isotope values could be caused partly by the small size of the planktic foraminifera (Metcalf et al., 2015), we assume that the main reason is the influx of fresh water, which changed the chemistry of the surface water. Such salinity oscillations in the surface water might additionally be supported by the small size of the planktic foraminifera, which indicates that they lived at or outside their environmental optima and might reflect decreased salinity, nutrient availability, carbonate saturation, and oxygen availability (Schmidt et al., 2004 and references herein).

The new SIS age data allow to correlate the middle Tarkhanian with the sea level rise and highstand of the Langhian megacycle Bur5/Lan1 and main phase of the MCO (Figs. 12 and 14). It thus seems plausible to assume that the middle Tarkhanian increase in foraminifera and mollusc species diversity and abundance, the high percentage of cosmopolitan species and also the increase in water depth can be explained by the growing influence of the MCO, causing a high-stand of the World Ocean and, as a consequence, the greatest transgression into the epicontinental

Eastern Paratethys sea.

#### 5.2.4. Late Tarkhanian (middle Langhian – see Fig. 12) (Bed 4 at Malyi Kamyshlak)

In the late Tarkhanian, the connection between the Eastern Paratethys and the open ocean continued, but was less stable (Goncharova, 1989; Goncharova et al., 2001). The beginning isolation of the Eastern Paratethys is well observable in our data, which show a sharp change in the species composition of the benthic biota and an increase in the proportion of endemic foraminifera species (up to 50% – see associations IV, V) (Figs. 13 and 14).

It is known that the late Tarkhanian is characterized by a significant change in the species composition of the benthic biota (molluscs, foraminifera, ostracods) in many areas of the Eastern Paratethys (e.g. Archangelsky, 1940; Ananiashvili, 1985; Muratov and Nevesskaya, 1986; Nevesskaya et al., 1984, 2003). Furthermore, a sharp decrease of molluscs compared to the middle Tarkhanian is observed. The characteristic mollusc association is represented by a *Leda-Abra* assemblage, with prevailing infauna (Merklin, 1950). Based on the molluscs, an open shelf environment (150–200 m deep) with normal-marine, stenohaline conditions, minor water mobility and low oxygenation of bottom water has been proposed (Merklin, 1950; Goncharova, 1989; Goncharova et al., 2001). This is largely in agreement with our benthic foraminifera data from the late Tarkhanian at Malyi Kamyshlak. The assemblages can be divided into the *Nonion* association (IV) and the *Nonion-*

*Quinqueloculina* association (V) (Fig. 7A; Appendix Fig. A1; Supplementary Fig. S5), both are characterized by a sharp decrease of species and also by a decrease in the number and the size of their tests in comparison to the middle Tarkhanian foraminifera (Figs. 13 and 14). The *Nonion* association (IV) has some similarity in genus and species composition with the middle Tarkhanian foraminifera association from Malyi Kamyshlak (Figs. 6 and 7A) and indicates an outer shelf area (after Ouda and Obaidalla, 1998; Murray, 2006; Katz et al., 2013; Nurzalia et al., 2018). Slight shoaling of the sea is indicated by the *Nonion-Quinqueloculina* association (V), which points to inner- to outer shelf conditions (after Ouda and Obaidalla, 1998; Murray, 2006; Katz et al., 2013; Nurzalia et al., 2018). As before, the presence of herbivore species of *Quinqueloculina*, *Triloculina*, *Discorbis*, *Ammonia* (?) and *Nonion* (after Murray, 2006) in both associations indicates a photic zone. The few fish otoliths reveal the same pattern as seen in the *Nonion* association; their composition is similar as in the middle Tarkhanian and suggests relatively deep water of an outer shelf.

Low oxygen conditions in the bottom water can be assumed based on the prevalence of Suboxic B indicators (according to Kaiho, 1994, 1999; Murray, 2006) in association IV (Fig. 13; Supplementary Fig. S5). Furthermore, variable epifauna/infauna ratios in associations IV and V (Fig. 13; Supplementary Fig. S5) suggest unstable sea-floor environments with fluctuating nutrient/oxygen content inside the sediments (after Rosoff and Corliss, 1992; Báldi, 2006; Murray, 2006). Nevertheless, the increase of epifaunal species in association V (Fig. 13), mainly due to miliolids (see Fig. 6; Supplementary Fig. S5), indicates a gradual increase in bottom water oxygenation and probably also inside the sediments (Jorissen et al., 1995) in the study area towards the end of the Tarkhanian. As described above for the middle Tarkhanian, significant differences between the isotopic values of benthic and planktic foraminifera support that the water column was stratified, in agreement with the model of Palcu et al. (2019). Furthermore, carbon and oxygen isotopic values of benthic foraminifera stayed similar between the middle and late Tarkhanian, which suggests similar quality of the bottom waters (Fig. 14). In contrast, a significant change in the surface water, compared to the middle Tarkhanian, is indicated by a clear change in the composition of the nannofossils, which fluctuate from *Coccolithus*- to *Sphenolithus*-dominated assemblages. Different surface water conditions are additionally confirmed by the decrease of  $\delta^{13}C$  in the isotope data of the planktic foraminifera from the upper Tarkhanian (Fig. 10). Both the nannofossil assemblages and the carbon stable isotope data point to reduced availability of nutrients and less eutrophic water (Fig. 15).

Our new age data indicate that the late Tarkhanian environmental changes and beginning of Eastern Paratethys isolation can be associated to the end of the MCO (Figs. 12 and 14). The slight increase in bottom water oxygenation (seen in foraminifera association V), and clear signs of less eutrophic waters (nannofossil assemblages, carbon isotope data of planktic foraminifera) suggest reduced freshwater influx, possibly because of the gradual aridification of the climate at the end of the MCO (Figs. 14 and 15).

#### 5.2.5. Early Chokrakian (middle Langhian – see Fig. 12) (Beds 5, 6 at Malyi Kamyshlak)

Data from other Tarkhanian-Chokrakian sections (Bogdanovich, 1965; Dzhanlidze, 1970; Krashennnikov et al., 2003) indicate that the Eastern Paratethys had a limited connection with the open ocean during the early Chokrakian (Fig. 14). The new data from Malyi Kamyshlak show that the number of endemic benthic foraminifera species (association VI) increases up to 60% per sample (vs. up to 50% in samples from the late Tarkhanian) (Fig. 13), which suggests an increasing degree of isolation of the Eastern Paratethys in the early Chokrakian.

Previous works showed that the benthic species composition (molluscs, foraminifers) of the early Chokrakian is largely similar to that of the late Tarkhanian in many areas of the Eastern Paratethys, suggesting that the bottom water environments did not significantly change (e.g.

Archangelsky, 1940; Ananiashvili, 1985; Vernyhorova, 2014). The molluscs species diversity remained low (*Leda-Abra* assemblage, after Merklin, 1950, presence of the pelagic gastropod *Limacina tarchanensis* (Kittl) after Davitashvili and Merklin, 1968) and normal-marine, stenohaline conditions of the pseudoabyssal zone with some deepening of the basin have been proposed (Merklin, 1950; Goncharova, 1989; Goncharova et al., 2001; these studies suggest that the lower Chokrakian deposits at Malyi Kamyshlak and Skelia were related to the late Tarkhanian age).

However, our new data allow to revise and refine the previous interpretations. Benthic foraminifera are represented by the *Bolivina-Nonion-Quinqueloculina* association (VI) (Appendix Fig. A1; Supplementary Fig. S5). The composition of genera is similar to the late Tarkhanian association V (Figs. 6 and 7; Appendix Fig. A1; Supplementary Fig. S5), but the overall species composition is different and species diversity has increased (Fig. 7A; Appendix Fig. A1; Supplementary Fig. S5). In detail, association VI consists of species inhabiting the inner-outer shelf, photic zone (e.g. Ouda and Obaidalla, 1998; Murray, 2006; Miriam et al., 2013; Nurzalia et al., 2018) and the proportion of oxic species continues to increase. This, as well as a gradual increase in the proportion of epibenthic species, may indicate a tendency towards more oligotrophic conditions and better bottom water oxygenation (Jorissen et al., 1995; Drinia, 2009). In addition, occasional changes of dominant species are observed: the infaunal species *Bolivina tarchanensis* and *Nonion commune* are replaced by epibenthic species of *Quinqueloculina* (Appendix Fig. A1; Supplementary Fig. S5) and an increase of herbivore species of *Quinqueloculina* and *Triloculina* occurs in the levels with dominant epibenthic species (Figs. 13–15; Supplementary Fig. S5).

Taking our new data and previous mollusc data together, the environment was a normal marine, open shelf habitat, probably of the lower sublittoral zone (after Hedgpeth, 1957; Longhurst, 2007), but not of the pseudoabyssal zone. The pelagic species *Vinciguerria merklini* and absence of benthic fish species (see above) suggest a relatively deep, outer shelf habitat, whereas the dominance of *Quinqueloculina* and *Triloculina* in some samples points to shoaling and/or increase in the degree of water transparency. Variable bottom water oxygenation, as indicated by the species composition of foraminiferal association VI (Figs. 7A and 13; Appendix Fig. A1; Supplementary Fig. S), suggests fluctuations between eutrophic and oligotrophic conditions, which is additionally corroborated by the calcareous nannofossils. Overall, *Sphenolithus* is dominant in the early Chokrakian assemblages, but its abundance and diversity are variable, most likely due to oscillations in nutrient availability. Moreover, reduced fresh-water influx can be inferred based on the slightly increased oxygen isotope values of the planktic foraminifera (compared to the late Tarkhanian, see Fig. 10). Also, the water-column stratification had decreased (Fig. 14), as carbon isotope values between planktic and benthic foraminifera are similar and differences in the  $\delta^{18}O$  values are diminished (Fig. 10).

Our new age model suggests that the begin of the Chokrakian can be tightly linked to the end of the MCO and onset of the MCT (Figs. 12 and 14). As for the late Tarkhanian, gradual increase in bottom water oxygenation (foraminifera association VI), and clear signs of less eutrophic waters (nannofossil assemblages, carbon isotope data of planktic foraminifera) suggest reduced freshwater influx because of the ongoing aridification of the climate (Figs. 14 and 15). Moreover, common occurrence of reworked taxa among the calcareous nannofossil assemblage points to a regressive phase (Holcová, 1999).

### 5.3. Reconstructions of the terrestrial vegetation

#### 5.3.1. Early Tarkhanian (early Langhian – see Fig. 12)

From the point of view of the development of terrestrial vegetation, the early Tarkhanian interval appears to be the warmest and wettest according to the semiquantitative ratio of paleotropical and arctic elements in the classical palynological diagram (Fig. 9). Based on the coexistence approach (CA) this phenomenon is also evident from high



CMT (mean temperature of the coldest month). With CMT > 10°C, winter temperatures are among the highest in the entire record. This coincides with the high percentage of the thermophilous zonal component (lowermost two samples). Azonal communities such as coastal swamp and deciduous riparian forest also attained highest proportions in the early Tarkhanian (Fig. 9). Summers were most humid at 19.67 m. Thereafter, there was a step-wise decline of the ratio of MPwarm on MAP.

PFT data indicate a high general plant diversity at the beginning of the lower part of the Tarkhanian, low diversity proportion of conifers and of drought-tolerant arboreal components (in the beginning only). Towards the top of the lower part of the Tarkhanian there is evidence for short-term cooling, which is indicated by the decrease of CMT and the lowest proportion of broadleaved evergreen (BLE) to broadleaved deciduous (BLD) trees (Appendix Fig. A4a and b). Precipitation and temperature show high variability in the early Tarkhanian and indicate also drier intervals. With MAT means mostly between 15 and 20°C, climate persisted to be warm temperate. Pollen in clumps were not detected. It seems that the environment corresponds to a relatively remote area from the shore, e.g. a more distant part of a delta.

### 5.3.2. Middle Tarkhanian (early Langhian – see Fig. 12)

Sediments from the middle Tarkhanian were not suitable for palynological studies.

### 5.3.3. Late Tarkhanian (middle Langhian – see Fig. 12)

The share of herbaceous vegetation increased. Poaceae attained about the same percentages as Chenopodiaceae, most of which are considered drought-tolerant elements. Moreover, coastal and aquatic herbs appeared (Fig. 9; Appendix Fig. A4). On the other hand, the share of sclerophytic and heliophytic, but riparian elements decreased. Gradual increase in oxygen level of the sea in the study area towards the end of the Tarkhanian indicates less contribution of organic matter from land associated with a reduction in permanent land drainage due to aridification (see above). This phenomenon could be associated with the small proportion of riparian habitats (especially alders whose growth is associated with eutrophic conditions) and their reduction towards the younger parts of the profile (upper Tarkhanian and Chokrakian).

Pollen grains in clumps as an indicator of low-energy transport from the growth site first appeared. Winter temperatures were still at a high level (>10°C), and rainfall in the warm season. WMT increased at the top of the upper Tarkhanian section which indicates an increase in seasonality. The very rare presence of mountain vegetation elements points to a flat relief without mountain chains.

### 5.3.4. Chokrakian (middle Langhian – see Fig. 12)

Various values (percentage of thermophilous elements, CA, PFT) indicate a weak, gradual cooling and drying of the warm season. The proportion of conifers shows a steady increase, whereas the diversity of evergreen components and the percentage of thermophilous elements first stayed at a high level, then significantly declined towards the top of the section. The ratio of MPwarm on MAP displays a step-wise decline to values around 9% as resulting from the upper Chokrakian samples. The reconstructed temperature records show a trend of moderate gradual cooling in the Chokrakian. CMTmin values dropped to 5°C. With MAT means mostly between ca. 18 and 21°C, climate persisted to be warm temperate.

A further reduction of the riparian elements is recorded. At the same time, Chenopodiaceae (20–28%) and Caryophyllaceae (up to 10%) were at their maximum occurrence. These data can be interpreted as extension of coastal salt marshes – overgrown by the halophilous flora (Chenopodiaceae/*Salicornia* with Caryophyllaceae, *Armeria*, *Daucaceae*) due to higher evaporation and decreased fresh-water influx (Fig. 9). These vegetation changes are in good agreement with the results of our study based on other methods (see above), according to which decreased fresh-water influx and shoaling of the sea happened due to a regressive

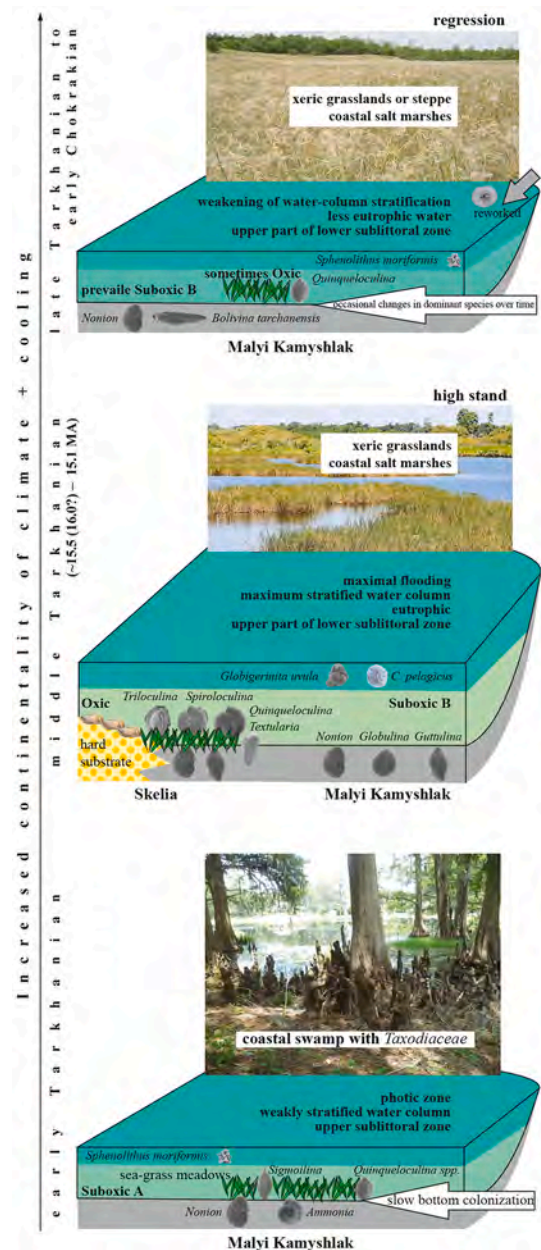


Fig. 15. Conceptual model of paleoenvironmental evolution within Tarkhanian and Chokrakian in the Kerch Peninsula area.

phase associated with the increasing isolation of the Eastern Paratethys. Precipitation decline in the warm season is most evident from the ratio of MPwarm/MAP. Moreover, a mean annual range of temperature (MART) > 15°C in the Chokrakian points to higher continentality of climate (Appendix Fig. A4).

### 5.4. Comparison of climatic evolution between the Eastern and the Central Paratethys during culmination of the MCO

Terrestrial ecosystems experienced substantial heterogeneity in the regional manifestation of the Miocene Climatic Optimum (MCO) (Harris et al., 2017). Palynofloras and phytolith assemblages suggest that open, grass-dominated, mosaic habitats, or steppe vegetation continued to spread during the middle Miocene in the eastern Mediterranean as part of an ecological transition that started in the Early Miocene (Leopold and Denton, 1987; Strömberg et al., 2007; Strömberg and McInerney, 2011; Harris et al., 2017; Smiley et al., 2018; Steinthorsdottir et al.,

2021). In addition, the Middle Miocene records the maximum advance of vegetation adapted to warm and/or wet climates to higher latitudes, as well as spreading of sclerophyllous forests, grass-dominated habitats, and initiation of modern deserts. Subhumid sclerophyllous forest was common in Eurasia, including west-central Europe, middle Asia, and Anatolia, where broad-leaved deciduous forest and subtropical forest also occurred (Kovar-Eder et al., 2008a, 2008b; Ivanov et al., 2011; Utescher et al., 2011; Bouchal et al., 2016), as well as more open, grass-dominated or steppe vegetation (Strömberg and McInerney, 2011; Tang and Ding, 2013).

The feature of the Middle Miocene vegetation around the Central Paratethys was significantly affected by the Alpine uplift in the western Alps and Carpathians (Kováč et al., 1994; Meulenkamp and Sissingh, 2003; Sharp et al., 2005; Campani et al., 2012). For the Karpatian (late Burdigalian) and early Badenian (early Langhian) of the Carpathian Foredeep and the Vienna Basin, very warm conditions with low seasonality, high precipitation and high abundances of palaeotropical (thermophilous) elements were observed (Doláková et al., 2021). The same pattern of climate was recorded based on the vegetations found in the Pannonian Basin (Jiménez-Moreno et al., 2005) and the Korneuburg Basin (Hofmann et al., 2002; Kern et al., 2011).

However, there are also several alternations between warmer and cooler phases in the Carpathian Foredeep and Vienna Basin that partly have been correlated with glacial events (Mi 2a and Mi 3a according to Miller et al., 1998) (Doláková et al., 2021). Periodic changes in climatic factors – especially temperatures and precipitation and increasing seasonality were interpreted in the frame of the culminating MCO and the beginning of the Miocene Climate Transition (MCT). Nevertheless, swamp tree pollen and annual precipitation rates point to the persistence of overall humid climate conditions and the almost continuous presence of subtropical conditions in all regions of the Central Paratethys (Kopecká et al., 2022). Evidence for the MCT and subsequent cooling during the Late Langhian – Early Serravalian (upper part of the nanoplankton zone NN5 and in NN6 – above the LO of *Helicosphaera waltrani* at 14.371 Ma) were recorded in the Carpathian foredeep and Vienna basin (Doláková et al., 2014; Holcová et al., 2015; Nehyba et al., 2016; Doláková et al., 2021). Reconstructed precipitation data and the presence of drought-tolerant plant functional types point to a seasonal climate with a trend to somewhat drier conditions during the Serravalian (with distinctly drier season, which was, however, not the warm season).

In comparison to time-equivalent vegetation data from the Carpathian foredeep, the palynospectra from the Malyi Kamyshlag section are characterized by slightly lower percentages of palaeotropical elements in the Tarkhanian and a clear decrease in the Chokrakian (Kováčová et al., 2011; Doláková et al., 2021). In addition, the reconstructed temperature and precipitation values indicate cyclical changes and also drier intervals especially in the upper Tarkhanian, and a trend of moderate gradual cooling and higher continentality in the Chokrakian.

A notable feature is the constant existence of Taxoioideae swamps (although they are decreasing upsection), which is probably associated with a very flat coastline at Malyi Kamyshlag. In the upper Tarkhanian and Chokrakian, the progressive increase in the proportion of herbal elements indicates a gradual opening of the landscape, occurrence of non-forested areas, and extension of coastal salt marshes (overgrown by the halophilous flora) accompanied by higher evaporation.

Taxonomic diversity changes periodically across the entire section, which may also be due to taphonomy – such as changes in the redox potential of seawater or sediment. This phenomenon is also observable in time-equivalent vegetation records from the Central Paratethys (i.e. Doláková et al., 2014; Holcová et al., 2015; Doláková et al., 2021). Another typical indicator for lower Langhian palynospectra in the Central Paratethys as well as at Malyi Kamyshlag is the increased diversity and quantity of “deciduous oak type” pollen grains. Nevertheless, a marked difference from the Central Paratethys is that all values from Malyi Kamyshlag (percentage of thermophilous elements, CA, PFT)

indicate a weak, gradual cooling and drying of the warm season, as well as significant climate continentality in the early Chokrakian (before 14.6 Ma, see Appendix Fig. A4). This indicates an earlier trend of climate change than in the Central Paratethys, where cooling and continentality has only been recorded from sediments younger than 14.3 Ma (see above). We assume that this earlier increase in climate continentality is a regional phenomenon of the Eastern Paratethys, associated with the sea regression in the late Tarkhanian and the existence of a large flat continent.

## 6. Conclusions

Our comprehensive analyses including (micro)palaeontology (foraminifera, calcareous nannofossils, molluscs, fish otoliths), palynology (spores and pollen), geochemistry (carbon and oxygen stable isotopes) and strontium isotope age dating resulted in a new age model for the studied sections of the Tarkhanian and lower Chokrakian (lower Langhian), which is >15.5 (~16.0?) – 14.75 Ma, with the middle Tarkhanian dated to ~15.5–15.1 Ma. The new age data were linked with the reconstructions of marine environments, coastal and inland vegetation and allowed to conclude possible relations to global climate change:

The middle Tarkhanian flooding can be correlated to the global sea level high-stand of sequence Bur 5/Lan 1 at ~15.2 Ma. This implies that the global sea level rise of the MCO is well detectable at the same time in the Eastern Paratethys, despite of its palaeogeographic location far away from the open sea.

The mostly stable open marine shelf conditions (near upper part of lower sublittoral zone) with stratification of the water column dominate the study area from the Tarkhanian to early Chokrakian. The water column stratification is most distinct in the middle Tarkhanian and decreased in the early Chokrakian. Changes in the benthic assemblages are associated with fluctuations in bottom water oxygenation and nutrient/oxygen content within the sediment, with increasing substrate density and/or shallower water, and possibly also with a change in the degree of illumination. The maximum species diversity of the benthic assemblages occurs in the middle Tarkhanian and thus appears to be associated with the culmination of the MCO.

A gradual transition to more arid and continental climate conditions occurs during the Tarkhanian to early Chokrakian. The wet and warm climate of the early Tarkhanian gradually changes to a more seasonal climate with cooler winters and drier summers in the late Tarkhanian and Chokrakian. Coastal swamp and deciduous riparian forest has their largest extend in the early Tarkhanian.

Our palynological results may be one of the first to indicate that a trend of cooling and aridification occurred earlier in the Eastern Paratethys (before 14.6 Ma) than in the Central Paratethys, where cooling and continentality has only been recorded from sediments younger than 14.3 Ma. This phenomenon can most likely be related to the regression of the late Tarkhanian sea and the wide, flat landscape of the study area in the Eastern Paratethys, where high mountain ranges were absent.

Supplementary data to this article can be found online at <https://doi.org/10.1016/j.marmicro.2023.102231>.

## CRediT authorship contribution statement

**Yuliia V. Vernyhorova:** Conceptualization, Methodology, Formal analysis, Investigation, Resources, Writing – original draft, Writing – review & editing, Visualization. **Katarína Holcová:** Conceptualization, Methodology, Formal analysis, Investigation, Writing – original draft, Writing – review & editing, Visualization. **Nela Doláková:** Conceptualization, Methodology, Formal analysis, Investigation, Writing – original draft, Writing – review & editing, Visualization. **Bettina Reichenbacher:** Conceptualization, Methodology, Formal analysis, Investigation, Writing – original draft, Writing – review & editing, Visualization. **Filip Scheiner:** Methodology, Formal analysis, Investigation. **Lukáš Ackerman:** Methodology, Formal analysis, Investigation.

**Jan Rejšek:** Methodology, Formal analysis, Investigation. **Lorenzo De Bortoli:** Methodology, Formal analysis, Investigation. **Jakub Trubač:** Methodology, Formal analysis, Investigation. **Torsten Utescher:** Conceptualization, Methodology, Formal analysis, Investigation, Writing – review & editing.

**Declaration of Competing Interest**

The authors declare that they have no known competing financial interests or personal relationships that could have appeared to influence the work reported in this paper.

**Data availability**

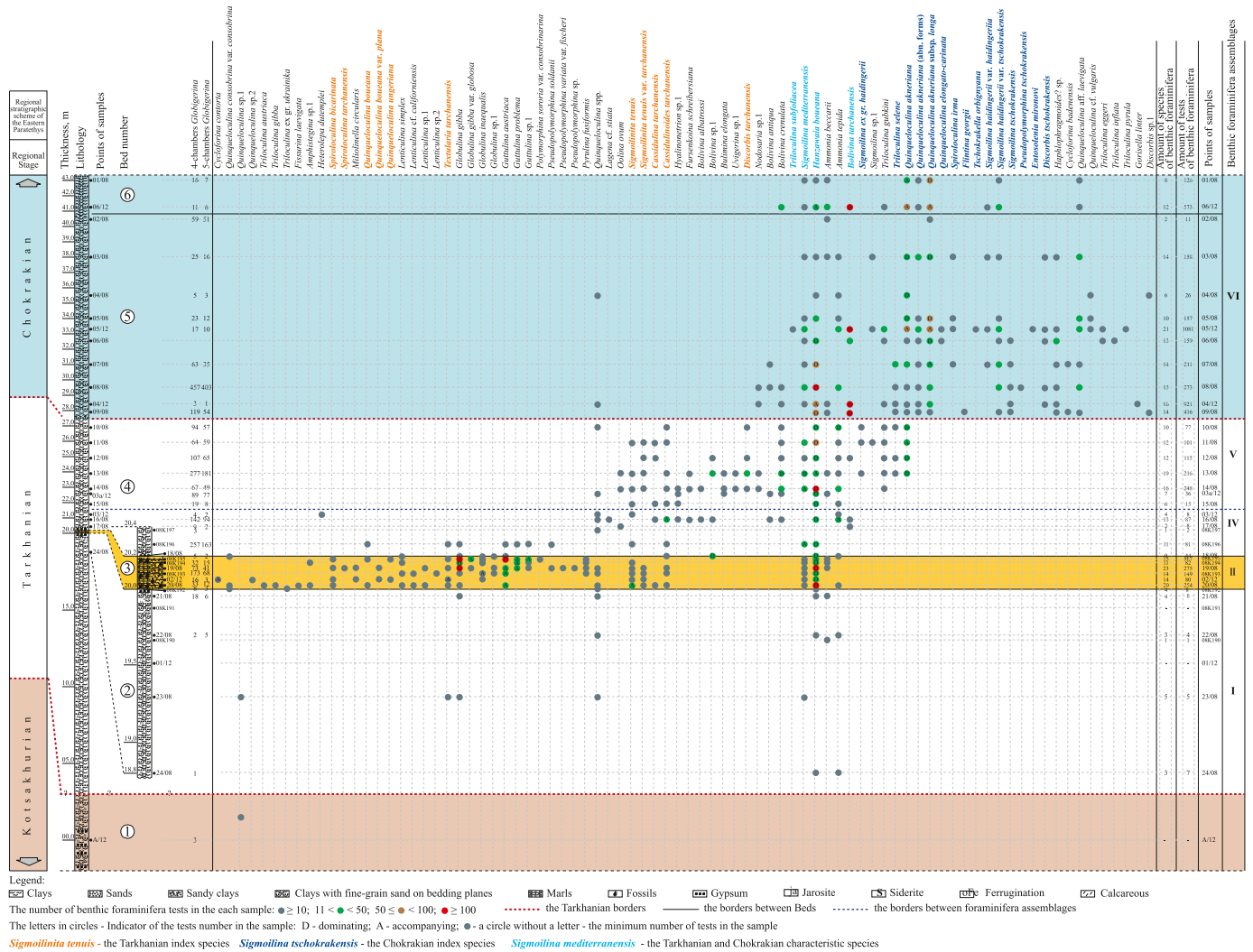
No data was used for the research described in the article.

**Acknowledgments**

This research was supported by Paleontological Society International Research Program (PaSIRP), Sepkoski Grants (2017). The geochemical analysis in this paper has been funded by the Czech Science Foundation,

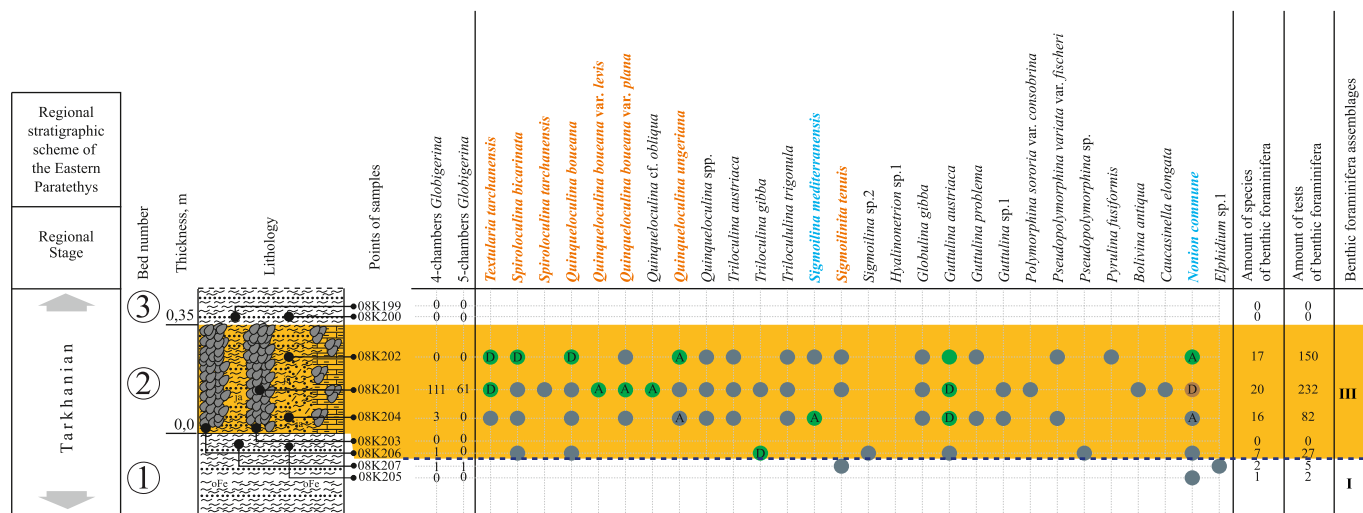
project 20-05872S. The authors from Charles University Prague were supported by institutional project COOPERATIO by the Center for Geosphere Dynamics UNCE/SCI/006. The institutional support was provided also by the research program RVO 67985831 (Institute of Geology of the Czech Academy of Sciences). Yuliia V. Vernyhorova was partially supported by the National Academy of Sciences of Ukraine, project no. 0122U001698. We are grateful to Alexander Bannikov for providing SEM images of the otoliths preserved in situ in skeletons of *Vinciguerrina merklini* from the collection of the Borissiak Palaeontological Institute of the Russian Academy of Sciences, Moscow. Scanning electroning microscopic of foraminifera were obtained in the Center for shared use of scientific equipment of the Laboratory of Physical Methods of Research, Institute of geological sciences of National Academy of Sciences of Ukraine (Kyiv, Ukraine) and in Institute of Geology and Palaeontology, Charles University in Prague. Palynological study was supported by the specific research project of Institute of Geological Sciences, Masaryk University Brno. We are very thankful to Assistant Editor Shijun Jiang and two anonymous reviewers whose constructive comments and suggestions helped to improve the manuscript.

**Appendix**



**Appendix Fig. A1.** Foraminifera distribution in deposits of the Malyi Kamyshlak section.





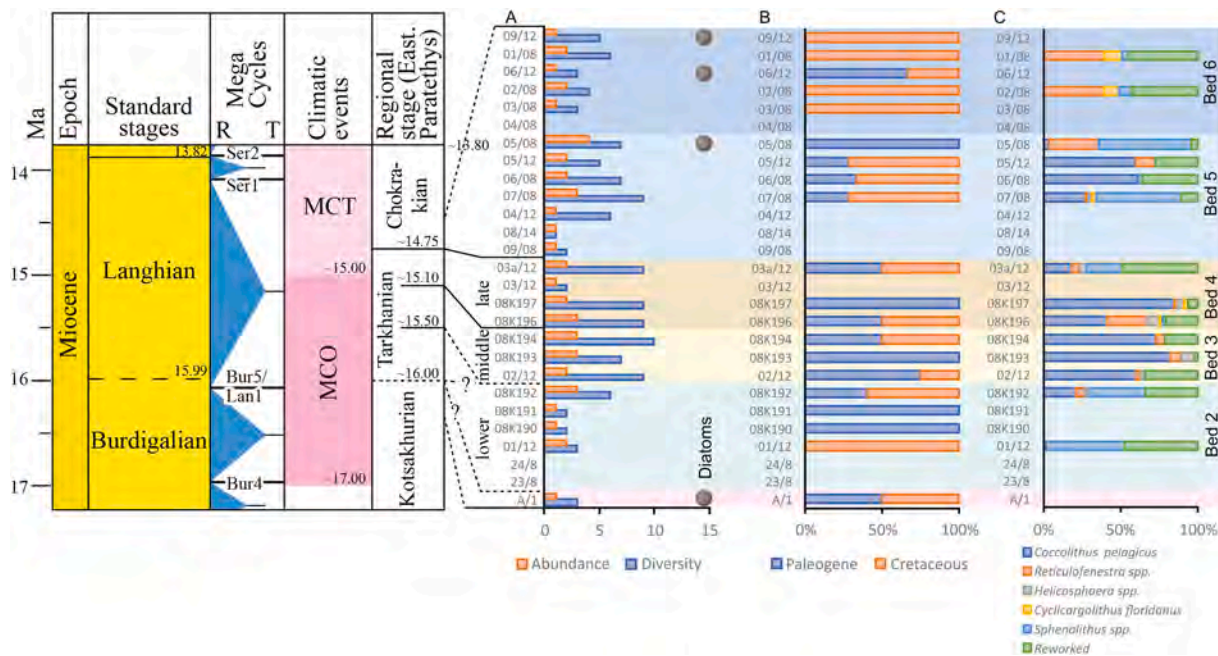
Legend: Clays, Sands, Sandy clays, Clays with fine-grain sand on bedding planes, Marls, Ferrugination, Calcareous, Jarosite, Siderite, Fossils, Oster bank

The number of benthic foraminifera tests in the each sample: ● ≥ 10; ● < 11 < 50; ● < 50 < 100

The letters in circles - Indicator of the tests number in the sample: D - dominating; A - accompanying; ● - a circle without a letter - the minimum number of tests in the sample

*Sigmoilinita tenuis* - the Tarkhanian index species *Sigmoilina mediterraneensis* - the Tarkhanian and Chokrakian characteristic species

Appendix Fig. A2. Foraminifera distribution in the Tarkhanian deposits of the Skelia section.



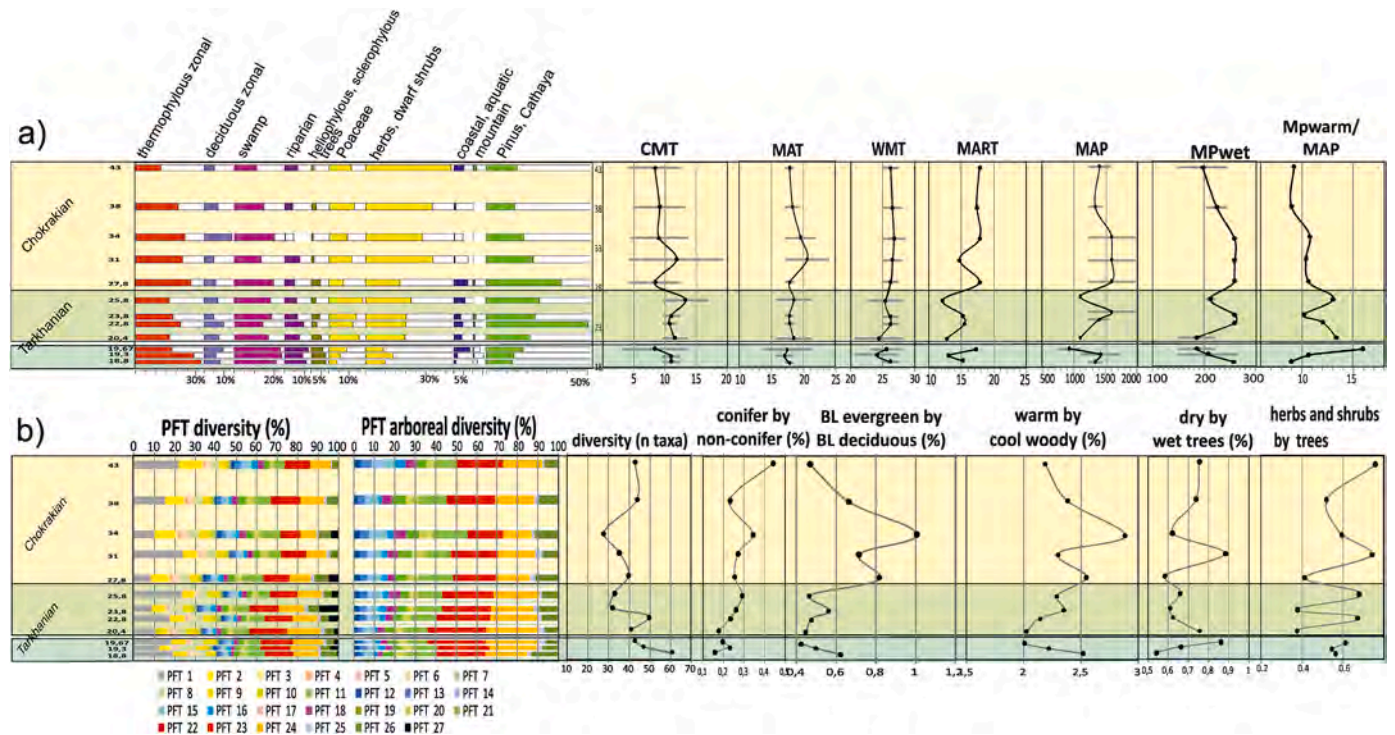
Appendix Fig. A3. Quantitative characteristics of the calcareous nannofossil assemblages:

A - Abundance: 1-rare, 2-common, 3-abundant, 4-very abundant; diversity is expressed as a number of species/sample, occurrence of diatoms in sample is recorded by pictograms;

B - relative abundances of reworked Paleogene and Cretaceous nannofossils;

C - relative abundances of nannofossil groups in assemblages.

Mega Cycles - after Hilgen et al., 2012. Climatic events - after Zachos et al., 2001; Holbourn et al., 2005; Shevenell et al., 2006.



**Appendix Fig. A4.** a) Pollen diagram combined with respect to their ecological demands according to Kvaček et al. (2006) and selected climate variables based on the coexistence approach;

b) Synthesized diagrams showing abundance of key pollen groups, PFT diversity spectra (using the 26 PFT system according to Popova et al. and an additional aquatic PFT 27), various diversity indices, and diversity of taxa. [Colour figure can be viewed at [ileyonlinelibrary.com](https://doi.org/10.1016/j.micropaleo.2023.102231)].

## References

- Agnini, C., Fornaciari, E., Rio, D., Tateo, F., Backman, J., Giusberti, L., 2007. Responses of calcareous nannofossil assemblages, mineralogy and geochemistry to the environmental perturbations across the Paleocene/Eocene boundary in the Venetian Pre-Alps. *Mar. Micropaleontol.* 63, 19–38. <https://doi.org/10.1016/j.micropaleo.2006.10.002>.
- Aleksandrova, V.N., 1952. On structural-geological survey at the Bulhanak and Aktash-Kazantip areas in the northern part of the Kerch Peninsula [O strukturno-geologicheskoi symke na Bulhanakskoi i Aktash-Kazantipskoi ploschchadiakh v severnoi chasti Kerchenskogo poluostrova]. Feodosia (in Russian).
- Ananiashvili, G.D., 1985. The Territory of Georgia and Adjacent Areas in the Tarkhanian Time [Teritoriya Gruzii i smezhnyye s nei regiony v Tarkhanskoye vremia], Metsniereba, Tbilisi (in Russian).
- Andreyeva-Grigorovich, A., 2002. Biostratigraphy and paleoecology of the upper Badenian and lower Sarmatian of the Carpathian foredeep on the basis of nannoplankton. *Bull. Acad. Serbe Sci. Arts* 125, 75–82.
- Andreyeva-Grigorovich, A.S., Savitskaya, N.A., 2000. Nannoplankton of the Tarkhanian deposits of the Kerch Peninsula (Crimea). *Geol. Carpath.* 5 (116), 399–406.
- Andriyashov, A.P., 1979. On some issues of vertical zoning of the marine benthic fauna. In: Studenetskiy, S.A. (Ed.), *Biological Resources of the World Ocean [O nekotorykh voprosakh vertikalnogo zonirovaniya morskoy donnoy fauny. V knige: Biologicheskie resursy Mirovogo okeana]* Moscow, Science. S. pp. 117–138 (In Russian).
- Andrusov, N.I., 1889. New geological research on the Kerch Peninsula. In: 1888 [Novye geologicheskie issledovaniya na Kerchenskom poluostrove], Memoires de la societe des naturalistes de la Nouvelle-Russie, Odessa, 14, pp. 59–130. No. 2. (in Russian).
- Andrusov, N.I., 1893. Geotectonics of the Kerch Peninsula [Geotektonika Kerchenskogo Poluostrova]. Edition by Imperarskoy Akademii Nauk, St. Petersburg (in Russian).
- Andrusov, N.I., 1961a. The Selected Papers [Izbrannye trudy], 1. Edition by Academy of Sciences of USSR, Moscow, p. 712 (in Russian).
- Andrusov, N.I., 1961b. The Selected Papers [Izbrannye trudy], Edition by Academy of Sciences of USSR, Moscow, Vol.2, 644. (in Russian).
- Archangelsky, A.D. (Ed.), 1940. Stratigraphy of the USSR. Vol. 12: Neogene USSR [Stratigrafiya SSSR. Tom 12: Neogen SSSR]. AN SSSR, Moscow, Leningrad (in Russian).
- Arkhangelsky, A.D., Blokhin, A.A., Menner, V.V., Osipov, S.S., Sokolov, M.I., Chepikov, K.R., 1930. A Short Review of the Geological Structure and the Oil Deposits of the Kertch Peninsula [Kratkiy ocherk geologicheskogo stroeniya i nefiannykh mestorozhdeniy Kerchenskogo poluostrova] Transactions of the Geological and Prospecting Service of USSR, Moscow, Leningrad, no. 13 (in Russian).
- Aubry, M.-P., 1989. Handbook of Cenozoic Calcareous Nannoplankton: Book 3. Ortholithae (Pentaliths, and Others), Heliolithae (Fasciculiths, Sphenoliths and Others). Micropaleontology Press, New York.
- Báldi, K., 2006. Paleoceanography and climate of the Badenian (Middle Miocene, 16.4–13.0 Ma) in the Central Paratethys based on foraminifera and stable isotope ( $\delta^{18}\text{O}$  and  $\delta^{13}\text{C}$ ) evidence. *Int. J. Earth Sci.* 95 (1), 119–142.
- Bannikov, A.F., 2010. Fossil Vertebrates of Russia and Adjacent Countries. Fossil acanthopterygians fishes (Teleostei, Acanthopterygii). GEOS, Moscow.
- Bannikov, A.F., Parin, N.N., 1997. The list of marine fishes from Cenozoic (Upper Paleocene – Middle Miocene) localities in southern European Russia and adjacent countries. *J. Ichthyol.* 37, 133–146.
- Barg, I.M., Ivanova, T.A., 2000. Stratigraphy and geological development of the Plain Crimea in the Miocene [Stratigrafiya i geologicheskoye razvitiye Ravninnogo Kryma v miotsene]. *Stratigr. Geol. Correl.* 8 (3), 83–93 (in Russian).
- Barg, I.M., Ivanova, T.A., 2001. Miocene stratigraphy and geological history of the Crimean Plain Region. *Stratigr. Geol. Correl.* 8 (3), 83–93.
- Barg, I.M., Stepaniak, Y.D., 2003. Stratigraphy and Geological Development of the Crimea and Kerch Peninsula in the Miocene Epoch [Stratigrafiya i Geologicheskoe Razvitiye Ravninnogo Kryma i Kerchenskogo Poluostrova v Miotsenovuyu Epokhu], Monolit, Dnepropetrovsk (in Russian).
- Barker, S., Greaves, M., Elderfield, H., 2003. A study of cleaning procedures used for foraminiferal Mg/Ca paleothermometry. *Geochem. Geophys. Geosyst.* 4 (9), 8407. <https://doi.org/10.1029/2003GC000559>.
- Benito, M.I., Suarez-Gonzalez, P., Quijada, I.E., Sonia Campos-Soto, S., Rodríguez-Martínez, M., 2020. Constraints of applying strontium isotope stratigraphy in coastal and shallow marine environments: insights from lower cretaceous carbonates deposited in an active tectonic setting (N Iberian Basin, Spain). *J. Iber. Geol.* 47, 151–169.
- Bogdanovich, A.K., 1952. Miliolidae and peneroplidae [Miliolidy i Peneroplidy]. *Proc. VNIGRI* 64 (in Russian).
- Bogdanovich, A.K., 1965. The Stratigraphic and Facies Distribution of Foraminifera in the Miocene of the Western Ciscaucasia and Questions of their Genesis [Stratigrafiyecheskoye i fatsialnoye raspredeleniye foraminifer v Miotsene Zapadnogo Predkavkaziya i voprosy ikh genezisa]. *Trudy KFNII, Leningrad*, 19, pp. 300–350 (in Russian).
- Bogdanovich, A.K., 1971. Entwicklungsetappen der Foraminiferen Fauna des Miozäns von Nordkaukasus und Fragen den Gense.
- Böhme, M., Winkhofer, M., Ilg, A., 2011. Miocene precipitation in Europe: temporal trends and spatial gradients. *Palaeogeogr. Palaeoclimatol. Palaeoecol.* 304 (3–4), 212–218. <https://doi.org/10.1016/j.palaeo.2010.09.028>.
- Boltovskoy, E., Totah, V., 1985. Diversity, similarity and dominance in benthic foraminiferal fauna along one transect of the Argentina shelf. *Rev. Micropaleontol.* 28 (1), 23–31.



- Bouchal, J.M., Zetter, R., Grímsson, F., Denk, T., 2016. The middle Miocene palynoflora and palaeoenvironments of Eskihsar (Yatağan Basin, southwestern Anatolia): a combined LM and SEM investigation. *Bot. J. Linn. Soc.* 182 (1), 14–79.
- Bralower, T.J., 2002. Evidence of surface water oligotrophy during the Paleocene – Eocene thermal maximum: nannofossil assemblage data from Ocean Drilling Program Site 690, Maud Rise, Weddell Sea. *Paleoceanography* 17 (PA000662).
- Bratishko, A., Schwarzhan, W., Reichenbacher, B., Vernyhovora, Y., Corić, S., 2015. Fish otoliths from the Konkian (Miocene, early Serravallian) of Mangyshlak (Kazakhstan) – testimony of an early endemic evolution in the Eastern Paratethys. *Paläontol. Z.* 89 (4), 839–889. <https://doi.org/10.1007/s12542-015-0274-4>.
- Brzobohatý, R., Nolf, D., 2002. Stomiiformes (Teleostei, Otolithen) aus dem Miozän der Karpatischen Vortiefe (Westkarpaten, Mähren) und der Zentralen Paratethys insgesamt. *Cour. Forsch. Senckenberg* 237, 139–150.
- Bugrova, E.M., Gladkov, V.I., Dmitrieva, T.V., Nevzorova, L.S., Sokolov, B.C., 2005. Guidebook of Microfauna, Volume 8: Cenozoic Foraminifera [Prakticheskoe Rukovodstvo Po Mikrofaune, tom 8: Foraminifery Kainozoya ] Proceedings of VSEGEI (In Russian).
- Cachão, M., Moita, M.T., 2000. *Coccolithus pelagicus*, a productivity proxy related to moderate fronts off Western Iberia. *Mar. Micropaleontol.* 39 (1–4), 131–155.
- Campani, M., Mulch, A., Kempf, O., Schlunegger, F., Mancktelow, N., 2012. Miocene paleotopography of the Central Alps. *Earth Planet. Sci. Lett.* 337–338 (1), 174–185.
- Čorić, S., Hohenegger, J., 2008. Quantitative analyses of calcareous nannoplankton from Baden-Sooss section (Austria). *Geol. Carpath.* 59, 447–460.
- Davitashvili, L.Sh., Merklin, R.L. (Eds.), 1966. Guide to the Ecology of Marine Bivalves [Spravochnik po ekologii morskikh dvustvorok]. Moscow, Nauka (In Russian).
- Davitashvili, L.Sh., Merklin, R.L. (Eds.), 1968. Guide to the Ecology of Marine Gastropods [Spravochnik po ekologii morskikh gastropod]. Moscow, Nauka (In Russian).
- Derjugin, K., 1915. La faune du dugolfe de Kola et les conditions de son existence. In: *Memoires l'Academie Imperiale des sciences. Classe des sciences physiques et mathematiques.* [Fauna Kol'skogo zaliva i usloviya ee sushhestvovaniya. Zapiski Imperatorskoj akademii nauk po otdeleniyu fiziko-matematicheskikh nauk]. Petrograd (In Russian).
- Derjugin, K., 1928. Die Fauna des Weissen Meeres und ihre Existenzbedingungen. *Explorations des mers d'U.R.S.S.* [Fauna Belogo morya i usloviya ee sushhestvovaniya. Issledovaniya morej SSSR] Fasc. 7–8, (In Russian).
- Doláková, N., Holcová, K., Nehyba, S., Hladilová, Š., Brzobohatý, R., Zágorský, K., Hrabovský, J., Seko, M., Utescher, T., 2014. The Badenian parastratotype at Židlochovice from the perspective of the multiproxy study. *N. Jb. Geol. Paläont.* 271 (2), 169–201.
- Doláková, N., Kováčová, M., Utescher, T., 2021. Vegetation and climate changes during the Miocene Climatic Optimum and Miocene climatic transition in the northwestern part of Central Paratethys. *Geol. J.* 56 (2), 729–743. <https://doi.org/10.1002/gj.4056>.
- Drinia, H., 2009. Palaeoenvironmental reconstruction of the Oligocene Afales Basin, Ithaki island, western Greece. *Central Eur. J. Geosci.* 1 (1), 1–18. <https://doi.org/10.2478/v10085-009-0001-z>.
- Dury, M., Hambuckers, A., Warnant, P., Henrot, A.J., Favre, E., Ouberdou, M., François, L., 2011. Responses of European forest ecosystems to 21 (st) century climate: assessing changes in interannual variability and fire intensity. *For. Biogeosci. For.* 4, 82–99.
- Dzhanelidze, O.I., 1963. Miliolidae of the Middle Miocene of Georgia, VIII. *Trudy Instituta paleobiologii Akademii nauk Gruzinskoj SSR*, pp. 133–192 (In Georgian).
- Dzhanelidze, O.I., 1970. Foraminifera from the Late and Middle Miocene of Georgia [Foraminifery Nizhnego I Srednego Miotsena Gruzii] Tbilisi, Metsniereba (In Russian).
- El Meknassi, S., Dera, G., Cardone, T., De Raféllis, M., Brahm, C., Chavagnac, V., 2018. Sr isotope ratios of modern carbonate shells: good and bad news for chemostratigraphy. *Geology* 46 (11), 1003–1006. <https://doi.org/10.1130/G45380.1>.
- Fornaciari, E., Stefano, A.D., Rio, D., Negri, A., 1996. Middle Miocene quantitative calcareous nannofossil biostratigraphy in the Mediterranean region. *Micropaleontology* 42 (1), 37–63.
- Golovina, L.A., 2012. On the question of stratigraphy of the Middle-Upper Miocene of southern Russia based on calcareous nannoplankton [K voprosu o stratigrafii sredne-verhnego miotsena yuga Rossii na osnove izvestkovogo nanoplanktona]. In: 15th All Russia Micropaleontological Conference on Modern Micropaleontology, Gelendzhik, pp. 305–308 (in Russian).
- Goncharova, I.A., 1989. Bivalves of the Tarkhanian and the Chokrakian basins [Dvustvorchatye molluski tarkhanskogo i chokrakskogo basseinov]. In: *Proceedings of the Paleontological Institute, Moscow*, 234 (in Russian).
- Goncharova, I.A., Khondkarian, S.O., Shcherba, I.G., 2001. The Tarkhanian-Karaganian stage in development of the Euxinian-Caspian Basin (Eastern Paratethys), part 1: Tarkhanian [Tarkhan-karaganskij etap razvitiya Evksino-Kaspijskogo basseina (Vostochnyj Paratetis), chast 1: Tarkhan]. *Stratigr. Geol. Correl.* 9 (5), 508–522 (in Russian).
- Gradianu, I., Prikluy, T., Gregorova, R., 2020. Revision of the genera *Vinciguerria* and *Ĵovinciguerria* from the Oligocene of Romania (Central Paratethys) – comments on selected characters. *Neues Jahrb. Geol. Palaontol. Abh.* 298, 251–267.
- Hammer, Ø., Harper, D.A.T., Ryan, P.D., 2001. *PAST: Paleontological Statistics Software.* [http://priede.bf.lu.lv/ftp/pub/TIS/datu\\_analize/PAST/2.17c/download.html](http://priede.bf.lu.lv/ftp/pub/TIS/datu_analize/PAST/2.17c/download.html).
- Haq, B.U., Schutter, S.R., 2008. A chronology of Paleozoic sea-level changes. *Science* 322, 64–68.
- Harris, E.B., Strömberg, C.A.E., Sheldon, N.D., Smith, S.Y., Vilhena, D., 2017. Vegetation response during the lead-up to the middle Miocene warming event in the Northern Rocky Mountains. *Palaeogeogr. Palaeoclimatol. Palaeoecol.* 485, 401–415.
- Hedgpeth, J.W., 1957. Chapter 6 Classification of marine environments. In: Ladd, Harry S. (Ed.), *Treatise on Marine Ecology and Paleocology*, Volume 2, Paleocology, 67. The Geological Society of America, Memoir, pp. 93–100. <https://doi.org/10.1130/MEM67V2>.
- Hilgen, F.J., Lourens, L.J., Van Dam, J.A., Beu, A.G., Boyes, A.F., Cooper, R.A., Krijgsman, W., Ogg, J.G., Piller, W.E., Wilson, D.S., 2012. The Neogene period. In: *The Geologic Time Scale*, 2012, pp. 923–978, 1–2.
- Hofmann, Ch.-Ch., Zetter, R., Draxler, L., 2002. Pollen- und Sporenvergesellschaften aus dem Karpatium des Korneuburger Beckens (Niederösterreich). *Beitr. Paläontol.* 27, 17–43.
- Hohenegger, J., Rögl, F., Čorić, S., Pervesler, P., Lirer, F., Roetzel, R., Scholger, R., Stingl, K., 2009. The Styrian Basin: a key to the Middle Miocene (Badenian/Langhian) Central Paratethys transgressions. *Aust. J. Earth Sci.* 102, 102–132.
- Holbourn, A., Kuhnt, W., Schulz, M., Erlenkeuser, H., 2005. Impacts of orbital forcing and atmospheric carbon dioxide on Miocene ice-sheet expansion. *Nature* 438, 483–487. <https://doi.org/10.1038/nature04123>.
- Holcová, K., 1999. Postmortem transport and re-orientation of foraminiferal tests: relations to cyclical changes of foraminiferal assemblages. *Palaeogeogr. Palaeoclimatol. Palaeoecol.* 145, 157–182.
- Holcová, K., Hrabovský, J., Nehyba, S., Hladilová, Š., Doláková, N., Demény, A., 2015. The Langhian (Middle Badenian) carbonate production event in the Moravian part of the Carpathian Foredeep (Central Paratethys): a multiproxy record. *Facies* 61, 1–26.
- Holcová, K., Kopecká, J., Scheiner, F., 2019. An imprint of the Mediterranean middle Miocene circulation pattern in a satellite sea during the Langhian: a case study from the Carpathian Foredeep (Central Paratethys). *Palaeogeogr. Palaeoclimatol. Palaeoecol.* 514, 336–348. <https://doi.org/10.1016/j.palaeo.2018.10.024>.
- Iaccarino, S.M., Di Stefano, A., Foresi, L.M., Turco, E., Baldassini, N., Cascella, A., Da Prato, S., Ferraro, L., Gennari, R., Hilgen, F.J., Lirer, F., Maniscalco, R., Mazzei, R., Riforgiato, F., Russo, B., Sagnotti, L., Salvadorini, G., Speranza, F., Verducci, M., 2011. High-resolution integrated stratigraphy of the upper Burdigalian – lower Langhian in the Mediterranean: the Langhian historical stratotype and new candidate for defining its GSSP. *Stratigraphy* 8 (2–3), 199–215.
- Ilyina, L.B., 1993. Handbook for Identification of the Marine Middle Miocene Gastropods of Southwestern Eurasia [Opredelitel' morskikh srednemiootsenovih gastropod Yugo-Zapadnoy Evrasii], 255. *Trudy Paleontologicheskogo Institute (in Russian)*.
- Ivanov, D., Utescher, T., Mosbrugger, V., Syabryaj, S., Djordjević-Milutinović, D., Molchanoff, S., 2011. Miocene vegetation and climate dynamics in Eastern and Central Paratethys (Southeastern Europe). *Palaeogeogr. Palaeoclimatol. Palaeoecol.* 304 (3–4), 262–275.
- Jiménez-Moreno, G., Rodríguez-Tovar, F.J., Pardo-Igúzquiza, E., Fauquette, S., Suc, J.P., Müller, P., 2005. High-resolution palynological analysis in late early-middle Miocene core from the Pannonian Basin, Hungary: climatic changes, astronomical forcing and eustatic fluctuations in the Central Paratethys. *Palaeogeogr. Palaeoclimatol. Palaeoecol.* 216, 73–97.
- Jorissen, F.J., de Stigter, H.C., Widmark, G.V., 1995. A conceptual model explaining benthic foraminiferal microhabitats. *Mar. Micropaleontol.* 26 (1–4), 3–15. [https://doi.org/10.1016/0377-8398\(95\)00047-X](https://doi.org/10.1016/0377-8398(95)00047-X).
- Kaiho, K., 1994. Benthic foraminiferal dissolved-oxygen index and dissolved-oxygen levels in the modern ocean. *Geology* 22, 719–722. [https://doi.org/10.1130/0091-7613\(1994\)022<0719:BFDIOIA>2.3.CO;2](https://doi.org/10.1130/0091-7613(1994)022<0719:BFDIOIA>2.3.CO;2).
- Kaiho, K., 1999. Effect of organic carbon flux and dissolved oxygen on the benthic foraminiferal oxygen index (BFOI). *Mar. Micropaleontol.* 37, 67–76.
- Katz, M.E., Browning, J.V., Miller, K.G., Monteverde, D.H., Mountain, G.S., Williams, R.H., 2013. Paleobathymetry and sequence stratigraphic interpretations from benthic foraminifera: insights on New Jersey shelf architecture. *IODP Expedition 313. Geosphere* 9 (6), 1488–1513. <https://doi.org/10.1130/GES00872.1>.
- Kern, A., Harzhauser, M., Mandic, O., Roetzel, R., Čorić, S., Bruch, A.A., Zuschin, M., 2011. Millennial – scale vegetation dynamics in an estuary at the onset of the Miocene climate optimum. *Palaeogeogr. Palaeoclimatol. Palaeoecol.* 304 (3–4), 247–261.
- Konenkova, I.D., Bogdanovich, E.M., 1994. The distribution of foraminifera and nannoplankton in the Tarkhanian – the Chokrakian deposits of the Malyi Kamysylak ravine (Kerch Peninsula) [Raspredeleniye foraminifer i nannoplanktona v tarkhan-chokrakskikh otlozheniyakh urochischa Malyi Kamysylak (Kerchenskij poluostrov)]. *Biosphere of the geological past of Ukraine.* In: *Proceedings of the Institute of Geological Sciences of the NAS of Ukraine, Kyiv*, pp. 95–96 (in Russian).
- Kopecká, J., Holcová, K., Brlek, M., Scheiner, F., Ackerman, L., Rejšek, J., Milovský, R., Baranyi, V., Gaynor, S., Galović, I., Brčić, V., Belak, M., Bakrač, K., 2022. A case study of paleoenvironmental interactions during the Miocene climate optimum in southwestern Paratethys. *Glob. Planet. Chang.* 211, 1–21. <https://doi.org/10.1016/j.gloplacha.2022.103784>.
- Kováč, M., Král, J., Márton, E., Plašienka, D., Uher, P., 1994. Alpine uplift history of the central western Carpathians: geochronological, paleomagnetic, sedimentary and structural data. *Geol. Carpath.* 45 (2), 83–96.
- Kováč, M., Márton, E., Oszczytko, N., Vojtko, R., Hók, J., Králíková, S., Plašienka, D., Klučiar, T., Hudáčková, N., Oszczytko-Clowes, M., 2017. Neogene palaeogeography and basin evolution of the Western Carpathians, Northern Pannonian domain and adjoining areas. *Glob. Planet. Chang.* 155, 133–154. <https://doi.org/10.1016/j.gloplacha.2017.07.004>.
- Kováč, M., Halászová, E., Hudáčková, N., Holcová, K., Hyžný, M., Jamrich, M., Ruman, A., 2018. Towards better correlation of the Central Paratethys regional time scale with the standard geological time scale of the Miocene Epoch. *Geol. Carpath.* 69, 283–300.
- Kováčová, M., Doláková, N., Kováč, M., 2011. Miocene vegetation pattern and climate change in the Northwestern Central Paratethys domain (Czech and Slovak Republic). *Geol. Carpath.* 62 (3), 251–266.



- Kovar-Eder, J., Teodoridis, V., 2018. The Middle Miocene Central European plant record revisited; widespread subhumid sclerophyllous forests indicated. *Foss. Impr.* 74 (1–2), 115–134.
- Kovar-Eder, J., Jechorek, H., Kvaček, Z., Parashiv, V., 2008a. The integrated plant record: an essential tool for reconstructing Neogene zonal vegetation in Europe. *Palaios* 23, 97–111.
- Kovar-Eder, J., Suc, J.-P., Kvaček, Z., 2008b. Definition of Relevant Botanical Terms and Vegetation Units. [www.neclimate.de](http://www.neclimate.de).
- Krasheninnikov, V.A., 1959. Foraminifera [Foraminifery]. In: Zhizhchenko, B.P. (Ed.), *Atlas of the Middle Miocene Fauna from North Caucasus and Crimea* [Atlas Srednemiotenovoi Fauny Severnogo Kavkaza i Kryma] – Gostoptekhizdat, Moscow, pp. 15–103 (In Russian).
- Krasheninnikov, V.A., Basov, I.A., Golovina, L.A., 2003. The Eastern Paratethys: Tarkhanian and Konkian Regional Stages (Stratigraphy, Micropaleontology, Bionomy, Paleogeographic Links) [Vostochnyi Paratetis: Tarhanskiy i Konkskiy Regioyarusy (Stratigrafiya, Mikropaleontologiya, Bionomiya, Paleogeograficheskii Svyazi)]. *Nauchnyi Mir*, Moscow (In Russian).
- Kvaček, Z., Kováč, M., Kovar-Eder, J., Doláková, N., Jechorek, H., Parashiv, V., Kováčová, M., Sliva, L., 2006. Miocene evolution of landscape and vegetation in the Central Paratethys. *Geol. Carpath.* 57 (4), 295–310.
- La Mesa, M., 1999. Age and growth of *Aphiaminuta* (Pisces, Gobiidae) from the central Adriatic Sea. *Sci. Mar.* 63, 147–155.
- La Mesa, M., Arneri, E., Caputo, V., Iglesias, M., 2005. The transparent goby, *Aphia minuta*: review of biology and fisheries of a paedomorphic European fish. *Rev. Fish Biol. Fish.* 15, 89–109.
- Laurent, J.M., François, L., Bar-Hen, A., Bel, L., Cheddadi, R., 2008. European bioclimatic affinity groups: data-model comparisons. *Glob. Planet. Chang.* 61 (1–2), 28–40.
- Leopold, E.B., Denton, M.F., 1987. Comparative age of grassland and steppe east and west of the northern Rocky Mountains. *Ann. Mo. Bot. Gard.* 74, 841–867.
- Loeblich Jr., A.R., Tappan, H., 1988. Foraminiferal Genera and their Classification. Springer US, p. 2031. <https://doi.org/10.1007/978-1-4899-5760-3>. XL.
- Longhurst, A.R., 2007. *Ecological Geography of the Sea*. Elsevier Science, p. 560. <https://doi.org/10.1016/B978-0-12-455521-1.X5000-1>.
- Mai, H.D., 1981. Entwicklung und klimatische Differenzierung der Laubwaldflora Mitteleuropas in Tertiär. *Flora* 171, 525–582.
- Mai, H.D., 1991. Palaeofloristic changes in Europe and the confirmation of the arctotertiary – palaeotropical concept. *Rev. Palaeobot. Palynol.* 68 (1), 29–36.
- McArthur, J.M., Howarth, R.J., Shields, G.A., Zhou, Y., 2020. Strontium isotope stratigraphy, Chapter 7, p.211–238. In: Gradstein F.M., Ogg J.G., Schmitz M.D. and Ogg G.M. *A Geologic Time Scale*, Elsevier B.V., Vol 1 of 2, 1357.
- Merklin, R.L., 1950. Lamellibranchia of the spiralis clays, their environment and the life [Plastinchatozhabernye spiralisovykh kly, ikh sreda i zhizn]. In: *Proceedings of the Paleontological Institute, Moscow, Leningrad*, 28 (In Russian).
- Metcalfe, B., Feldmeijer, W., de Vringer-Picon, M., Brummer, G.-J.A., Peeters, F.J.C., Ganssen, G.M., 2015. Late Pleistocene glacial-interglacial shell-size-isotope variability in planktic foraminifera as a function of local hydrography. *Biogeosciences* 12, 4781–4807. <https://doi.org/10.5194/bg-12-4781-2015>.
- Meulenkamp, J.E., Sissingh, W., 2003. Tertiary paleogeography and tectonostratigraphic evolution of the Northern and Southern Peri-Tethys platforms and the intermediate domains of the African – Eurasian convergent plate boundary zone. *Palaeogeogr. Palaeoclimatol. Palaeoecol.* 196 (1–2), 209–228.
- Miller, P.J., 1986. Gobiidae. In: Whitehead, P.J.P., Bauchot, M.-L., Hureau, J.-C., Nielsen, J., Tortonese, E. (Eds.), *Fishes of the North-Eastern Atlantic and the Mediterranean (FNAM)*. UNESCO, Paris, pp. 1019–1085.
- Miller, K.G., Mountain, G.S., Browning, J.V., Komins, M., Sugarman, P.J., Christie-Blick, N., Katz, M.E., 1998. Cenozoic global sea level, sequences, and the New Jersey transect: results from coastal plain and continental slope drilling. *Rev. Geophys.* 36, 569–601.
- Mosbrugger, V., Utescher, T., 1997. The coexistence approach – a method for quantitative reconstructions of Tertiary terrestrial palaeoclimate data using plant fossils. *Palaeogeogr. Palaeoclimatol. Palaeoecol.* 134, 61–86.
- Muratov, M.V., Nevevskaia, L.A. (Eds.), 1986. *Stratigraphy of the USSR. Neogene System* [Stratigrafiya SSSR. Neogenovaya sistema] Moscow, Semivol. 1 (In Russian).
- Murray, J.W., 2006. *Ecology and Applications of Benthic Foraminifera*. Cambridge University Press, p. 426. <https://doi.org/10.1017/CBO9780511535529>.
- Nehyba, S., Holcová, K., Gedl, P., Doláková, N., 2016. The lower Badenian transgressive-regressive cycles – a case study from Oslavany (Carpathian Foredeep, Czech Republic). *Neues Jahrb. Geol. Paläontol. Abh.* 279 (2), 209–238.
- Nelson, J.S., Grande, T.C., Wilson, M.V.H., 2016. *Fishes of the World*, Fifth edition. John Wiley Sons, inc., Hoboken, New Jersey.
- Nevevskaia, L.A., Bogdanovich, A.K., Vyalov, O.S., Zhizhchenko, B.P., Il'ina, L.B., Nossovsky, M.F., 1975. A stage stratigraphic scale of Neogene deposits for the south USSR [Yarusnaya shkala neogenovykh otlozheniy yuga SSSR]. In: Senes, J. (Ed.), *Proceedings of the VI-th Congress of the Regional Committee on Mediterranean Neogene Stratigraphy (RCMNS)*, Bratislava, I, pp. 267–289.
- Nevevskaia, L.A., Goncharova, I.A., Il'ina, L.B., Paramonova, N.P., Popov, S.V., Bogdanovich, A.K., Gabunia, L.K., Nossovsky, M.F., 1984. Regional stratigraphic scale of the Neogene of Eastern Paratethys [Regional'naya stratigraficheskaya shkala Neogena Vostochnogo Paratetisa]. *Sov. Geol.* 9, 91–101 (In Russian).
- Nevevskaia, L.A., Goncharova, I.A., Paramonova, N.P., Popov, S.V., Babak, E.V., Bagdasaryan, K.G., Voronina, A.A., 1993. *Handbook for identification of the bivalvia of Southwestern Eurasia* [Opredelitel miotsenovykh dvustvorchatih molluskov Yugo-Zapadnoy Evrazii]. 247. *Trudy Paleontologicheskogo instituta* (In Russian).
- Nevevskaia, L.A., Goncharova, I.A., Il'ina, L.B., Paramonova, N.P., Khondkarian, S.O., 2003. The Neogene stratigraphic scale of the Eastern Paratethys [Stratigraficheskaya shkala neogena Vostochnogo Paratetisa]. *Stratigr. Geol. Correl.* 11 (2), 105–127 (in Russian with English abstract).
- Nolf, D., 2013. *The Diversity of Fish Otoliths, Past and Present*. Royal Belgian Institute of Natural Sciences, Brussels.
- Nosovsky, M.F., Barg, I.M., Pishvanova, L.S., Andreyeva-Grigorovich, A.S., 1976. On the Volume of the Tarkhanian Stage in the South of USSR [Ob obime tarkhanskogo yarusa na yuge SSSR], *Stratigraphy of the Northern Black sea region and the Crimea, Dnepropetrovsk*, pp. 22–31 (In Russian).
- Nurzalia, W., Saelan, W., Hohenecker, J., 2018. Depth distribution of benthic foraminifera in the middle and deeper sublittoral to uppermost bathyal zones northwest of Okinawa, Japan. *Bull. Geol. Soc. Malaysia* 65, 77–90.
- Okada, H., McIntyre, A., 1979. Seasonal distribution of modern coccolithophores in the western North Atlantic Ocean. *Mar. Biol.* 54 (4), 319–328.
- Otto, D., Rasse, D., Kaplan, J., Warnant, P., François, L., 2002. Biospheric carbon stocks reconstructed at the Last Glacial Maximum: comparison between general circulation models using prescribed and computed sea surface temperatures. *Glob. Planet. Chang.* 33 (1–2), 117–138.
- Ouda, Kh., Obaidalla, N., 1998. Ecology and distribution of the recent subtidal foraminifera along the Egyptian Red Sea shore, between Mersa Alam and Ras Banas. *Rev. Esp. Micropaleontol.* 30 (3), 11–34.
- Palcu, D.V., Golovina, L.A., Vernyhorova, Y.V., Popov, S.V., Krijgsman, W., 2017. Middle Miocene paleoenvironmental crises in Central Eurasia caused by changes in marine gateway configuration. *Glob. Planet. Chang.* 158, 57–71. <https://doi.org/10.1016/j.gloplacha.2017.09.013>.
- Palcu, D.V., Popov, S.V., Golovina, L.A., Kuiper, K.F., Liu, S., Krijgsman, W., 2019. The shutdown of an anoxic giant: magnetostratigraphic dating of the end of the Maikop Sea. *Gondwana Res.* 67, 82–100. <https://doi.org/10.1016/j.gr.2018.09.011>.
- Pearson, P., 2012. Oxygen isotopes in foraminifera: overview and historical review. *Paleontol. Soc. Pap.* 18, 1–38. <https://doi.org/10.1017/S108933260002539>.
- Pearson, P.N., Burgess, C.E., 2008. Foraminifer test preservation and diagenesis: comparison of high latitude sites, 59–72. In: Austin, W.E.N., James, R.H. (Eds.), *Biogeochemical Controls on Paleocceanographic Environmental Proxies*. Geological Society of London. Special Publications, 303.
- Perch-Nielsen, K., 1985. Cenozoic Calcareous Nannofossils. In: Bolli, H.M., Sanders, J.B., Perch-Nielsen, K. (Eds.), *Plankton Stratigraphy*. Cambridge University Press, Cambridge, pp. 427–554.
- Piller, W.E., Harzhauser, M., Mandic, O., 2007. Miocene Central Paratethys stratigraphy – current status and future directions. *Stratigraphy* 4, 151–168.
- Pin, C., Gannoun, A., Dupont, A., 2014. Rapid, simultaneous separation of Sr, Pb, and Nd by extraction chromatography prior to isotope ratios determination by TIMS and MC-ICP-MS. *J. Anal. At. Spectrom.* 29 (10), 1858–1870.
- Planderová, E., 1990. Miocene Microflora of Slovak Central Paratethys and its Biostratigraphical Significance. *Geological Institute Dionýz Štúr Bratislava*, pp. 1–144.
- Pobedina, V.M., Voroshilova, A.G., Rybina, O.I., Kuznetsova, Z.V., 1956. *Spravochnik po mikrofaune sredne- i verkhnemiocenovykh otlozhenii Azerbaidzhana* (Handbook about Microfauna Middle and Upper Miocene Deposits of Azerbaijan). Azerbaidzhanskoe gosudarstvennoe izdatelstvo nefyanoi nauchno-tehnicheskoi literatury, Baku.
- Popov, S.V., Akhmetiev, M.A., Lopatin, A.V., Bugrova, E.M., Sytchevskaya, E.K., Scherba, L.G., Andreyeva-Grigorovich, A.S., Zaporozhec, N.I., Nikolaeva, I.A., Kopp, M.I., 2009. Paleogeography and Biogeography of Paratethys Basins [Paleogeographiya i biogeographiya basseinov Paratetisa]. *Scientific World*, Moscow (In Russian).
- Popov, S.V., Rostovtseva, Yu.V., Pinchuk, T.N., Patina, I.S., Goncharova, I.A., 2019. Oligocene to Neogene paleogeography and depositional environments of the Euxinian part of Paratethys in Crimean – Caucasian junction. *Mar. Pet. Geol.* 103, 163–175. <https://doi.org/10.1016/j.marpetgeo.2019.02.019>.
- Popov, S.V., Voronina, A., Goncharova, I.A., 1993. *Stratigraphy and Bivalvia of Oligocene-Lower Miocene of the Eastern Paratethys* [Stratigrafiya i dvustvorchatyie molluski oligotsena-nizhnego miotsena Vostochnogo Paratetisa]. *Nauka*, Moscow (In Russian).
- Popova, S., Utescher, T., Gromyko, D.V., Mosbrugger, V., Herzog, E., François, L., 2013. Vegetation change in Siberia and the Northeast of Russia during the Cenozoic Cooling – a study based on diversity of plant functional types. *Palaios* 28, 418–432.
- Raffi, I., Wade, B.S., Pálke, H., Beu, A.G., Cooper, R., Crundwell, M.P., Krijgsman, W., Moore, T., Raine, I., Sardella, R., Vernyhorova, Y.V., 2020. Chapter 29 – The Neogene period. In: Gradstein, Felix M., Ogg, James G., Schmitz, Mark D., Ogg, Gabi M. (Eds.), *Geologic Time Scale 2020*. Elsevier, pp. 1141–1215. <https://doi.org/10.1016/B978-0-12-824360-2.00029-2>.
- Rio, D., Fornaciari, E., Raffi, I., 1990. Late Oligocene through early Pleistocene calcareous nannofossils from the western equatorial Indian Ocean (Leg 115). In: Duncan, R.A., et al. (Eds.), *Proceedings of the Ocean Drilling Program*, 115. Ocean Drilling Program, College Station TX, pp. 175–221. *Sci. Res.*
- Rögl, F., 1998. Paleogeographic considerations for Mediterranean and Paratethys seaways (Oligocene to Miocene). *Ann. Naturhist. Mus. Wien* 99A, 279–310.
- Rögl, F., 1999. Mediterranean and Paratethys. Facts and hypotheses of an Oligocene to Miocene paleogeography (short overview). *Short note. Geol. Carpath.* 50, 339–349.
- Rögl, F., 2001. Mid-Miocene circum-Mediterranean paleogeography. In: EEDEN Workshop Stratigraphy & Paleogeography, 4. *Berichte Inst. Geol. Paläont. K.F.-Universität Graz*, Austria, pp. 49–59, 15–18.3.2001. 8 figs. - Graz.
- Rögl, F., Spezzaferri, S., 2003. Foraminiferal paleoecology and biostratigraphy of the Mühlbach section (Gaiendorf Formation, lower Badenian), Lower Austria. *Ann. Naturhist. Mus. Wien* 104A, 23–75.

- Rosoff, D.B., Corliss, B.H., 1992. An analysis of recent deep-sea benthic foraminiferal morphotypes from the Norwegian and Greenland seas. *Palaeogeogr. Palaeoclimatol. Palaeoecol.* 91 (1–2), 13–20. [https://doi.org/10.1016/0031-0182\(92\)90028-4](https://doi.org/10.1016/0031-0182(92)90028-4).
- Rostovtseva, Yu.V., 2012. Lithostratigraphy of the spiralis clays of the Kerch Peninsula [Litostratigraficheskoe raschlenenie spirialisovykh glin Kerchenskogo poluostrova]. Paleontological research to improve of stratigraphic schemes of the Phanerozoic sediments. In: Materials of the XXXIV Session of the Paleontological Society of NAS of Ukraine, Kyiv, pp. 93–94 (in Russian).
- Sant, K., Palcu, D., Mandic, O., Krijgsman, W., 2017. Changing seas in the Early–Middle Miocene of Central Europe: a Mediterranean approach to Paratethyan stratigraphy. *Terra Nova* 29, 273–281.
- Scheiner, F., Holcova, K., Milovský, R., Dolakova, N., Rigova, J., 2019. Response of benthic foraminiferal communities to changes in productivity and watermass conditions in the epicontinental Paratethys during the middle Miocene. *Mar. Micropaleontol.* 151. <https://doi.org/10.1016/j.marmicro.2019.101750>.
- Schmidt, D.N., Renaud, S., Bollmann, J., Schiebel, R., Thierstein, H.R., 2004. Size distribution of Holocene planktic foraminifer assemblages: biogeography, ecology and adaptation. *Mar. Micropaleontol.* 50, 319–338.
- Schwarzans, W., 2017. A review of otoliths collected by W. Weiler from the Badenian of Romania and by B. Strashimirov from Badenian equivalents of Bulgaria. *Cainozoic Res.* 17, 167–191.
- Schwarzans, W., Brzobohatý, R., Radwańska, U., 2020. Goby otoliths from the Badenian (middle Miocene) of the Central Paratethys from the Czech Republic, Slovakia and Poland: a baseline for the evolution of the European Gobiidae (Gobiiformes; Teleostei). *Boll. Soc. Paleontol. Ital.* 59, 125–173.
- Sharp, Z.D., Masson, H., Lucchini, R., 2005. Stable isotope geochemistry and formation mechanisms of quartz veins; extreme paleoaltitudes of the Central Alps in the Neogene. *Am. J. Sci.* 305 (3), 187–219.
- Shevenell, A., Kenneth, J.P., Lea, D.W., 2006. Middle Miocene ice sheet dynamics, deep-sea temperatures, and carbon cycling: a Southern Ocean perspective. *Geochim. Geophys. Geosyst.* 9 <https://doi.org/10.1029/2007GC001736>. Q02006. 2008.
- Shnyukov, Y.F., Sheremetev, V.M., Maslakov, N.A., Kutny, V.A., Gusakov, I.N., Trofimov, V.V., 2006. Mud Volcanoes of the Kerch-Taman Region [Griazevye Vulkany Kerchensko-Tamanskogo Regiona]. GlavMedia, Krasnodar (In Russian).
- Smiley, T.M., Hyland, E.G., Cotton, J.M., Reynolds, R.E., 2018. Evidence of early C4 grasses, habitat heterogeneity, and faunal response during the Miocene Climatic Optimum in the Mojave Region. *Palaeogeogr. Palaeoclimatol. Palaeoecol.* 490, 415–430.
- Steinhilber, M., Coxall, H.K., de Boer, A.M., Huber, M., Barbolini, N., Bradshaw, C. D., Burls, N.J., Feakins, S.J., Gasson, E., Henderiks, J., Holbourn, A.E., Kiel, S., Kohn, M.J., Knorr, G., Kürschner, W.M., Lear, C.H., Liebrand, D., Lunt, D.J., Mörs, T., Pearson, P.N., Pound, M.J., Stoll, H., Strömberg, C.A.E., 2021. The Miocene: the future of the past. *Paleoceanogr. Paleoclimatol.* 36, 1–71.
- Strashimirov, B., 1972. Otolity ot tarkhana na Severoistochna Bulgaria. In: *Annuaire de l'École supérieure des mines et de géologie, Sofia*, 18, pp. 301–313.
- Strömberg, C.A.E., McInerney, F.A., 2011. The Neogene transition from C-3 to C-4 grasslands in North America: assemblage analysis of fossil phytoliths. *Paleobiology* 37 (1), 50.
- Strömberg, J.C., Beauchamp, V.B., Dixon, M.D., Lite, S.J., Paradzick, C., 2007. Importance of low-flow and high-flow characteristics to restoration of riparian vegetation along rivers in and south-western United States. *Freshw. Biol.* 52 (4), 651–679.
- Stuchlik, L. (Ed.), 1994. Neogene pollen flora of central Europe. Part 1. *Acta Paleobot. (Suppl.1)*, 1–56.
- Studencka, B., Gontsharova, I.A., Popov, S.V., 1998. The bivalve fauna as a basis for reconstruction of the Middle Miocene history of the Paratethys. *Acta Geol. Pol.* 48, 285–342.
- Tang, Z.-H., Ding, Z.-L., 2013. A palynological insight into the Miocene aridification in the Eurasian interior. *Palaeoworld* 22 (3–4), 77–85.
- Teodoridis, V., Kovar-Eder, J., Mazouch, P., 2011a. The IPR-vegetation analysis applied to modern vegetation in SE China and Japan. *PALAIOS* 26 (10), 623–638.
- Teodoridis, V., Kovar-Eder, J., Marek, P., Kvaček, Z., Mazouch, P., 2011b. The integrated plant record vegetation analysis: internet platform and online application. *Acta Mus. Nat. Pragae, Ser. B. Hist. Nat.* 67 (3–4), 159–164. Praha.
- Toffanin, F., Agnini, C., Fornaciari, E., Rio, D., Giuberti, L., Luciani, V., Spofforth, D.J. A., Pälke, H., 2011. Changes in calcareous nannofossil assemblages during the Middle Eocene Climatic Optimum: clues from the central-western Tethys (Alano section, NE Italy). *Mar. Micropaleontol.* 81, 22–31. <https://doi.org/10.1016/j.marmicro.2011.07.002>.
- Trabelsi, R., Elloumi, J., Hamza, A., Ayadi, N., Zghal, I., Ayadi, H., 2017. Variability of foraminifera associations in seagrass ecosystems in shallow water during winter (Kerkennah – Southern Tunisian coasts). *J. Mar. Biol. Assoc. UK* 98 (Special Issue 8), 1945–1954. <https://doi.org/10.1017/S0025315417001667>. Special Section: European Marine Biology Symposium Papers 2018, December 2018.
- Utescher, T., Mosbrugger, V., 2015. The Palaeoflora Database. At. <http://www.geologie.unibonn.de/Palaeoflora>.
- Utescher, T., Böhme, M., Mosbrugger, V., 2011. The Neogene of Eurasia: spatial gradients and temporal trends – the second synthesis of NECLIME. *Palaeogeogr. Palaeoclimatol. Palaeoecol.* 304, 3–4, 1,196–201.
- Utescher, T., Bruch, A.A., Erdei, B., François, L., Ivanov, D., Jacques, F.M.B., Kern, A.K., Liu, Y.-S.(C.), Mosbrugger, V., Spicer, R.A., 2014. The coexistence approach – theoretical background and practical considerations of using plant fossils for climate quantification. *Palaeogeogr. Palaeoclimatol. Palaeoecol.* 410, 58–73.
- Vernigorova, J.V., Fikolina, L.A., Obsharskaya, N.N., 2012. Structural and facies zonation of the Neogene sediments of the Kerch Peninsula [Strukturno-fatsialnoye raionirovaniye neogenovykh otlozheniy Kerchenskogo poluostrova]. *Geol. J.* 3, 74–94 (in Russian).
- Vernyhorova, Yu.V., 2014. Lytho- and biofacial features of the Neogene deposits of the Kerch Peninsula [Lito- i biofatsialni osoblyvosti neogenovykh vidkladiv Kerchenskoho pivostrova]. Kyiv. In: Proceedings of the Institute of Geological Sciences of the NAS of Ukraine. Kyiv, 7, pp. 112–157 (In Ukrainian).
- Vernyhorova, Yu.V., Ryabokon, T.S., 2020. The stratigraphy of the Oligocene-lower Miocene deposits of Southern Ukraine. *Turk. J. Earth Sci.* 29 (8) <https://doi.org/10.3906/yer-1905-24>. Article 8.
- Walanus, A., Nalepka, D., 1999. POLPAL. Program for counting pollen grains, diagrams plotting and numerical analysis. *Acta Paleobot.* 2, 659–661.
- Warnant, P., François, L., Strivay, D., Gérard, J.C., 1994. CARAIB: a global model of terrestrial biological productivity. *Glob. Biogeochem. Cycles* 8 (3), 255–270.
- Wei, W., Wise, S.W., 1990. Biogeographic gradients of middle Eocene-Oligocene calcareous nannoplankton in the South Atlantic Ocean. *Palaeogeogr. Palaeoclimatol. Palaeoecol.* 79, 29–61. [https://doi.org/10.1016/0031-0182\(90\)90104-F](https://doi.org/10.1016/0031-0182(90)90104-F).
- Weiler, W., 1950. Die Otolithen aus dem Jung-Tertiär Süd-Rumäniens. 2. Mittel-Miozän, Torton, Buglow und Sarmat. *Senckenbergiana* 31, 209–258.
- Winter, A., Jordan, R., Roth, P.H., 1994. Biogeography of living coccolithophores in ocean waters. In: Winter, A., Siesser, W.G. (Eds.), *Coccolithophores*. Cambridge University Press, Cambridge, pp. 13–37.
- Young, J.R., 1994. Functions of coccoliths. In: Winter, A., Siesser, W.G. (Eds.), *Coccolithophores*. Cambridge University Press, Cambridge, pp. 63–82.
- Young, J.R., Bown, P.R., Lees, J.A., 2021. Nannotax3 Website. International Nannoplankton Association. Accessed January–November 2021. <https://www.mikrotax.org/Nannotax3>.
- Zachos, J., Pagani, M., Sloan, L., Thomas, E., Billups, K., 2001. Trends, rhythms, and aberrations in global climate 65 Ma to present. *Science* 292, 686–693. <https://doi.org/10.1126/science.1059412>.
- Zágoršek, K., Holcová, K., Trsoň, T., 2007. Bryozoan event from Middle Miocene (early Badenian) lower neritic sediments from the locality Kralice nad Oslavou (Central Paratethys, Moravian part of the Carpathian Foredeep). *Int. J. Earth Sci. (Geol. Rundsch.)* 97, 835–850.